# The molecular function of Sin1, an evolutionarily conserved subunit of TOR complex 2

村山　真一

奈良先端科学技術大学院大学

バイオサイエンス研究科　細胞シグナル研究室

（塩﨑　一裕　教授）

２０１７／８／２４

バイオサイエンス研究科　博士論文要旨

| | | | |
|---|---|---|---|
| 推薦教員 | 細胞シグナル研究室 （塩﨑一裕） | | |
| 氏名 | 村山真一 | 提出 | 平成29年8月24日 |
| 題目 | The molecular function of Sin1, an evolutionarily conserved subunit of TOR complex 2 | | |


A serine/threonine-specific protein kinase, Target Of Rapamycin (TOR) regulates cell growth and metabolism by integrating various extracellular stimuli, such as nutrients, stress, as well as growth factors in metazoans. From yeast to humans, TOR kinase operates by forming two different protein complexes, TOR complex 1 (TORC1) and 2 (TORC2), each of which has a unique set of regulatory subunits that determine the substrate specificity. The metazoan phosphoinositide 3-kinase (PI3K) pathway mediates signals from various growth factors and the hormone insulin, resulting in the phosphorylation and activation of the AGC-family kinase AKT (also known as PKB). TORC2 has been identified as the kinase complex that phosphorylates AKT at its C-terminal hydrophobic motif (HM). However, the exact molecular basis for the substrate specificity and recognition by TORC2 is not well understood. In the fission yeast *Schizosaccharomyces pombe*, TORC2 phosphorylates and activates the AKT-homolog Gad8 kinase for cellular survival under stress conditions. It was previously reported that Sin1 is one of the TORC2-specific subunits essential for Gad8 phosphorylation as is human SIN1 for AKT phosphorylation. In addition, the interaction of Sin1 with Gad8 was detected by a yeast two-hybrid screen. In this study, I present evidence that the Conserved Region in the Middle (CRIM) of Sin1 mediates essential functions of Sin1 as a TORC2 subunit; (1) substrate binding, (2) activation, and (3) assembly of TORC2.

(1) I first demonstrated the physical interaction of Sin1 with Gad8 through a co-immunoprecipitation assay. Previously, our laboratory reported that a small GTPase Ryh1 in its GTP-bound form positively regulates TORC2-Gad8 signaling. I found that GTP-locked Ryh1 promotes the Sin1-Gad8 interaction, thus increasing the TORC2-dependent phosphorylation of Gad8 in its HM. Although a direct association between Sin1 and Gad8 was not evident, this observation indicated that Sin1 functions as a critical mediator of TORC2 activity to the downstream effecter Gad8. Through deletion analysis of the Sin1 protein, the Gad8/AKT-associating domain (GAD) was mapped to a central region that overlaps with the CRIM domain conserved among the Sin1 orthologs. Random mutagenesis of the GAD region revealed that the integrity of GAD is essential in mediating the Sin1-Gad8 interaction. Moreover, Gad8 phosphorylation was induced by artificially fusing the GAD fragment to another TORC2 subunit Ste20, illustrating that the GAD region is sufficient for the substrate-recruiting function of Sin1. The NMR solution structure of Sin1 CRIM has an ubiquitin-like fold with an acidic loop structure protruding from the molecular surface. Interestingly, the amino acid sequence of the acidic loop is highly conserved more than the rest of the CRIM region, implying the importance of this loop structure. Indeed, site-directed mutagenesis unveiled the critical role that the acidic loop plays in substrate binding.

The fusion protein technique was also employed to test if absence of Sin1 affects the catalytic activity of Tor1; a direct presentation of Gad8 with Tor1 was enabled by fusing Gad8 to Ste20. The forced recruitment of Gad8 to TOR kinase was sufficient to induce the phosphorylation of the fusion protein at the HM site, independently of Sin1, indicating that Sin1 is not essential for the intrinsic kinase activity of Tor1. Moreover, I found that the *Δsin1* mutation does not affect the interaction of Tor1 with the other subunits, indicating that Sin1 is dispensable for the TORC2 assembly. On the other hand, when Gad8 is fused to the TORC1 subunit Mip1, the Mip1-Gad8 fusion protein was found to be phosphorylated at the HM site in a TORC1-dependent manner, supporting the notion that the unique subunit of the TOR complexes determines the substrate specificity.

(2) In order to gain a complete picture of the Sin1-Gad8 interface, truncation and random mutagenesis studies were carried out with the Gad8 protein. Single amino acid substitutions that disrupted the interaction of Gad8 with Sin1 were isolated within the N-terminal, non-catalytic region of Gad8 as well as the N-lobe of its kinase domain. I verified loss of the interaction between the Gad8 variants and Sin1 in *in-vitro* co-purification assays. The isolated Gad8 variants gave little information about the Sin1 binding site on Gad8, probably because these substitutions affect the Gad8 conformation and structure. Unexpectedly, some of the Gad8 N-terminal variants require very limited interaction with Sin1 to be phosphorylated at the HM site, implying a role of the N-terminal region in Gad8 activation. In addition, the analysis of the L303P variant and a theoretical model of the active form of Gad8 suggest that the proper positioning of the phosphorylated C-terminal loop against the kinase domain after activation may be important for Gad8 activity.

(3) I demonstrated that the Sin1 GAD region is not necessary for the incorporation of Sin1 into TORC2. The analysis using the truncation variants revealed that association of TOR kinase with Sin1 is largely dependent on a short region of Sin1 spanning 251-260 residues in the N-terminal region of the CRIM, just next to the GAD.

I have shown that AKT kinase can replace the function of Gad8 in the stress tolerance of fission yeast, indicating the evolutionarily conserved role of the orthologous AGC family kinases. Furthermore, similar to the Sin1-Gad8 interaction in *S. pombe*, human TORC2 has been proposed to interact with AKT through the CRIM domain of human SIN1. Dysregulation in TORC2-AKT signaling in human has been linked to cancer and type-2 diabetes. Hence, the identification and characterization of the substrate-docking moiety of TORC2 is of great therapeutic interest. The present study has established Sin1 as the substrate-recruiting subunit of TORC2 and demonstrated that the three of the major functions of Sin1, the substrate binding and activation as well as integration into TORC2, are mediated by the CRIM domain. Hence, the SIN1 CRIM domain appears to be a potent target of pharmacological intervention. Future studies will elucidate how the positioning of the substrate-binding site, particularly the acidic loop, of the Sin1 CRIM relative to the FRB domain of Tor1 contributes to the substrate recognition and activation and is modulated by the upstream signaling.

# Table of Contents

# 1. INTRODUCTION

How nutrient signals control the key events that trigger cell cycle progression has been one of the key questions to understand the molecular mechanisms by which cell division is coordinately regulated with cell growth in response to environmental fluctuations. Cell reproduction is the most nutrient-demanding process to coordinate cellular growth with fine and intricate operations of chromosome segregation followed by cell division. Failure in coordinating such process is likely to pose detrimental consequences on cellular physiology and fate. Hence, the status of cellular growth and metabolism which affect the rate of the cell division is tightly regulated by signaling pathways so that cells can reproduce only when nutritional and environmental conditions are favorable. An elaborate signaling network that integrates various extracellular stimuli modulates cellular growth and metabolism in response to environmental fluctuations.

From yeast to humans, nutrient sensing coupled with various cellular processes, including cell cycle control, is the most fundamental faculty for cells to survive and reproduce. Simple unicellular microorganism such as yeasts have been used as genetically amenable model system to dissect cellular response to nutrients. Yeast cells are incapable of autonomous movements and highly susceptible to nutrient deprivation; therefore, they require a sensitive nutrient-sensing system, with which they can determine when to proliferate or arrest the cell cycle for the initiation of sexual differentiation that produces spores highly resistant to harsh conditions. Cells in multicellular organisms, on the other hand, are constantly supplied with nutrient through the circulatory system and thus, require an additional mechanism to control cell proliferation – growth factors (hormones) coordinate cell proliferation by regulating the core cell cycle machinery. Cancer cells can proliferate without

signal input in a deregulated manner, while diabetic adipocytes become irresponsive to the hormone insulin and hence incapable of uptaking glucose.

Cell proliferation is achieved by two separate processes; cell growth and division, which are now understood to be regulated through distinct signaling pathways (Fingar and Blenis, 2004). In order to keep a defined cell size, however, the cells must double the cell sizes before undergoing cell division (Fingar and Blenis, 2004; Jorgensen, 2004). Hence, in most cell types, cell division is tightly coupled with cell growth even under changing environments. Indeed, both cell division and cell growth contribute to tumorigenesis; aggressive cell proliferation must be supported by unrestrained cell growth. Therefore, cancer cells must find a way to unleash cell growth and/or bypass the restraints on cell growth to sustain their rapid proliferation. However, mutational events that lead to hypertrophic cell growth alone seldom result in malignant transformation. On the other hand, constitutively activated mitogenic signaling that deregulates cell cycle control is a highly potent inducer of cellular transformation and frequently observed in a wide variety of cancers.

### 1.1. Target of Rapamycin (TOR) kinase(s) regulate cell growth and cell cycle progression by forming TOR complex 1 (TORC1) and TOR complex 2 (TORC2)

Yeasts have been serving as an excellent model system to dissect the molecular mechanisms of the coordinated regulation of cell growth and division. Yeast strains defective in a certain cell cycle gene arrest the cell cycle and grow larger beyond the defined cell size (e.g., *cdc25* mutants in the fission yeast *Schizosaccharomyces pombe*). On the other hand, upon nitrogen starvation, fission yeast cells commit to two consecutive rounds of the cell division cycle without cell growth before arresting in G1 phase (Yanagida et al., 2011). This starvation response indicates that the signaling pathways which regulate cell growth and division are distinct, and yet they seem to be coordinately regulated in most cases. The molecular

machinery that coordinates the cell growth and division is thought to operate in G1 phase. Evidently, in human cancers, activating mutations are frequently observed in the genes whose products constitute the signaling pathways that regulate cell cycle progression through G1 phase (Foster et al., 2010). In G1 phase, cells determine whether or not to initiate DNA synthesis by monitoring the sufficiency of nutrients and growth factors. When the nutrients and/or the growth factors are scarce, cells not only halt their growth but also arrest in G1 until the environment becomes favorable. Once cells commit to the mitotic cell cycle by passing a certain point in G1 phase, which is referred to as START in budding yeast and the restriction point in mammalian cells, they no longer respond to deprivation of nutrients and/or growth factors.

Rapamycin is the macrolide antibiotic isolated from a soil bacterium based on its anti-fungal activity that effectively inhibits yeast cell growth (Heitman et al., 1991). Rapamycin has been instrumental in dissecting the signaling pathways that respond to the nutrients and the growth factors. The phenotypes of rapamycin-treated yeast cells significantly overlap with those of nutritionally starved cells, including cell cycle arrest in G1, reduced protein synthesis, accumulated glycogen and trehalose, resistance to high temperatures, and altered transcription patterns (Barbet et al., 1996). Rapamycin was also found to be effective on mammalian cells, arresting lymphocytes in G1 with reduced cell sizes, whereas other cell types treated with the drug manifest smaller cell sizes even in nutrient- and growth factor-rich conditions (Fingar and Blenis, 2004). This phenotypic feature can be attributed to accelerated mitotic onset by rapamycin treatment or upon nutritional starvation; accelerated initiation of cell division before enough cell growth would decrease the cell size of daughter cells. Therefore, the phenotypes caused by rapamycin imply that the drug might target nutrient and/or growth factor signaling pathways that coordinate cell growth and progression through G1 phase. It can thus be conceived that the cellular target(s) of rapamycin might be involved

in aberrant cell cycle progression of cancer cells when deregulated (Brown et al., 1994; Chou and Blenis, 1995; Price et al., 1992).

Yeast genetics has greatly helped to identify the genes encoding the cellular target of rapamycin (TOR) and to elucidate the molecular mechanisms of the rapamycin action as well as the nutrient-sensing signaling pathway sensitive to this drug. Mutations that conferred resistance to rapamycin were mapped to the genes encoding FKBP12 and TOR kinases (Heitman et al., 1991; Kunz et al., 1993). The yeast genome encodes two isoforms of TOR kinase, while other eukaryotes have only one TOR homologue (Heitman et al., 1991; Helliwell et al., 1994; Kunz et al., 1993). Yeast genetics and biochemical analysis revealed that FKBP12 binds rapamycin and the FKBP12-rapamycin complex inhibits the protein products of the TOR genes, which are serine/threonine-specific protein kinases of about 260 kDa. TOR is a member of phosphatidylinositol 3-kinase-related kinase (PIKK) family, and shares a similar domain architecture with other family members (Figure 1). A large area of the N-terminal region contains multiple HEAT (huntingtin, elongation factor 3, a subunit of protein phosphatase 2A and TOR1) repeats. Following the HEAT repeats, there are the FRAP, ATM and TRRAP (FAT) domain, the FKBP12-rapamycin binding (FRB) domain, the kinase domain (Kinase), and the carboxy-terminal FATC domain. In budding yeast, while deletion of *TOR1* alone does not affect normal cell cycle progression, simultaneous depletion of *TOR1* and *TOR2* results in G1 cell cycle arrest, indicating that *TOR2* has an overlapping and complementing function with *TOR1* in cell cycle progression through G1 phase (Helliwell et al., 1994). On the other hand, deletion of the *TOR2* gene is lethal with cells arresting throughout the cell cycle (Helliwell et al., 1994), indicating that *TOR2* plays a function essential for cell viability, which is insensitive to rapamycin. Subsequent biochemical studies revealed that, from yeast to humans, the TOR kinase forms two distinct multi-subunit complexes, TOR complex 1 (TORC1) and 2 (TORC2) with different subunit

composition (Loewith et al., 2002; Wedaman et al., 2003). Specifically, the mass spectrometric and biochemical analyses of the immunoprecipitates of Tor1 and Tor2 revealed that Kog1 (kontroller of growth 1), and Lst8 (lethal with EC13 protein 8) are assembled with either Tor1 or Tor2 to form TORC1, while TORC2 contains Avo1, Avo2, Avo3 (adheres voraciously to Tor2) and Lst8 in addition to the core kinase Tor2 (Loewith et al., 2002). The FKBP12-rapamycin complex binds to only TORC1 through the FRB domain of Tor1/Tor2, but not to TORC2 and therefore, rapamycin effectively inhibits only TORC1 (Helliwell et al., 1998; Loewith et al., 2002). Thus, whilst TORC1 mediates a rapamycin-sensitive signaling pathway, TORC2 is part of a rapamycin-insensitive signaling pathways (Loewith et al., 2002). These studies clearly demonstrate that, in budding yeast, Tor1 is a main component of TORC1, while Tor2 forms TORC2 but it can also assemble TORC1 (Loewith et al., 2002). This is exactly the reason why the *tor1* deletion strain has no defect in cell cycle progression; because the *TOR1* function is shared by *TOR2*, the *tor1* deletion alone does not result in the inactivation of TORC1 (Helliwell et al., 1998; Loewith et al., 2002). Repressed expression of *KOG1* enables selective disruption of the TORC1 function and phenocopies the rapamycin-treated cells that arrest in G1, suggesting that TORC1 activity is required for passing START in G1 phase (Loewith et al., 2002).

In mammalian cells, the phosphorylation of the AGC-family kinase S6K1 and the eIF4-binding protein 4EBP1 was found to be sensitive to rapamycin, suggesting those proteins as mTORC1 substrates (Figure 2) (Brown et al., 1995; Brunn et al., 1997; Hara et al., 1997; 1998; Kuo et al., 1992; Price et al., 1992; Saltiel, 1996). However, in the early days of mTOR research, the immunoprecipitates of mTOR kinase prepared in the presence of a detergent was found to be inactive in *in vitro* kinase assays with recombinant 4EBP1 as substrate. This observation raised the possibility that mTOR requires regulatory subunits to phosphorylate its substrates (Nishiuma et al., 1998). Continued efforts revealed that mTOR complexes are

sensitive to a particular detergent, and a modified protocol with a milder detergent showed co-precipitation of interacting proteins with mTOR (Hara et al., 2002; Kim et al., 2002; Loewith et al., 2002). The analysis of the co-precipitated proteins by mass spectroscopy identified Raptor (regulatory-associated protein of mTOR) as the defining subunit of the rapamycin-sensitive mTOR complex, mTORC1 (Figure 3) (Hara et al., 2002; Kim et al., 2002; Loewith et al., 2002). Raptor was found to be homologous to Kog1 as well as the previously described fission yeast Mip1 (Mei2 Interacting Protein) (Shinozaki-Yabana and Watanabe, 2000), all of which have WD repeats at its C-terminal region. Furthermore, the mTORC1-dependent phosphorylation of S6K1 and 4EBP1 required the presence of the functional Raptor, which was shown to bind to S6K1 and 4EBP1 (Hara et al., 2002; Kim et al., 2002). Hence, mTORC1 promotes cell growth in response to nutrient and growth factors by regulating S6K1 and 4EBP1, which are implicated in protein synthesis and cap-dependent translation, respectively (Inoki et al., 2005b). In addition to the essential subunit Raptor, mTORC1 also contains mLST8, which is conserved as LST8 in budding yeast and Wat1 (also known as Pop3) in fission yeast (Figure 3).

In budding yeast, the rapamycin-insensitive function of Tor2 was shown to be mediated by TORC2 (Loewith et al., 2002), but the identity of the signaling pathways and the physiological processes in which TORC2 participates were to be addressed separately. Akt is a member of the AGC protein kinase family and is activated in a phosphatidylinositol-3 kinase (PI3K) dependent manner in response to growth factors (Figure 2). Activated Akt, in turn, promotes cell cycle progression through G1 phase (Chang et al., 2003; Fatrai et al., 2006; Liang and Slingerland, 2003). Consistent with its role in the G1 cell cycle control, Akt activity is upregulated in many human cancers (Altomare and Testa, 2005; Luo et al., 2003; Mei Sun, 2001; Testa and Bellacosa, 2001; Vivanco and Sawyers, 2002). Akt needs to be phosphorylated at two sites in the activation loop and the hydrophobic motif to become fully

active upon growth factor stimulation. Phosphorylation within the activation loop was known to be mediated by PDK1(Alessi et al., 1996; Biondi et al., 2001). But the identity of the kinase that mediates the phosphorylation of the hydrophobic motif in the C-terminal region had long been a mystery, and it was tentatively named as PDK2 (Alessi et al., 1997; Balendran et al., 1999).

Mass spectrometric and biochemical analyses of mTOR-immunoprecipitates as well as a search for proteins homologous to the budding yeast TORC2 subunits identified the mammalian TORC2 (mTORC2) components, which are well conserved among species (Frias et al., 2006; Jacinto et al., 2006; 2004; Loewith et al., 2002; Pearce et al., 2007; Sarbassov et al., 2004; Yang et al., 2006). These studies revealed that mTORC2 is a multi-subunit kinase complex composed of SIN1 (stress activated MAP kinase interacting protein)(Wilkinson et al., 1999), Rictor (rapamycin-insensitive companion of mTOR)(Sarbassov et al., 2004) and mLST8 together with mTOR as a core kinase (Figure 3). In addition, Protor1/2 (Protein observed with RICTOR) is incorporated into mTORC2 through the association with Rictor (Pearce et al., 2007). mLST8 is common to both mTORC1 and mTORC2, but appears to affect only mTORC2 activity (Guertin et al., 2006; Wang et al., 2012). The organization of TORC2 is also conserved in fission yeast with Sin1, Ste20, Wat1 (mLST8 equivalent) and Bit61 (Figure 3) (Hayashi and Yanagida, 2011; Hayashi et al., 2007; Ikeda et al., 2008; Matsuo et al., 2007) as its regulatory subunits. Notably, a reverse genetics approach on Rictor revealed that mTORC2 specifically phosphorylates and activates Akt and PKC, but not the mTORC1 substrate S6K1, all of which are members of the AGC kinase family (Sarbassov et al., 2004; 2005). Later, another AGC-family kinase SGK1 was also demonstrated to be under the regulation of mTORC2 (García-Martínez and Alessi, 2008). Through these discoveries, mTORC2 was determined to be the long-sought PDK2 kinase (Sarbassov et al., 2005). Similar TORC2-dependent activation mechanisms have been found for the budding yeast

Ypk1/2 kinases and the fission yeast Gad8 kinase (Ikeda et al., 2008; Kamada et al., 2005; Matsuo et al., 2003; Roelants et al., 2004).

Figure 1.

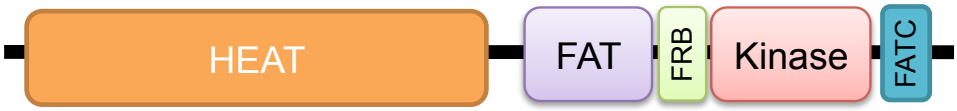


**Figure 1. Schematic representation of the domain architecture of TOR**

Figure 2.

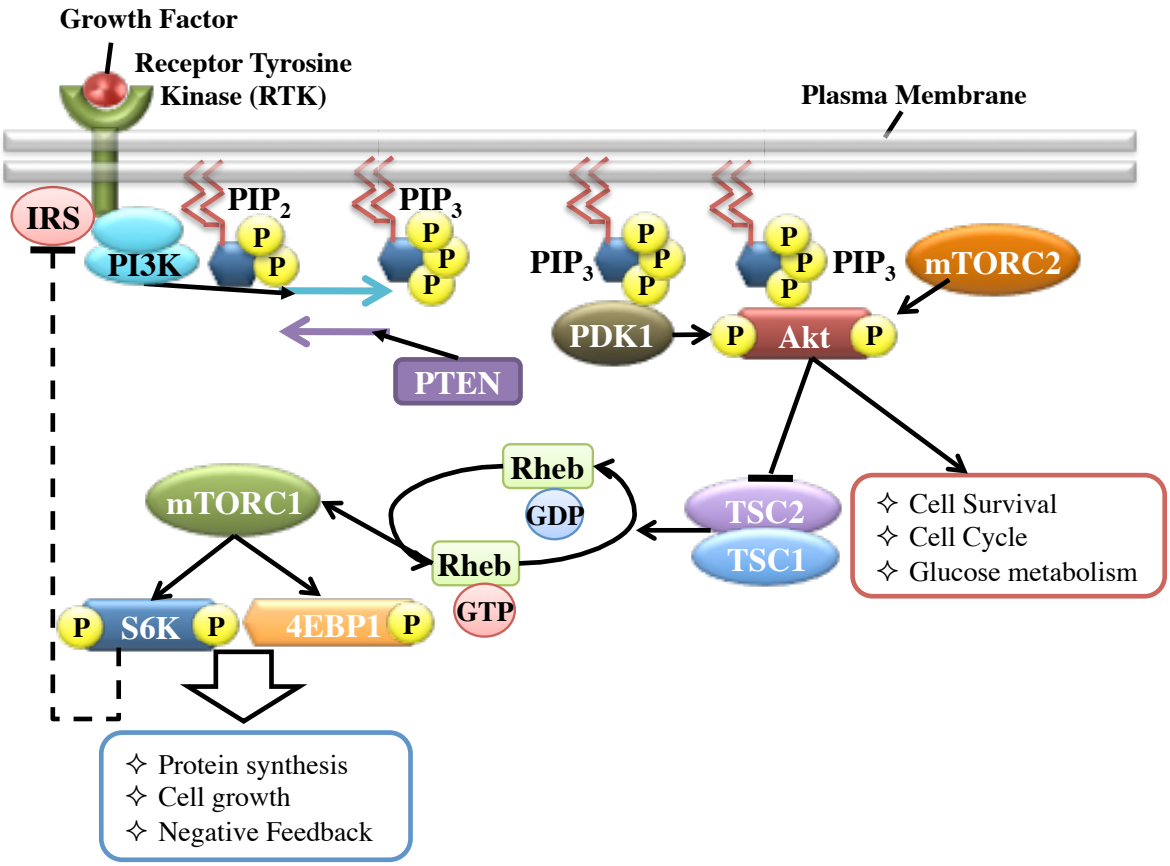


**Figure 2. The PI3K pathway and TORC2-Akt signaling**

Figure 3.

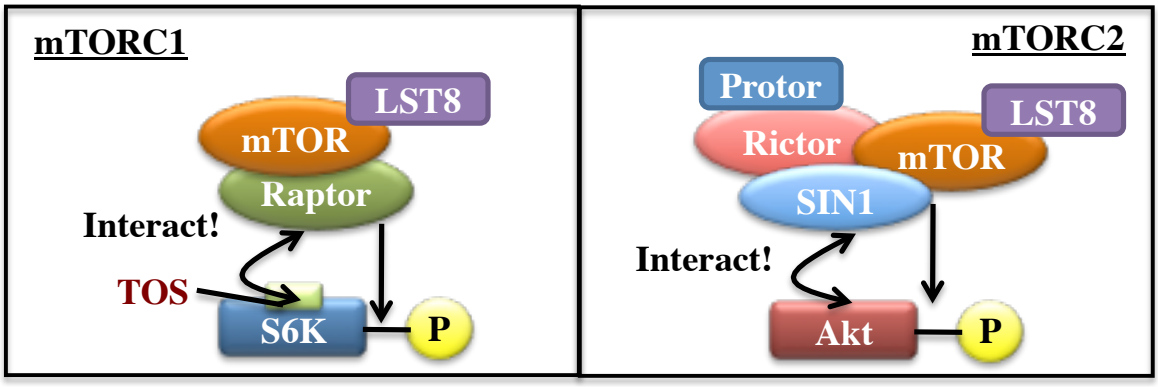


| H. sapiens | S. pombe | S. cerevisiae |
|---|---|---|
| mTOR | Tor1 | TOR2 |
| Rictor | Ste20 | AVO3 |
| SIN1 | Sin1 | AVO1 |
| mLST8 | Wat1 | LST8 |
| PROTOR | Bit61 | BIT61 |

**Figure 3. Subunits of TOR complex 2 are conserved between species**

## 1.2. The distinctive subunit compositions of TORC1 and TORC2 predict differential substrate specificities

In animals, the substrate specificity of the TOR complexes must be conferred by their specific regulatory subunits, because the protein product of a single TOR gene forms both mTORC1 and mTORC2. The mTORC2-substrates Akt, PKC and SGK as well as the mTORC1-substrate S6K are members of the AGC kinase family and their amino acid sequences are homologous to each other. A clue to understand how the two TOR complexes discern the structurally related substrates first came from the notion that Raptor in mTORC1 recognizes a short amino-acid sequence termed TOR signaling (TOS) motif in its substrates (Figure 4) (Ali and Sabatini, 2005; Nojima et al., 2003; Schalm et al., 2003). The two major mTORC1 substrates, S6K1 and 4EBP1, possess a TOS motif in their N-terminal region, and it has been shown that Raptor binds both S6K1 and 4EBP1 through their TOS motifs. However, no TOS-motif is readily identified in other mTORC1 substrates, such as ATG13 (Hosokawa et al., 2009), implying that additional mechanisms may be employed for mTORC1 to recognize other substrates. Because budding yeast and fission yeast have two TOR kinases, it remains possible that TOR kinases themselves have some ability to discern specific substrates. In budding yeast, a TOS like-motif is found in the N-terminus of Ypk2 kinase, which is regulated by TORC2, but not found in the TORC1 substrates, such as the Atg1-Atg13 kinase complex and Sch9 (the S6K1 ortholog) (Jacinto and Lorberg, 2008). In fission yeast, no TOS-like motif has been reported and therefore, TORC1 might interact with its substrates through another molecular mechanism (Kamada et al., 2010).

On the other hand, how TORC2 specifically recognizes its substrates remains elusive, but it would be most likely to be dependent upon its regulatory subunits. The mTORC2 subunit SIN1 is conserved from yeasts to human and has been shown to be an essential subunit of mTORC2, being required for Akt phosphorylation and regulation (Cloonan, 2006; Jacinto et al., 2006; Yang et al., 2006). Furthermore, it has been demonstrated that Akt is co-

precipitated with SIN1, but not with Rictor in an immunoprecipitation assay (Jacinto et al., 2006). The "conserved region in the middle" (CRIM) of SIN1 (Schroder et al., 2004) has also been shown to be required for substrate binding by mTORC2 (Cameron et al., 2011). However, the reverse genetics approach to analyze the TOR complexes inevitably encounters the problem that the gene deletion would cause the disruption of the complex integrity and/or the kinase activity of TOR itself. Therefore, it has been inconclusive which subunit of mTORC2 is truly responsible for the recruitment of its substrates. The recently published 3D structures of TORC1 and TORC2 suggest that the TOR complexes interact with the substrates at two site; the substrate recruiting subunits, Raptor in mTORC1 and most likely SIN1 in mTORC2, as well as the FRB domain of TOR kinase (Aylett et al., 2016; Gaubitz et al., 2015; Yang et al., 2013). The substrate binding subunit might as well regulate the substrate accessibility to the kinase active site of TOR, by modulating the positioning of the substrate binding subunit against the active site and the FRB domain. The FRB domain functions as the secondary substrate binding unit or the "gatekeeper" to navigate the phosphorylation site of the substrate into the active site (Aylett et al., 2016; Gaubitz et al., 2015). In budding yeast TORC2, the FRB domain is masked by the C-terminal region of Avo3 (Rictor), making TORC2 insensitive to the FKBP12-rapamycin complex that binds to the FRB domain (Gaubitz et al., 2015). These studies indicate that the spatial arrangement of the FRB domain with the substrate-binding subunit as well as other subunits such as LST8 may contribute to the substrate discrimination (Yang et al., 2013). Therefore, the substrate selectivity of the TOR complexes may not only be determined by their unique substrate-binding subunits, but also by the spatial organization of their subunits.

Identification of the substrate-binding site is important not only for understanding the molecular basis of the substrate specificity, but also for developing protein-protein interaction inhibitors (PPI inhibitors). PPI inhibitors can be superior to kinase inhibitors or allosteric

inhibitors in terms of selectivity and efficacy (Arkin, 2004; Betzi et al., 2009). Although mTOR kinase inhibitors with relatively high specificity have emerged (Benjamin et al., 2011; Janes et al., 2010), these ATP-competitive inhibitors in no way distinguish mTORC1 and mTORC2 because both complexes contain the same mTOR kinase. Allosteric inhibitors are also difficult to develop, because binding pockets to target allosteric inhibitors are usually difficult to predict within a protein structure using current knowledge and technology (Arkin, 2004). On the other hand, PPI inhibitors are expected to be very specific and many of them have been developed by *in-silico* design based on the crystal structures of target proteins. Because the mTORC2-Akt pathway is aberrantly activated in many cancer cells, drugs that specifically inhibit the mTORC2 pathway will be valuable for combating cancer. Furthermore, mTORC2-specific inhibitors are much awaited not just for the disease treatment but also as a molecular tool to dissect the mTORC2 signaling pathway.

**Figure 4.**

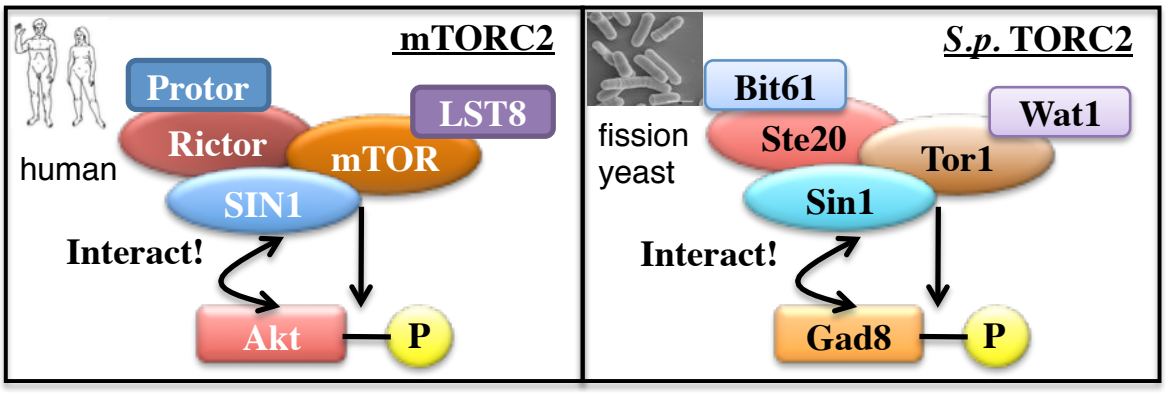


**Figure 4. TORC1 and TORC2 signaling complex in mammals**

**Copyright**: Human and fission yeast images are taken from Wikimedia Commons, a collection of freely usable media files. Licenses for free use of both images are confirmed. Human illustration is originally taken from NASA homepage. Microscopic view of a fission yeast culture is originally derived from The Cell Cycle. Principles of Control. David O Morgan.

### 1.3. The molecular mechanisms of Akt activation

In order to understand the role of mTORC2 in Akt activation, it is important to know the molecular mechanisms of Akt activation. There are three Akt isoforms, Akt1, Akt2 and Akt3, and they are activated by the same mechanism. mTORC2 phosphorylates Akt1 at two sites, Thr450 in turn motif (TM) and Ser473 in hydrophobic motif (HM) in its C-terminal loop. The TM site is phosphorylated during translation of the Akt polypeptide and the phosphorylation is required for the proper folding of Akt (Facchinetti et al., 2008; Ikenoue et al., 2008). Upon binding to $PIP_3$ in the plasma membrane, Akt1 is phosphorylated by PDK1 at Thr308 in the activation loop. For full activation, Akt1 needs to be phosphorylated at Ser473 residue in the C-terminal hydrophobic motif by mTORC2, and the HM site phosphorylation increases Akt1 activity about ten-fold. Indeed, Akt1 mutated at the HM site (S473A) showed markedly reduced activity in phosphorylating downstream substrates (Chen and Sarbassov, 2011; Frias et al., 2006; Jacinto et al., 2006; Sarbassov et al., 2004; Yang et al., 2006). To summarize, Akt takes 3 steps to be fully activated, which is explained below with Akt1 as an example (Figure 5).

(1) Localization to the plasma membrane through the interaction with $PIP_3$; the PH domain detaches from the C-terminal lobe of the kinase domain

(2) Co-localization with PDK1 which phosphorylates Akt1 at Thr308 in the activation loop

(3) mTORC2 phosphorylates Akt1 at Ser473 in the C-terminal HM site, and αC-helix of the N-lobe in the Akt1 kinase domain becomes structured. The phosphorylated HM site is then placed in the hydrophobic groove formed between αB- and αC-helices of the N-lobe.

As shown in Figure 5, the αC-helix in the N-lobe is disordered when Akt is in the inactive form (Yang et al., 2002b). It was suggested that the phosphorylated HM site of Akt interacts

with the αC-helix, inducing its rearrangement into a properly structured α-helix. In this state, the C-terminal loop with the phosphorylated HM site is tethered to the hydrophobic groove formed between αB- and αC-helices of the N-lobe. Other AGC family kinases such as PKC and SGK1 are also reported to be phosphorylated at their hydrophobic motifs in an mTORC2-dependent manner (Hauge et al., 2007; Ikenoue et al., 2008; Lu et al., 2010). Although SGK1 and PKC do not possess PH domain and the phosphorylation of SGK1 and PKC is thought to occur mostly in cytosol, these AGC family kinases are shown to go through conformational changes similar to those described above for Akt upon phosphorylation and activation by mTORC2 (Kannan et al., 2007).

**Figure 5.**

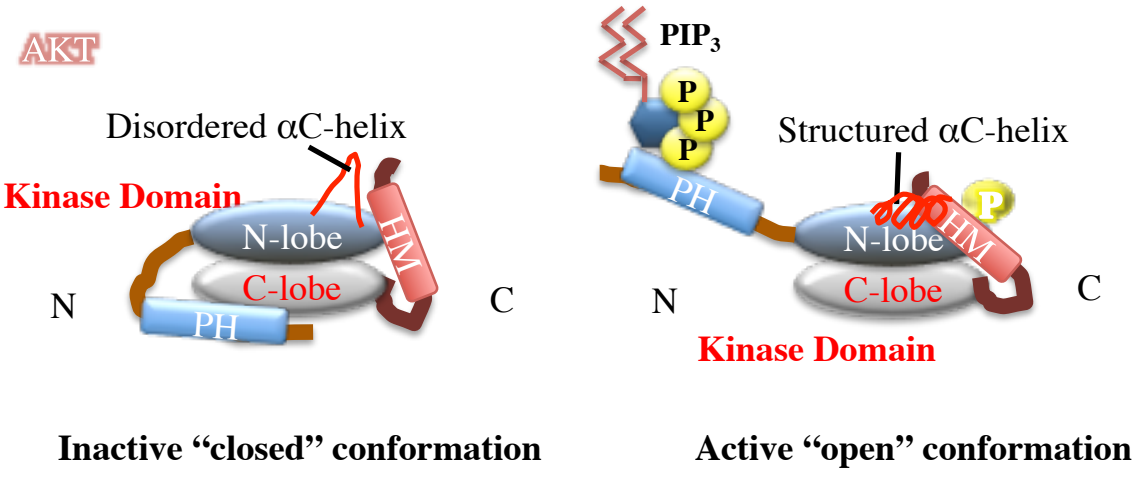


**Figure 5. AKT conformation in inactivate and active states**

## 1.4. The molecular function of the TORC2-specific subunit Sin1

Sin1 is first identified as a protein that physically interacts with the fission yeast Spc1 MAPK through a yeast two-hybrid screen (Wilkinson et al., 1999). The phenotypes of the *sin1* mutant were described to overlap with those of the *Δspc1* strain, including stress sensitivity and mating deficiency. It was also shown that, although Sin1 is not required for the phosphorylation of Spc1, it is required for the stable expression of Atf1, a stress response transcription factor under the regulation of Spc1. Another key observation was that the transcription of the genes regulated by the Spc1-Atf1 pathway in response to stress was diminished in the *sin1* mutant strain. However, reexamination by completely deleting the *sin1* gene, as opposed to the partial deletion used by the earlier study, demonstrated that Atf1 is stably expressed and that the Spc1-regulated gene expression in response to stress is not altered even in the absence of Sin1 (Ikeda et al., 2008). Rather, it was made clear that as an essential subunit of TORC2, Sin1 functions independently of the Spc1 pathway, playing a major role in cellular stress resistance. Furthermore, the role of Sin1 as a subunit of TORC2 is well conserved among species, as has been demonstrated for its budding yeast ortholog, Avo1 and human SIN1 (Jacinto and Lorberg, 2008).

The multiple alignments of Sin1 amino acid sequences from various species revealed 5 domains with different degrees of conservation, which was tentatively named as Sin1 conserved domains (SCD) (Wang and Roberts, 2005). The most prominent Sin1 domain is the evolutionarily conserved CRIM domain or SCD III found in all the Sin1 orthologs (Schroder et al., 2007; 2004; 2005; Wang and Roberts, 2005). The identity of amino acid residues is as high as 25-30% within the CRIM domain between of *S. pombe* Sin1 and *H. sapiens* SIN1, implying that the CRIM region might play an important role.

Human Sin1 was once isolated as multi-copy suppressor of the constitutively active form of *RAS* in *S. cerevisiae* (Colicelli et al., 1991). Indeed, the C-terminal region of SIN1

(SCD IV) shows homology to the Ras-binding domain (Wang and Roberts, 2005). It was shown that hSIN1 physically interacts with human Ras *in vitro*, and that Sin1 and Ras are co-localized in the cell (Schroder et al., 2007). Significance of this interaction is not yet fully understood, but it was suggested that the Sin1-Ras interaction might prevent cells from undergoing apoptosis by mitigating the activity of the oncogene Ras. SIN1 also carries a PH domain towards its C-terminus (SCD V) and the PH-domain of SIN1 was indeed demonstrated to bind phosphorylated derivatives of phosphatidylinositol lipids including $PIP_3$ and to localize onto the plasma membrane (Pan and Matsuura, 2012; Schroder et al., 2007). Correspondingly, the membrane localization of the budding yeast TORC2 was shown to be mediated by the Sin1 homolog Avo1 (Berchtold and Walther, 2009). Within the N-terminal part of Sin1, there exist two major sequence clusters SCD I & II, which, however, have not been characterized in any organisms yet. Except for CRIM, the other four sequence clusters are very weakly conserved in the fission yeast Sin1. The role of Sin1 and its PH-domain in targeting TORC2 to the plasma membrane has been questioned in fission yeast, because the localization of TORC2 appears to be unaffected even in the absence of Sin1 (Tatebe et al., 2010). In addition, the functions of the SCDs have not been explored in fission yeast including the CRIM domain. Because Sin1 must be interacting with multiple subunits of TORC2 and with the TORC2 substrates, these domains are expected to play a role in protein-protein interactions. For example, human SIN1 has been shown to be essential for the stable formation of mTOR complex 2; in the absence of SIN1, the interaction between mTOR and Rictor is lost and no TORC2 is assembled (Chen and Sarbassov, 2011).

## 1.5. The signaling pathways upstream of TOR and the molecular mechanisms of TORC2 activation

In response to extracellular cues, the two TOR complexes regulate many critical cellular

processes through phosphorylation of distinct sets of substrates. Hence, the activation of TOR complexes must be subject to strict temporal and/or spatial regulations. The signaling events upstream of mTORC1 are relatively well defined. Tuberous sclerosis is a rare genetic disease attributed to the constitutive activation of TORC1 signaling due to inactivating mutations in the TSC1 or TSC2 genes (Figure 2) (Manning and Cantley, 2003). The TSC1 and TSC2 proteins form a complex that functions as a GTPase-activating protein (GAP) for the small GTPase Rheb (Ras homolog enriched in brain protein)(Garami et al., 2003; Inoki et al., 2003; Zhang et al., 2003). The GTP-bound form of Rheb interacts with TORC1, promoting the association of TORC1 with its substrate to activate TORC1 signaling (Sato et al., 2009; Urano et al., 2005). Inactivation of TSC1 or TCS2 leads to an increase in the GTP-bound form of Rheb, resulting in constitutive activation of the TORC1 pathway (Manning and Cantley, 2003). Although tuberous sclerosis is accompanied by benign tumors, these tumors rarely progress into a malignant state (Inoki et al., 2005a). HEK293T cells carrying mTOR mutations that selectively activate mTORC1 but not mTORC2 show no decrease in the cell size in response to nutrient starvation, indicating that the cell cycle progression is not advanced (Hardt et al., 2011). This phenotype can be explained by a low level of G2/M cyclin-CDK activity in the presence of constitutively active mTORC1, implying that the mTORC1 activity opposes to initiation of mitosis. These observations indicate that, although mTORC1 plays major roles in promoting cell growth, mTORC1 activation alone is not sufficient for malignant transformation, maybe because of the limited roles of mTORC1 in promoting cell cycle progression.

On the other hand, the activation mechanism of mTORC2 remains largely elusive. The following three possible mechanisms have been explored in the literature.

(1) the kinase activity is directly modulated by protein modification such as phosphorylation,

(2) the complex is co-localized with the substrate upon stimulation to a specific cellular compartment, or

(3) the regulatory subunits undergo a conformational change, promoting the complex stability or the complex-substrate interaction.

(1) Kinase assays using the immunoprecipitates of mTOR have been employed to evaluate the activity of mTOR kinase (Brunn et al., 1997). However, mammalian cells have only one mTOR kinase that forms mTORC1 and mTORC2 and therefore, the intrinsic activity of mTOR kinase in those distinct complexes cannot be measured by this approach. On the other hand, yeast cells have two TOR kinases, each of which is the main component of TORC1 or TORC2, allowing the evaluation of the activity of each complex by the kinase assay of the individual TOR isoforms (Ikeda et al., 2008; Petersen and Hagan, 2005). Yet, it should be noted that because the subunits of the TOR complex are also co-precipitated, the kinase assay dose not necessarily measure the intrinsic activity of TOR kinases, but rather reflects the activity of the complex.

(2) Activation of Akt is thought to occur at the plasma membrane where the other signaling components that activate Akt are localized, implying that mTORC2 might as well be recruited onto the plasma membrane to activate Akt. However, some of the regulators of Akt signaling such as PI3K, PTEN, PDK1 and Akt can be found on ER (Betz and Hall, 2013). The localization of PTEN and Akt to mitochondria was also observed (Betz and Hall, 2013). Indeed, studies implied that mTORC2 associates with both ER and mitochondria (Betz et al., 2013; Betz and Hall, 2013). To enable the simultaneous association with ER and mitochondria, the mitochondria-associated ER membrane (MAM) has been suggested to be the site of mTORC2 localization and the substrate activation (Betz et al., 2013; Betz and Hall, 2013; Poston et al., 2013). Moreover, ribosomes, which are implicated in mTORC2 activation (Oh et al., 2010; Zinzalla et al., 2011), can be recruited to ER and possibly to MAM (Betz and

Hall, 2013; Lakkaraju et al., 2012). In budding yeast, TORC2 is predominantly localized to the plasma membrane through the Avo1 subunit that contains the PH-domain in its C-terminal region (Berchtold and Walther, 2009). Human SIN1, which is an Avo1 ortholog, carries a PH-domain in the C-terminal region as well (Schroder et al., 2007). A recent report has demonstrated that SIN1 and hence mTORC2 can also be recruited onto the plasma membrane through this PH domain (Liu et al., 2015). These observations suggest that mTORC2 can be found at multiple major organelles in the cell, obscuring the site of TORC2 activation. It is a subject of ongoing research whether mTORC2 is activated in all the places where it is found, or whether mTORC2 activated at a particular location shuttles among other organelles.

(3) Several lines of evidence indicate that the stability and integrity of the mTOR complexes can be affected in response to signals. In human cells, using the catalytically inactive mutant of mTOR, Chen *et al*. has shown that SIN1 is phosphorylated in a mTOR-dependent manner and that phosphorylated SIN1 is more readily incorporated into the mTORC2 complex (Chen and Sarbassov, 2011). In response to nutrient starvation, the expression levels of PI3K-related kinases (PIKKs) including mTOR and the Tel2-Tti1-Tti2 (TTT) complex, which functions as a chaperone for all PIKKs, are diminished in a time-dependent manner (Fernández-Sáiz et al., 2013). Moreover, the structural integrity of the TTT complex and its interaction with mTORC1 are significantly disrupted as well (Kim et al., 2013). Structure studies of mTORC1 revealed that mTORC1 exists as a dimer in which two sets of each subunit participate (Aylett et al., 2016; Yip et al., 2010; Yuan and Guan, 2016). It was shown that the mTORC1 dimer was dissociated in one hour after nutrients deprivation and that the TTT complex preferentially affected mTORC1 but not mTORC2 under this experimental condition (Fernández-Sáiz et al., 2013; Kim et al., 2013). However, because S6K1 and Akt, for example, are dephosphorylated within five minutes after starvation, the stability of the TOR complexes is unlikely to be involved in the immediate response to signal

extinction. Rather, the dissociation of the complex and loss of the expressions may be important in averting aberrant signal inputs in the absence of nutrients, which might result in detrimental effects to the cell viability.

Another possible mechanism of substrate activation by mTORC2 is that the conformational change of mTORC2 induced by upstream signaling promotes interaction between mTORC2 and its substrates, as in the case of TORC1 activation by TSC1/TSC2/Rheb (Urano et al., 2005). Recent studies suggest that the positioning of the substrate-binding domain relative to the FRB domain determines the accessibility of the substrate to the catalytic site of mTOR kinase (Aylett et al., 2016; Gaubitz et al., 2015; 2016; Yuan and Guan, 2016), and this positioning might be modulated by upstream signaling molecules. Thus, identifying the substrate-recognition subunit of TORC2 and elucidating how this subunit is incorporated into the complex are important to understand the molecular mechanisms of the activation of TORC2 and its substrates.

### 1.6. Fission yeast TORC2-Gad8 axis

Because of its rod shape and genetic amenability, fission yeast has been employed to dissect the molecular link between the cell size and division cycle. Fission yeast has two distinct mTOR homologs and, for historical reasons, the kinase that forms TORC1 is termed Tor2 while the one that forms TORC2 is Tor1. In contrast to other model organisms, a *tor1* deletion mutant strain is viable, indicating that loss of TORC2 activity does not affect the cell viability in fission yeast (Ikeda et al., 2008; Kawai et al., 2001). In fission yeast, TORC2-defective strains such as *Δtor1* show elongated cell morphology with longer doubling time. Although TORC2 in other organisms is implicated in the polarized localization of actin (Jacinto et al., 2004; Kamada et al., 2005; Loewith et al., 2002; Schmidt et al., 1996; Wullschleger et al., 2006), it is not clear whether TORC2 has a similar role in fission yeast. Instead, it is well

established that TORC2 regulates the cellular responses to various environmental stresses in fission yeast (Hayashi and Yanagida, 2011; Ikeda et al., 2008; Matsuo et al., 2007; Otsubo and Yamamato, 2008). Temperature-sensitive mutations of *tor2 (tor2*$^{t.s.}$) induce the mating program by arresting the cell cycle in G1 phase at the restrictive temperature, mimicking the nitrogen starvation response (Alvarez and Moreno, 2006; Matsuo et al., 2007; Uritani et al., 2006). In contrast, the *Δtor1* strain fails to arrest in G1 upon nitrogen starvation and hence is unable to commit to mating and sporulation (Hayashi and Yanagida, 2011; Hayashi et al., 2007; Kawai et al., 2001; Weisman et al., 2007). Thus, Tor2 and Tor1 function in an opposite manner in regards with the induction of the mating program (Weisman et al., 2007), and the *Δtor1 tor2*$^{t.s.}$ double mutant strain show severer stress-sensitive phenotypes than those of the individual single mutants, implying that Tor1 and Tor2 regulate independent pathways (Uritani et al., 2006). Indeed, TORC1 has been shown to act on sexual development through the Mei2 pathway independent of TORC2 (Alvarez and Moreno, 2006; Matsuo et al., 2007).

The TORC2–Akt pathway is highly conserved in fission yeast, with the AGC-family Gad8 kinase as an Akt equivalent (Ikeda et al., 2008; Matsuo et al., 2003). Following the initial reports of the *tor1*$^{+}$ gene in fission yeast (Kawai et al., 2001; Weisman and Choder, 2001), the *tor1*$^{+}$ gene was also identified through a genetic screen for mutants that cannot arrest cell cycle progression in G1 under nitrogen starvation and are sterile (Matsuo et al., 2003). Gad8 was identified as a multi-copy suppressor of the *tor1* defective cells. The Gad8 deletion strain was highly sensitive to stresses to the same degree as the TORC2-defective cells. Gad8 was shown to be phosphorylated in a Tor1-dependent manner at two sites; Ser527 in the turn motif and Ser546 in the hydrophobic motif, analogous to the mTORC2-dependent phosphorylation of Akt. The phosphorylation in the turn motif facilitates the proper folding of newly synthesized Akt and is probably constitutive (Facchinetti et al., 2008; Ikenoue et al., 2008). This may also be the case for Gad8 in fission yeast and the alanine substitution of

Ser527 significantly reduces the activity of Gad8 (Jacinto and Lorberg, 2008; Matsuo et al., 2003). The phosphorylation at Ser546 in the hydrophobic motif is responding to signals (Cohen et al., 2014; Hatano et al., 2015) and the substitution of Ser546 with alanine reduces the Gad8 activity by one seventh of the wild-type (Matsuo et al., 2003). Thus, the contribution of the hydrophobic motif phosphorylation in Gad8 is very similar to that in human Akt, because the activity of Akt is reduced to one tenth in the absence of the Ser473 phosphorylation in the hydrophobic motif (Sarbassov et al., 2005). Gad8 is also phosphorylated at Ser387 in the activation loop (T-loop) by the fission yeast PDK1 counterpart Ksg1, which is essential for Gad8 activity (Matsuo et al., 2003). In mammals, PDK1 phosphorylates multiple AGC family kinases including S6K1, SGK and Akt in their T-loop. Interestingly, the phosphorylation of the hydrophobic motif is prerequisite for the T-loop phosphorylation for S6K1 and SGK, but not for Akt (Biondi et al., 2001). In fission yeast, the Gad8 phosphorylation at Ser546 in the hydrophobic motif is not essential for the phosphorylation at T-loop by Ksg1, but seems to promote the Ksg1 dependent T-loop phosphorylation (Matsuo et al., 2003).

The TORC2-dependent Gad8 phosphorylation and the stress sensitivity of TORC2-defective mutant strains were employed to characterize the TORC2 subunits. The deletion mutants of the *ste20*, *pop3* (*wat1)*, and *sin1* genes were all sensitive to environmental stresses such as high temperature, high osmotic stress, and high calcium concentration, reinforcing the notion that the activity of TORC2 is essential for cells to survive stress conditions (Ikeda et al., 2008; Matsuo et al., 2007). Furthermore, Ste20, Sin1 and Wat1 were shown to be essential for the Gad8 phosphorylation at Ser546 in the hydrophobic motif (Ikeda et al., 2008). These observations suggest that TORC2 and its signaling mechanisms are conserved among a wide variety of eukaryotes including fission yeast.

Kominami *et al*. (1998) reported isolation of the *sat* (*s*tarvation induced *a*rres*t*) mutants

that exhibit a remarkably overlapping phenotypic features with those of the TORC2-defective strains; increased stress sensitivity as well as sterility due to a failure in G1 arrest upon nitrogen starvation (Kominami et al., 1998; Tatebe et al., 2010). Indeed, in the three *sat* mutant strains (*sat1, sat4* and *sat7*), the Gad8 phosphorylation at Ser546 was markedly reduced indicating compromised TORC2 activity (Tatebe et al., 2010). In a parallel approach to identify the upstream regulators of TORC2, a *S. pombe* gene deletion library was first screened for those strains that are stress sensitive. The identified strains were subsequently tested for reduced Gad8 phosphorylation at Ser546 through immunoblotting with the antibodies raised against phosphorylated Ser546. This attempt successfully re-isolated *sat1* and *sat7*/*ryh1* mutants, but no other genes were found to affect TORC2 activity when deleted. Ryh1 is a Rab-family small GTPase and homologous to mammalian Rab6, while Sat1 and Sat4 form a guanine nucleotide exchange factor (GEF) complex that promotes GTP loading onto Rhy1, thereby activating the TORC2-Gad8 pathway. Indeed, it was shown that expression of the GTP-bound form of Ryh1 induces the phosphorylation of Gad8 at Ser546. As the possible molecular mechanisms of the TORC2 activation by Ryh1, the following three major points were then examined, which are corresponding to the discussion in section 5 about the molecular mechanisms of TORC2 activation.

1) In an *in vitro* kinase assay, the activity of Tor1 kinase purified from the yeast cells expressing the GTP-bound form of Ryh1 was found to be similar to that from the wild-type cells.
2) There was no apparent change in the localization of TORC2 in the *Δryh1* background compared to the wild-type background.
3) The complex assembly of TORC2 was not significantly affected even in the absence of Ryh1.

On the other hand, it was demonstrated that the GTP-bound form of Ryh1 promotes the Sin1-Gad8 interaction (Tatebe et al., 2010). However, the underlying molecular mechanism that enables GTP-bound Ryh1 to enhance the TORC2-Gad8 interaction remains elusive. It is possible that a conformational change of TORC2 is induced upon its activation, resulting in the improved complex integrity and stability, which are favorable for substrate binding as has been discussed above for mTORC2. Therefore, not only the way how the substrate-recruiting subunit is incorporated into TORC2, but also the conformational as well as the positional information of the substrate binding site would be crucial to elucidate the molecular mechanism of the substrate activation by TORC2.

In this study, I have successfully demonstrated that *S. pombe* Sin1 physically interacts with Gad8 and that the Sin1-Gad8 interaction through the conserved central domain of Sin1 (Gad8/Akt-associating domain; GAD) within the CRIM domain is essential for the substrate recognition by TORC2 (**Section 3.1**). Furthermore, based on the NMR solution structure of *S. pombe* Sin1 CRIM, detailed mutagenesis analysis was conducted. Next, the study to indentify Sin1 binding site within Gad8 was conducted (**Section 3.2**). Based on the available AKT crystal structures of the active and inactive form, the residue, which undergoes a major drop in the surface exposure ratio after activation, was indentified to form the pocket responsible for Sin1 docking. To further understand the substrate-recruiting function of Sin1, Tor1 associating domain (TAD) within Sin1 were also defined and characterized (**Section 3.3**). Remarkably, the substrate-binding GAD and the kinase binding TAD are located next to each other within the evolutionarily conserved Sin1 CRIM region, indicating that the Sin1CRIM functions to bring the substrate and the kinase in close proximity. Importantly, human Akt can complement the *Δgad8* phenotypes, implying that the molecular mechanisms of TORC2-Gad8 signaling are conserved between fission yeast and humans.

# 2. MATERIALS AND METHODS

## 2.1. Yeast Strains and General Techniques

*S. pombe* strains used in this study are listed in Table 1. Growth media and basic techniques for S. pombe have been described (Moreno and Klar, 1991; Laboratory, 1993). Stress sensitivity of *S. pombe* strains was assessed by streaking or spotting on YES agar plates at 37˚C and those containing 2M sorbitol, 1M KCl or 0.1M CaCl2. QuikChange kit (Stratagene) was used for site-directed mutagenesis with oligonucleotide pairs shown in Table 2. The megaprimer method was used to delete a target region of the Sin1 protein.

## 2.2. Budding Yeast Transformation

The budding yeast cells transformed with the bait plasmids were grown in SD (–Trp) minimum liquid medium until $OD_{600}$ reached 0.5-1.5. This pre-culture was then inoculated to a main culture at 0.1 $OD_{600}$/mL and continued to be cultured until the culture concentration reached 0.5 $OD_{600}$/mL. The cells were harvested by centrifugation and suspended in1xLiAc/TE200 $\mu$l. The cell suspensions were divided into two 100 $\mu$l aliquots (One for Screen and the other for control), which were incubated at 30ºC for 1 hr. The appropriate amounts of the DNA fragments (e.g. 20ng for an insert and 180ng for a linearized vector) were added to the cells with 100ug carrier DNA and incubated at 30ºC for 15 min. The cells were suspend with 700ul of 1xPEG/LiAc/TE and further incubated at 30ºC for 45 min. After heat shock at 42ºC for 15min, the cells were cooled down on ice for 1min. After centrifugation, the supernatants were removed and the cell pellets were suspended in SD (–Trp, –Leu), which were then spread on SD (–Trp, –Leu) minimal agar plates. After 2-3 days incubation at 30ºC and counting the number of colonies, the replica-plates on SD (–Trp, –Leu,

–His) minimal agar plates and those supplemented with 3-AT were made and further incubated at 30ºC for 1-2 days. As shown in Figure 6A, those that cannot grow without histidine supplement were isolated for re-examination and subsequent analysis.

### 2.3. Reverse Yeast Two-Hybrid Screening

David Richter from our lab did the reverse yeast two-hybrid screens in this study. In this screening methods, Sin1 variants that cannot interact with Gad8 was isolated through negative selection by histidine auxotrophy based on yeast two hybrid assay; while the cells expressing wild-type Sin1 can grown on the histidine minus plate because the interaction of Sin1 with Gad8 allow the cells produce an enzyme mediating histidine synthesis, those expressing the Sin1 variants cannot. Using primers having homologous regions on both sides for a destination vector, the SpSin1CRIM (247-400 a. a.) region was PCR-amplified with Ex-Taq polymerase (Takara Bio Inc.). The length of the sequence subjected to the mutagenesis was determined so that roughly 1 single amino acid change occurs per the sequence mutagenized. The resultant DNA fragments were introduced into the budding yeast HF7c strain carrying the bait plasmid pGBT9-*gad8*$^{+}$ with the prey plasmid, pGAD-GH which was linearized with BamHI and SalI to remove the insert. Through the GAP repair mechanism, the intrinsic homologous recombination process of budding yeast, the mutagenized SpSin1CRIM fragments are sub-cloned into the destination vector producing the plasmids expressing Sin1CRIM variants carrying an amino acid substitution. The Sin1 variants were then tested for loss of the interaction with Gad8 in yeast two-hybrid assay (Figure 6B). Practically, the yeast cells that cannot grow on the selective media without histidine or those supplemented with 3AT drug were identified and isolated through replica plating technique (Figure 6C). Isolated transformants were subjected to immunoblotting against GAL4 transcriptional activation domain-SpSin1CRIM fusion protein to eliminate all the nonsense mutations.

Inability to grown on the selective media was re-examined by streaking on fresh histidine minus agar plates as well as by transforming fresh cells with pGAD GH-mutant SpSin1CRIM plasmids. Hence, the yeast cells carry both the bait plasmids and the prey plasmids at this stage. In order to isolate pGAD GH-mutant Sin1 plasmids, the plasmids were recovered from the yeast cells and introduced into the MH4 *E. coli* strain defective in leucine synthesis. Because the prey plasmid pGAD GH carries the genes required for leucine synthesis, only the cells carrying pGAD GH plasmids can grow on the M9 minimum medium which does not contain leucine. The MH4 cells selected in M9 medium were next grown in TB (Terrific Broth) liquid medium at 37ºC overnight and the plasmids were purified and DNA-sequenced to identify mutations.

The same procedure was employed to isolate Gad8 variants with a single amino acid substitution. For the identification of Gad8 interacting domain, a series of truncated Sin1 was tested for its interaction with Gad8 in the yeast two-hybrid assay.

## 2.4. Homology Modeling

For the alignment between the Gad8 C2 domain (residues 44-228) and Synaptotagmin-2 (ESYT2_HUMAN: 4p42), Dr. Kawabata employed PSI-BLAST due to its lower sequence identity. For the active form of Akt2 (1o6k) which lacks some parts of the sequence information, to avoid sequence lagging around missing parts, the alignment between Gad8 (GAD8_SCHPO) and Akt2 (AKT2_HUMAN) was first generated, and subsequently aligned with the sequence of 1o6k by an in-house program developed by Dr. Kawabata. The resultant sequence alignments were subjected to homology modeling using Modeller 9.11.

For the inactive from of Gad8, the multiple alignment of Gad8 with homologous kinases in other species; Ypk1, Ypk2, Akt1, Akt2, Sgk1, and PKC, was first generated using the built-in program in UCSF Chimera. Using the inactive form of Akt2 (1mrv) as template,

the homology modeling was performed with modeler 9.11 to obtain a 3D structure of an inactive form of Gad8.

### 2.5. Immunoblotting

Bio-Rad mini-protean system is used for immunoblotting. SDS-PAGE gels were run for 57 min at 200V and transfer onto nitrocellulose membrane for 60min at 100V. The membrane was incubated with the appropriate antibodies.

### 2.6. GST-Sin1 recombinant protein purification

BL21 *E. coli* strain was transformed with the pGEX-KG expression plasmid carrying the recombinant Sin1. The culture of exponentially growing BL21 at 0.4-0.8$OD_{600}$/mL was transferred from 37˚C to 16˚C shaker and IPTG was added to the culture to induce the expression of the recombinant GST-Sin1 proteins. The culture was kept incubated for 24hr to 37hr until the cell concentration of the culture reaches 2-3 $OD_{600}$/mL. All procedures described below were performed on ice or at 4°C. The cells were collected in the centrifuge tubes of the appropriate size depending on the culture volume, and in case of 250mL centrifuge tubes, the centrifugation was done for 15min at 8000rpm. The cell pellets were re-suspended in the ice-cold TBS buffer. The cell suspensions were aliquoted into 30OD cells in a 1.5mL centrifuge tubes, which were then pelleted for the subsequent use and storage. The 30OD cell pellets were re-suspended in the ice-cold TBS (20mM Tris-HCl [pH7.5], 150mM NaCl) buffer and were subjected to the sonication [1set (1sec x 20times), x3]. After adding Triton X-100 at 1% final concentration, the lysate was subjected to centrifugation for 15min at 20,800 x g. The supernatant was incubated with glutathione sepharose beads for 1hr, followed by extensive wash with the ice-cold TBS-T (TBS [pH7.5] + 1% Triton X-100) buffer. For storage at -20˚C,

glycerol was added to the beads suspension to give 30% final concentration.

## 2.7. Protein-Protein Interaction Assays

Protein-protein interactions were tested by co-precipitation experiments followed by immunoblotting analysis. Luminescent Image Analyzer LAS-4000 (Fujifilm) was used for quantification. All procedures described below were performed on ice or at 4°C. Cell lysates were prepared in the "TORC2" lysis buffer composed of 20 mM HEPES-KOH [pH 7.5], 150 mM potassium glutamate or sodium glutamate, 0.25% Tween-20, 50 mM NaF, 10 mM sodium pyrophosphate, 10 mM p-nitrophenyl phosphate, 10 mM β-glycerophosphate and, the protease inhibitor mix (PMSF, aprotinin, leupeptin and the protease inhibitor cocktail for use in purification of Histidine-tagged proteins [Sigma P8849]), and followed by centrifugation for 15min at 20,800 x g. The supernatant for incubation were normalized to the total protein inputs, which were quantified by Bradford assay (Bio-Rad Protein assay, 500-0006). To detect the interaction of Sin1:myc and Gad8:FLAG, the supernatant was incubated for 2 hr with EZview; Red Anti-c-Myc affinity gel (Sigma), followed by extensive wash. In all the following assays, the elusions from the precipitates were performed with SDS sample buffer at 65˚C for 10-15min. After elution, the resultant samples were subjected to immunoblotting analysis with anti-c-Myc (Santa Cruz Biotechnology) and anti-FLAG epitope tag (Stratagene) antibodies. The mixture of 1: 10 [= "Femto" : "Pico" of SuperSignal West Chemiluminescent Substrate series (Thermo Scientific)] was used for the development of signals from HRP.

The associations between FLAG:Tor1 and each of Myc-tagged TORC2 subunits were tested as follows. The supernatant prepared in the same way as above was incubated for 2 hr with Anti-FLAG M2 affinity gel (Sigma) for FLAG-Tor1 immunoprecipitation, and with EZview; Red Anti-c-Myc affinity gel (Sigama) for the immunoprecipitation of Myc-tagged TORC2 subunits. After extensive wash and elution, the samples were analyzed by

immunoblotting with antibodies against c-Myc (Santa Cruz Biotechnology) and FLAG epitope tag (Stratagene).

For pulldown of GST-Sin1 (247-400 a. a.) with Gad8:FLAG, the GST-Sin1 (247-400 a.a.) was expressed from pREP1 plasmids. The supernatant prepared as descried above was incubated with glutathione-sepharose for 2hr, followed by extensive wash and elution. Immunoblotting analysis was performed with antibodies against the GST and the FLAG epitope-tag (Stratagene). For pulldown of the purified recombinant GST-Sin1 with FLAG:Tor1 and/or Gad8:FLAG, the GST-Sin1 bound glutathione-sepharose beads were washed with the lysis buffer 3 times, and then incubated with the supernatant prepared as descried above. After extensive wash and elution, the precipitates were subjected to CBB-staining analysis for GST-Sin1 detection and immunobloting analysis with anti-FLAG antibodies.

**Table 1. *S. pombe* strains used in this study**

| Strain ID | Genotype | Source Reference |
|---|---|---|
| CA101 | *h-* | Laboratory |
| CA4593 | *h- leu1-32 ura4-D18 tor1::ura4+* | [1] |
| CA4855 | *h- leu1-32 ura4-D18 tor1::ura4+ ste20:3FLAG(kanR)* | This study |
| CA5021 | *h- leu1-32 ste20::kanR* | [2] |
| CA5126 | *h- leu1-32 sin1::kanR* | [2] |
| CA5142 | *h- leu1-32 ura4-D18 gad8::ura4+* | [3] |
| CA5827 | *h- leu1-32 ura4-D18 tor1::ura4+ gad8::ura4+* | This study |
| CA6271 | *h- leu1-32 ste20:3FLAG(kanR)* | This study |
| CA6281 | *h- leu1-32 gad8:3FLAG(kanR)* | [4] |
| CA6323 | *h- leu1-32 tor1D2137A* | This study |
| CA6435 | *h- leu1-32 Ste20:myc(KanR)* | [4] |
| CA6530 | *h- leu1-32 FLAG:tor1+(hph)* | [4] |
| CA6855 | *h- leu1-32 FLAG:tor1+(hph) bit61:13myc(kanMX6)* | [5] |
| CA6859 | *h- leu1-32 bit61:13myc(kanMX6)* | [5] |
| CA6870 | *h- leu1-32 FLAG:tor1+(hph) sin1::kanR* | This study |
| CA6984 | *h- leu1-32 sin1:13myc(kanMX6)* | [4] |
| CA6993 | *h- leu1-32 sin1:13myc(kanMX6) gad8:3FLAG(kanR)* | [4] |
| CA7087 | *h- leu1-32 FLAG:tor1+(hph) ste20:myc(KanR)* | This study |
| CA7092 | *h- leu1-32 FLAG:tor1+(hph) sin1:13myc(kanMX6)* | This study |
| CA7098 | *h- leu1-32 FLAG:tor1+(hph) ste20::kanR* | This study |
| CA7124 | *h- leu1-32 FLAG:tor1+(hph) pop3::kanR* | This study |
| CA7143 | *h- leu1-32 FLAG:tor1+(hph) ste20:myc(KanR) sin1::kanR* | This study |
| CA7147 | *h- leu1-32 FLAG:tor1+(hph) sin1:13myc(kanMX6) gad8::ura4+* | This study |
| CA7150 | *h- leu1-32 FLAG:tor1+(hph) sin1:13myc(kanMX6) bit61::ura4+* | This study |
| CA7151 | *h- leu1-32 FLAG:tor1+(hph) ste20:myc(KanR) pop3::kanR* | This study |

**Table 1. *S. pombe* strains used in this study**

| Strain ID | Genotype | Source Reference |
|---|---|---|
| CA7155 | *h- leu1-32 FLAG:tor1+(hph) ste20:myc(KanR) bit61::ura4+* | This study |
| CA7172 | *h- leu1-32 FLAG:tor1+(hph) sin1::kanR bit61:13myc(kanMX6)* | This study |
| CA7183 | *h- leu1-32 wat1:13myc(KanMX6)* | This study |
| CA7189 | *h- leu1-32 ura4-D18 FLAG:tor1+(hph) ste20:myc(KanR) gad8::ura4+* | This study |
| CA7200 | *h- leu1-32 FLAG:tor1+(hph) sin1:13myc(kanMX6) pop3::kanR* | This study |
| CA7213 | *h- leu1-32 FLAG:tor1+(hph) wat1:13myc(KanMX6)* | This study |
| CA7217 | *h- leu1-32 FLAG:tor1+(hph) ste20::kanR bit61:13myc(kanMX6)* | This study |
| CA7222 | *h+ leu1-32 ura4-D18 his7-366 FLAG:tor1+(hph) ste20::kanR sin1:13myc* | This study |
| CA7286 | *h- leu1-32 FLAG:tor1+(hph) sin1::kanR wat1:13myc(KanMX6)* | This study |
| CA7307 | *h- leu1-32 ura4-D18 FLAG:tor1+(hph) bit61:13myc(kanMX6) gad8::ura4+* | This study |
| CA7317 | *h- leu1-32 ura4-D18 FLAG:tor1+(hph) wat1:13myc(KanMX6) bit61::ura4+* | This study |
| CA7318 | *h- leu1-32 ura4-D18 FLAG:tor1+(hph) wat1:13myc(KanMX6) gad8::ura4+* | This study |
| CA7319 | *h- leu1-32 FLAG:tor1+(hph) pop3::kanR bit61:13myc(kanMX6)* | This study |
| CA7329 | *h- leu1-32 ura4-D18 FLAG:tor1+(hph) ste20::kanR wat1:13myc(KanMX6)* | This study |
| CA7470 | *h- leu1-32 ste20::kanR sin1::kanR* | This study |
| CA7523 | *h- leu1-32 ste20:3FLAG(hph) pop3::kanR* | This study |

## Reference


[1] Ikeda, K., Morigasaki, S., Tatebe, H., Tamanoi, F., and Shiozaki, K. (2008). Fission yeast TOR complex 2 activates the AGC-family Gad8 kinase essential for stress resistance and cell cycle control. Cell Cycle 7, 358–364.

[2] Matsuo, T., Kubo, Y., Watanabe, Y., and Yamamoto, M. (2003). Schizosaccharomyces pombe AGC family kinase Gad8p forms a conserved signaling module with TOR and PDK1-like kinases. Embo J. 22, 3073–3083.

[3] Tatebe, H., and Shiozaki, K. (2010). Rab small GTPase emerges as a regulator of TOR complex 2. Small Gtpases 1, 180–182.

[4] Tatebe, H., Morigasaki, S., Murayama, S., Zeng, C.T., and Shiozaki, K. (2010). Rab-family GTPase regulates TOR complex 2 signaling in fission yeast. Curr Biol 20, 1975–1982.

[5] Uritani, M., Hidaka, H., Hotta, Y., Ueno, M., Ushimaru, T., and Toda, T. (2006). Fission yeast Tor2 links nitrogen signals to cell proliferation and acts downstream of the Rheb GTPase. Genes Cells 11, 1367–1379.

**Table 2. Primers used for site-directed mutagenesis**

| Allele | Sense and antisense oligonucleotide sequences | Restriction enzymes used to identify the mutation |
|---|---|---|
| | 5`– –3` | |
| ***sin1 A319D*** | AAGAATGTTTTGGTCTCTGAGGaTATCGGTTATATTTTACTTCAA<br>TTGAAGTAAAATATAACCGATAtCCTCAGAGACCAAAACATTCTT | EcoRV |
| ***sin1 L348S*** | CAAAATCCGAATTATTGGAATTcACGTATTGTTGAAGATGACGGG<br>CCCGTCATCTTCAACAATACGTgAATTCCAATAATTCGGATTTTG | EcoRI |
| ***sin1 Y327D*** | ATCGGTTATATTTTACTgCAggACGTTAACCAGCAACTCGTGCCC<br>GGGCACGAGTTGCTGGTTAACGTccTGcAGTAAAATATAACCGAT | PstI |
| ***sin1 L364S*** | GCTAGATGAAGATTTTCCCGCTTccGAtCGTGTAGGTCCATTATC<br>GATAATGGACCTACACGATCGGAAGCGGGAAAATCTTCATCTAGC | PvuI |
| ***sin1 Q330P*** | CTTCAATACGTTAACCcGCAgCTgGTGCCCCCAATAGAAG<br>CTTCTATTGGGGGCACCAGCTGCGGGTTAACGTATTGAAG | PvuII |
| ***sin1 L310H*** | GCCCTTATTTGTAGAgCaCCGAAAGAATGTTTTGGTCTCTGAGGC<br>GCCTCAGAGACCAAAACATTCTTTCGGTGCTCTACAAATAAGGGC | BsiHKAI |
| ***sin1 I294T*** | CAAATGCCCTCCGTTTAAACAcTTATTTTCCTTCGAGCGAAAGTC<br>GACTTTCGCTCGAAGGAAAATAAgTGTTTAAACGGAGGGCATTTG | TstI |
| ***sin1 F296S*** | GCCCTCCGTTTAAACATcTATagTCCTTCGAGCGAAAGTCCTTC<br>GAAGGACTTTCGCTCGAAGGActATAgATGTTTAAACGGAGGGC | SfcI |
| ***sin1 L310P*** | CAAAGCCCTTATTTGTAGAgCcCCGAAAGAATGTTTTGGTCTCTG<br>CAGAGACCAAAACATTCTTTCGGgGcTCTACAAATAAGGGCTTTG | BanII |
| ***sin1 G355E*** | CGTATTGTTGAAGAcGACGaGGAGCTAGATGAAGATTTTCCCGC<br>GCGGGAAAATCTTCATCTAGCTCCtCGTCgTCTTCAACAATACG | BseRI |
| ***sin1 G368D*** | CCCGCTTTGGACCGTGTgGaTCCATTATCAAAATTTGGTTTTGAC<br>GTCAAAACCAAATTTTGATAATGGAtCcACACGGTCCAAAGCGGG | BamHI |
| ***sin1 S371P*** | GGACCGTGTAGGTCCATTAcCAAAATTTGGTTTTGACGCATTTGC<br>GGACCGTGTAGGTCCATTAcCAAAATTTGGTTTTGACGCATTTGC | PflMI |
| ***sin1 F378S*** | CAAAATTTGGTTTTGACGCgTcTGCTTTAGTTAAAGCCACTCCTG<br>CAGGAGTGGCTTTAACTAAAGCAgAcGCGTCAAAACCAAATTTTG | MluI |
| ***gad8 D153A*** | GGGATTATCAGGCAACTTTTGcCGTTTCCCGTTATTCCAAACTC<br>GAGTTTGGAATAACGGGAAACGgCAAAAGTTGCCTGATAATCCC | BstAPI |

Figure 6.

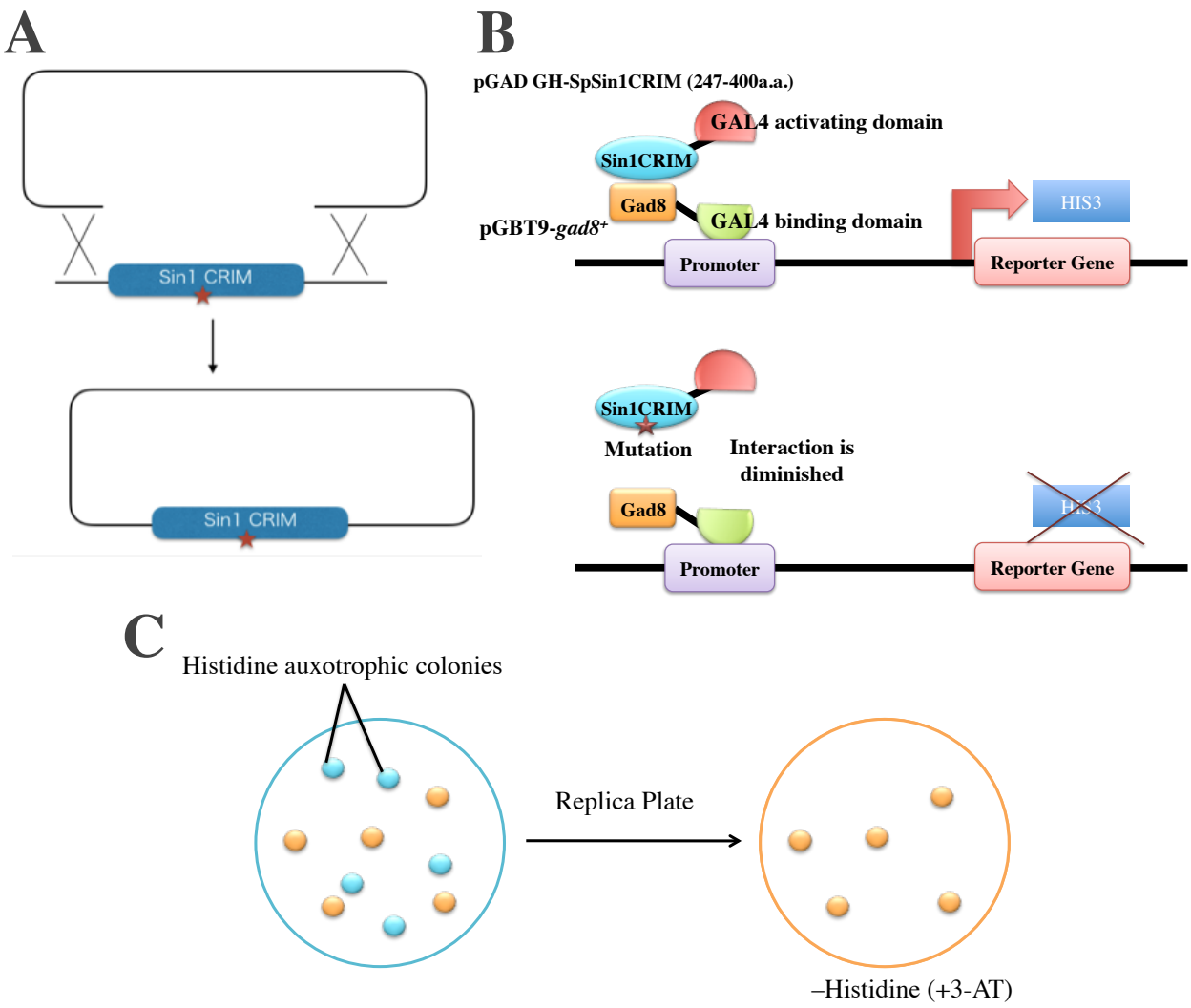


**Figure 6. The procedure of reverse yeast two-hybrid assays.**

(A) **Vector construction:** By employing the intrinsic homologous recombination mechanism of the budding yeast so called GAP repair, the pGAD GH prey plasmid was constructed having Sin1CRIM generated by random mutagenesis. Sin1CRIM fragments with 60-100bp homologous region on both side were PCR-amplified and introduced into budding yeast cells with the vector fragment linearized with restriction enzymes.

(B) **The molecular mechanism of reverse yeast two-hybrid system:** The Sin1CRIM-Gad8 interaction brings the GAL4 activating domain portion to come closer to a promoter, allowing expression of a reporter gene. Because mutations on Sin1CRIM diminish the interaction between Sin1CRIM and Gad8, GAL4 activating domain can no longer act on the promoter shutting off the expression of the reporter gene.

(C) **Replica plating:** The budding yeast HF7c cells carrying the pGBT-*gad8*+ bait plasmid were transformed with Sin1CRIM amplified with mutational PCR and the linearized pGAD GH prey plasmid for GAP repair as in (A), which were then spread on plates to obtain colonies. The resultant colonies were replica-plated onto a selective medium without histidine. Those colonies that were not able to grow on the histidine minus plate (represented by emerald-green in color) were picked up for re-examination and subsequent analysis.

# 3. RESULTS

## 3.1. Identification and characterization of the TORC2 substrate binding site on Sin1

### 3.1.1. The fission yeast TORC2-Gad8 pathway as a model of the TORC2-Akt pathway

Both Akt in humans and Gad8 in fission yeast are members of the AGC protein kinase family and are under the regulation of TORC2. The non-catalytic N-terminal region of Akt and Gad8 consists of the PH domain and the C2 domain, respectively. Although both PH domain and C2 domain have a role in membrane targeting (Jacinto and Lorberg, 2008; Steinberg, 2008), these two domains are structurally distinct. On the other hand, the sequence alignment between Gad8 and Akt from their catalytic domains to the C-termini shows that these kinases are highly homologous (sequence identity = 45%, sequence similarity = 61.4%) and structurally related (Figure 7A). However, how much Akt and Gad8 are functionally related was not known. Considering the role of the TORC2 pathway in response to nutrient uptake in both organisms, the TORC2 pathway and the constituent proteins are likely to be highly conserved, as are the many signaling pathways essential for cell physiology and viability. In order to know if Akt can phenotypically complement the loss of Gad8 in fission yeast, Akt was expressed from a plasmid in *Δgad8* cells, and the growth rate of the strain was tested under conditions such as high osmolarity and high temperature. *Δgad8* strains transformed with either the empty vector or a plasmid that expresses Gad8 served as controls. As shown in Figure 7B, the cells expressing Akt could grow on the stress plates at the rate comparable to the cells expressing Gad8, while those carrying the empty vector failed to form colonies. The experiment indicates that the protein kinases downstream of TORC2 are not only structurally but also functionally conserved between human and fission yeast. Thus, it is expected that the

*S. pombe* TORC2-Gad8 pathway can serve as a useful experimental model to understand the molecular mechanisms that govern the TORC2-Akt pathway in humans.

**Figure 7.**

**A**

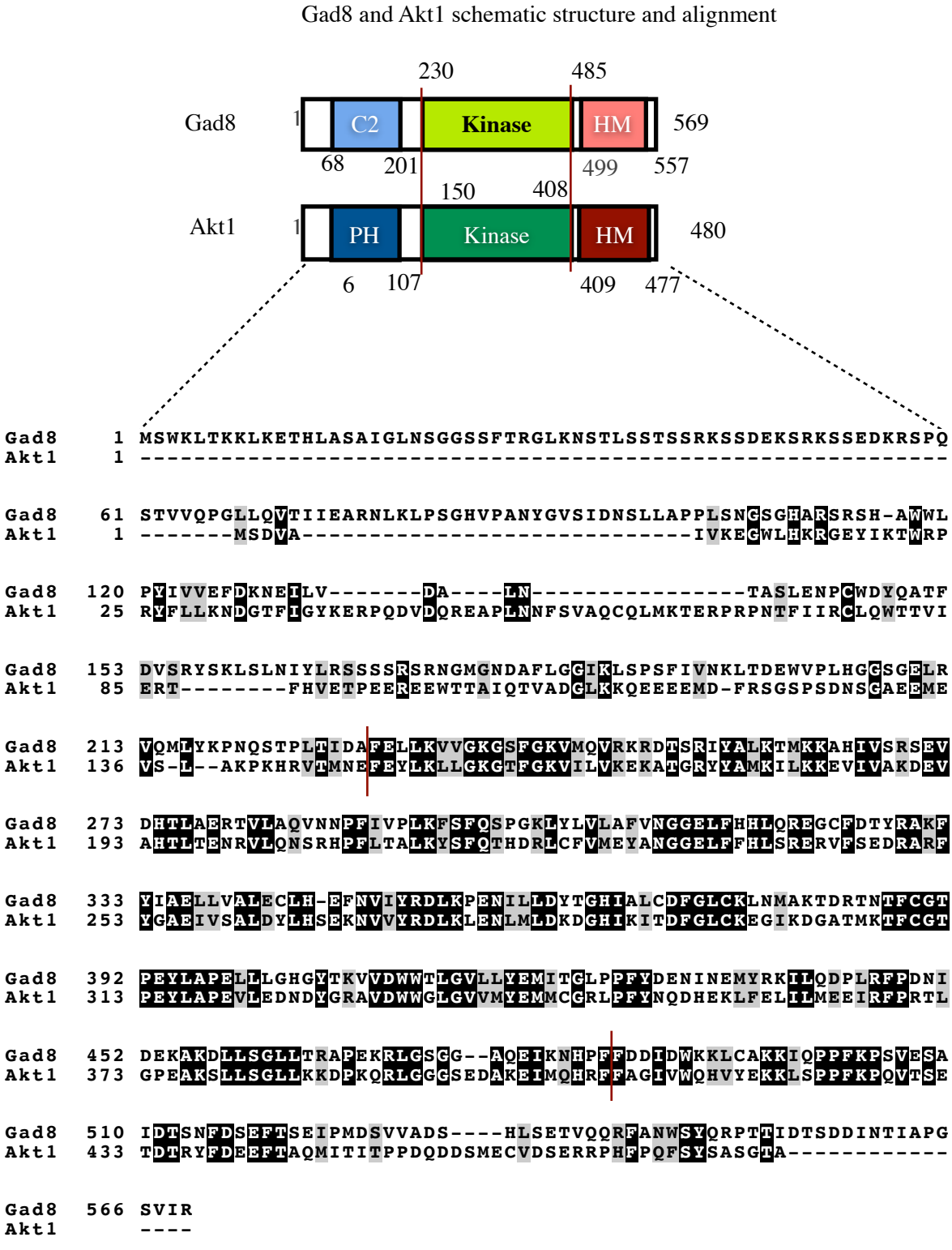
Gad8 and Akt1 schematic structure and alignment
230
485
Gad8
1
C2
Kinase
HM
569
68
201
499
557
150
408
Akt1
1
PH
Kinase
HM
480
6
107
409
477
Gad8 1 MSWKLTKKLKETHLASAIGLNSGGSSFTRGLKNSTLSSTSSRKSSDEKSRKSSEDKRSPQ
Akt1 1 ----------
Gad8 61 STVVQPGLLQVTIIEARNLKLPSGHVPANYGVSIDNSLLAPPLSNGSGHARSRSH-AWWL
Akt1 1 -------MSDVA----------IVKEGWLHKRGEYIKTWRP
Gad8 120 PYIVVEFDKNEILV-------DA----LN----------TASLENPCWDYQATF
Akt1 25 RYFLLKNDGTFIGYKERPQDVDQREAPLNNFSVAQCQLMKTERPRPNTFIIRCLQWTTVI
Gad8 153 DVSRYSKLSLNIYLRSSSSRSRNGMGNDAFLGGIKLSPSFIVNKLTDEWVPLHGGSGELR
Akt1 85 ERT--------FHVETPEEREEWTTAIQTVADGLKKQEEEEMD-FRSGSPSDNSGAEEME
Gad8 213 VQMLYKPNQSTPLTIDAFELLKVVGKGSFGKVMQVRKRDTSRIYALKTMKKAHIVSRSEV
Akt1 136 VS-L--AKPKHRVTMNEFEYLKLLGKGTFGKVILVKEKATGRYYAMKILKKEVIVAKDEV
Gad8 273 DHTLAERTVLAQVNNPFIVPLKFSFQSPGKLYLVLAFVNGGELFHHLQREGCFDTYRAKF
Akt1 193 AHTLTENRVLQNSRHPFLTALKYSFQTHDRLCFVMEYANGGELFFHLSRERVFSEDRARF
Gad8 333 YIAELLVALECLH-EFNVIYRDLKPENILLDYTGHIALCDFGLCKLNMAKTDRTNTFCGT
Akt1 253 YGAEIVSALDYLHSEKNVVYRDLKLENLMLDKDGHIKITDFGLCKEGIKDGATMKTFCGT
Gad8 392 PEYLAPELLLGHGYTKVVDWWTLGVLLYEMITGLPPFYDENINEMYRKILQDPLRFPDNI
Akt1 313 PEYLAPEVLEDNDYGRAVDWWGLGVVMYEMMCGRLPFYNQDHEKLFELILMEEIRFPRTL
Gad8 452 DEKAKDLLSGLLTRAPEKRLGSGG--AQEIKNHPFFDDIDWKKLCAKKIQPPFKPSVESA
Akt1 373 GPEAKSLLSGLLKKDPKQRLGGGSEDAKEIMQHRFFAGIVWQHVYEKKLSPPFKPQVTSE
Gad8 510 IDTSNFDSEFTSEIPMDSVVADS----HLSETVQQRFANWSYQRPTTIDTSDDINTIAPG
Akt1 433 TDTRYFDEEFTAQMITITPPDQDDSMECVDSERRPHFPQFSYSASGTA----------
Gad8 566 SVIR
Akt1 ----

**Figure 7.**

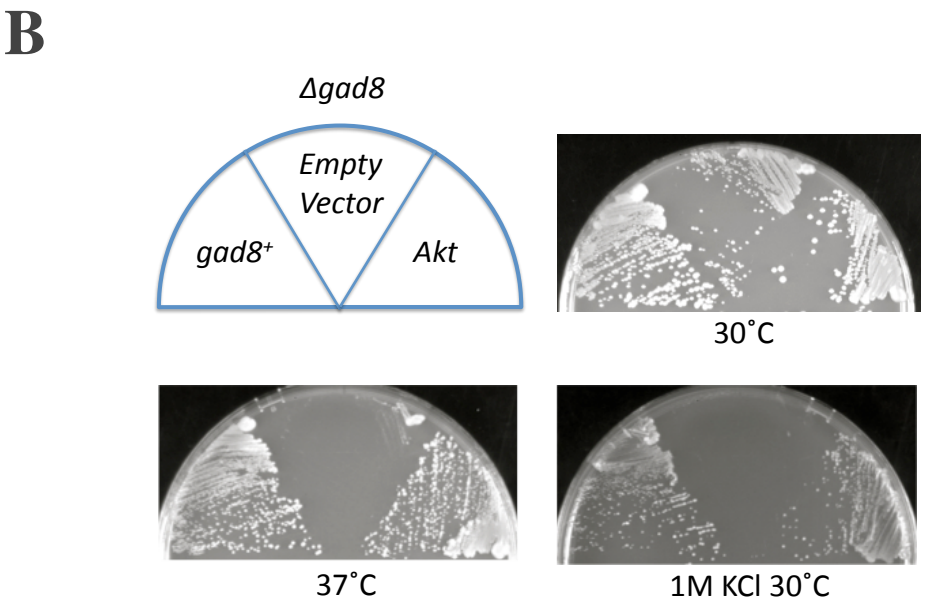


**Figure 7. Human Akt can replace fission yeast Gad8**

(A) Schematic diagram represents the architecture of Gad8 and human Akt1. The pairwise sequence alignment by Clustal W Omega shows conserved amino acid residues; Identical residues are shaded black and conserved residues are shaded grey at a 50% level of consensus. Sequence identity and sequence similarity of Gad8 and Akt1 from their catalytic domains to C-termini are 45% and 61.4%, respectively. Red lines are drawn as the boundaries of the non-catalytic N-terminal region and the kinase domain as well as the kinase domain and the C-terminal region. C2 = C2 domain, PH = Pleckstrin homology domain, Kinase = Kinase domain. (B) *Δgad8* strains expressing Gad8 or Human Akt1 were streaked onto EMM agar plates with thiamine and a YES agar plate with 1 M KCl, and incubated at the indicated temperatures. A *Δgad8* strain carrying the empty vector was included as a control.

### 3.1.2. Sin1 physically interacts with Gad8 to mediate TORC2 activity on Gad8

It has been demonstrated that the active, GTP-bound form of Ryh1 increases the TORC2-dependent phosphorylation of Gad8 at Ser546 in its C-terminal hydrophobic motif (Tatebe et al., 2010). However, the molecular mechanism with which Ryh1 mediates this event remained elusive. It was previously shown that small GTPase Rheb activates TORC1 signaling by enhancing the TORC1-S6K interaction in its GTP-bound form (Urano et al., 2005). In an analogous way, it can be assumed that TORC2-Gad8 docking would be a possible target of the Ryh1 action. In this regard, the identification of the TORC2 subunit responsible for substrate binding will give an valuable insight into the regulation of TORC2 by Ryh1. In order to identify the substrate binding subunit of TORC2, a yeast two-hybrid screen was carried out using Gad8 as bait. This attempt successfully isolated the Sin1 subunit of TORC2 as an interacting protein of Gad8 (Tatebe et al., 2017). To test if the interaction could be observed in fission yeast cells, I carried out a co-immunoprecipitation assay using a *gad8:FLAG sin1:myc* strain that expresses Gad8:FLAG and Sin1:myc proteins from their respective chromosomal loci along with a *gad8:FLAG* strain and a *sin1:myc* strain as negative controls (Figure 8A). The interaction between Sin1 and Gad8 was successfully detected in the *gad8:FLAG sin1:myc* strain, whereas no signals indicating the presence of Sin1 in the precipitates were detected from both of the control strains, confirming that Gad8 physically interacts with Sin1 in fission yeast.

Previous observations indicated that neither the activity of Tor1 kinase, the complex formation of TORC2, nor the localization of TORC2 was affected by expression of the GTP-bound form of Ryh1 (Tatebe et al., 2010). Therefore, it was hypothesized that the GTP-locked Ryh1 might promote the interaction between Sin1 and Gad8. Small GTPases can be genetically manipulated to be an active GTP-locked form or an inactive GDP-locked form through the substitution of a particular amino acid residue (Figure 8B). In the case of Ryh1,

the Ryh1Q70L variant exclusively binds GTP with inactivated GTP hydrolysis, while the Ryh1T25N variant exclusively binds GDP because of prevented GDP dissociation (He et al., 2006). It has been shown that while Ryh1QL positively regulates the phosphorylation of Gad8 at Ser546, Ryh1TN suppresses the Ser546 phosphorylation (Tatebe et al., 2010). To test if Ryh1 affects the Sin1-Gad8 interaction, Ryh1QL as well as Ryh1TN was expressed as glutathione *S*-transferase (GST) fusion proteins in a *gad8:FLAG sin1:myc* strain. In these settings, an immunoprecipitation assay with anti-FLAG beads was performed to assess the Sin1-Gad8 interaction. A significant increase in the amount of co-precipitated Sin1 was observed in the cells expressing Ryh1QL compared to the cells expressing GST alone or Ryh1TN, indicating that the Sin1-Gad8 interaction was augmented by Ryh1QL (Figure 8C). It should also be noted that, in the marked contrast to the GST alone control and the GDP-bound Ryh1TN, the smear-like ladder bands below the band of Sin1 in the lysate were not observed in the lane of the GTP-bound Ryh1QL. A smear-like ladder profile might represent a degraded form of Sin1, which is predicted to be not incorporated into TORC2. Therefore, the absence of the smear-like ladder indicates that the degraded form of Sin1 is present very little in the Ryh1QL expressing cells. Collectively, these observations suggest that Sin1 might serve as the substrate binding subunit of TORC2, and that the affinity of Sin1 to Gad8 can be modulated by changing the cellular level of the GTP-bound from of Ryh1.

In the course of the above experiments, I have noted that the extended induction of Ryh1QL expression resulted in suppression of cell growth. As shown in the growth curve, the growth of the cells expressing Ryh1*wt* or Ryh1QL began to slow down 18hrs after the thiamine withdrawal, which induces expression of the GST-Ryh1 genes from the *nmt1* promoter (Maundrell, 1990), while those expressing GST alone or Ryh1TN grew normally (Figure 8D). It is likely that Ryh1 engages the activation of TORC2 through augmentation of the Sin1-Gad8 interaction at around the time when the growth suppression occurs. Next,

Ryh1*wt* as well as Ryh1QL was expressed from plasmids under the control of the inducible *nmt1* promoter in a *sin1:myc gad8:FLAG* strain; expectedly the expression levels of Ryh1 were increased in a time dependent manner. The immunoprecipitation assay against Gad8:FLAG were carried out and the samples were collected at the indicated time points , which are analyzed for the presence of co-precipitated Sin1 to estimate the changing degree of the Sin1-Gad8 interaction. As shown in (Figure 8E), at early time point(s) such as 15 hrs (also 18 hrs in Ryh1*wt*) after induction of the gene expression, only a trace amount of co-precipitated Sin1 was observed in the immunoprecipitates by anti-FLAG beads. On the other hand, in the later time point such as 21 hrs (also 18 hrs in Ryh1QL) when the growth suppression became evident, the co-precipitation of Sin1 with Gad8 was observed in significant amounts. Ryh1QL was faster in promoting the Sin1-Gad8 interaction than Ryh1*wt,* demonstrating that the accumulated GTP-bound form of Ryh1 is responsible for the phenotype. It should be noted that the timing and the degree of the cell growth suppression were no different between the Ryh1*wt* and Ryh1QL expressing cells (Figure 8D), implying that Gad8 activity may reach the maximum level before the enhanced Sin1-Gad8 interaction becomes evident. Corresponding to the previous observation (Figure 8C), the GTP-bound form of Ryh1 seems to suppress the degradation of Sin1 during the immunoprecipitation assay (Figure 8E). Moreover, the disappearance of the degraded Sin1 was noticeably coincident with the appearance of the co-precipitated Sin1 with Ryh1*wt* and Ryh1QL (Figure 8E). There can be two possible explanations or both for the observed phenomena. One is that the GTP-bound form of Ryh1 might promote the eradication of unincorporated Sin1 by enhanced degradation. The other is that the GTP-bound form of Ryh1 might protect incorporated Sin1 from being degraded by inducing the conformational changes of TORC2, which leads to improved complex integrity. The results from the immunoprecipitation assays between Tor1 and the other subunit suggested that the absence of Ryh1 did not noticeably

affect the complex stability of TORC2 (Tatebe et al., 2010). Therefore, it is possible that the conformational changes of the complex are so minute that the complex formation of TORC2 may be affected, if any, at the level not readily detected in an immunoprecipitation assay.

**Figure 8.**

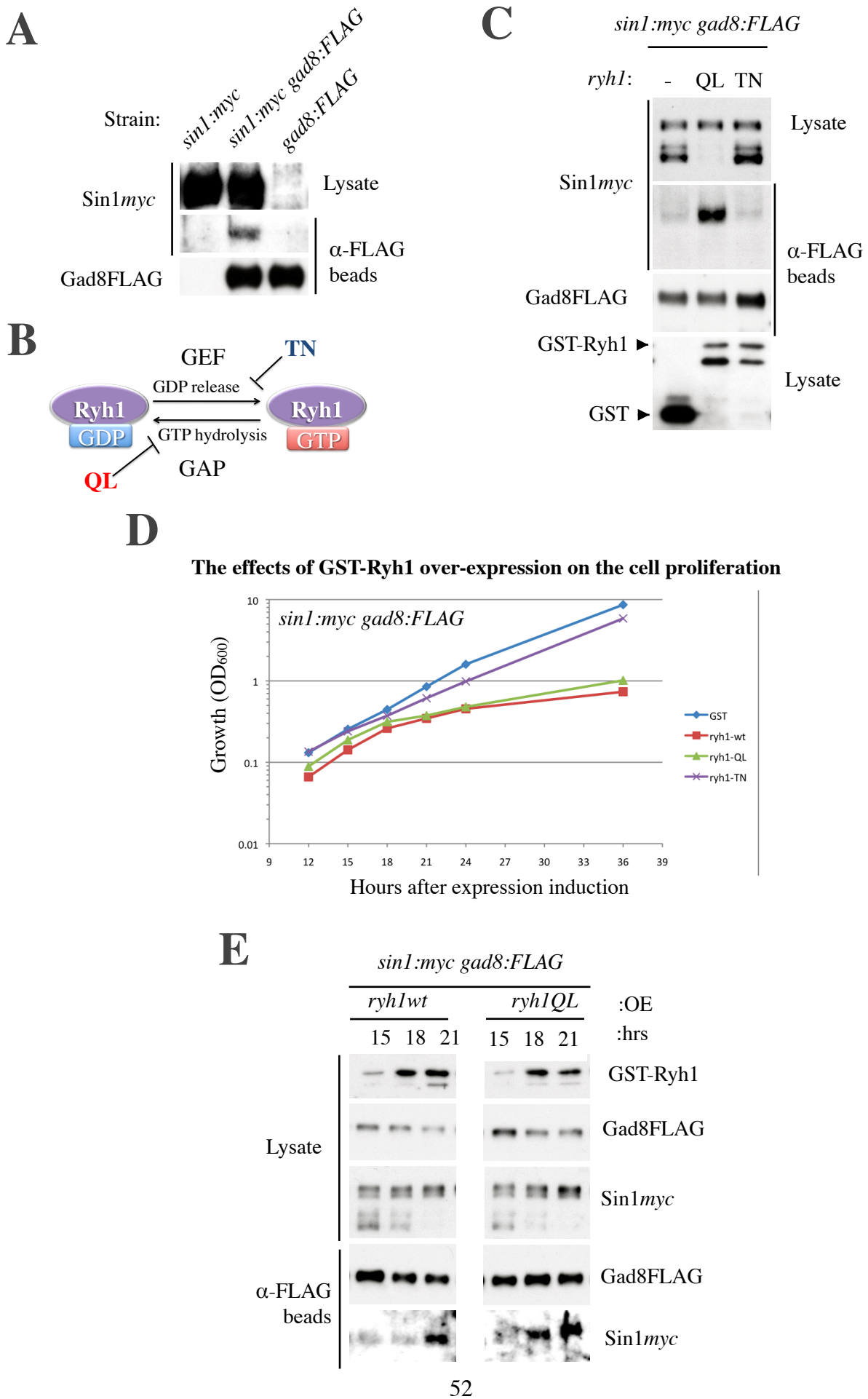
A
Strain:
sin1:myc
sin1:myc gad8:FLAG
gad8:FLAG
Sin1myc
Lysate
α-FLAG beads
Gad8FLAG
B
GEF
TN
GDP release
Ryh1
GDP
Ryh1
GTP
GTP hydrolysis
QL
GAP
C
sin1:myc gad8:FLAG
ryh1:
-
QL
TN
Lysate
Sin1myc
α-FLAG beads
Gad8FLAG
GST-Ryh1
Lysate
GST
D
The effects of GST-Ryh1 over-expression on the cell proliferation
sin1:myc gad8:FLAG
Growth (OD600)
10
1
0.1
0.01
9
12
15
18
21
24
27
30
33
36
39
Hours after expression induction
GST
ryh1-wt
ryh1-QL
ryh1-TN
E
sin1:myc gad8:FLAG
ryh1wt
ryh1QL
:OE
:hrs
15
18
21
15
18
21
GST-Ryh1
Lysate
Gad8FLAG
Sin1myc
α-FLAG beads
Gad8FLAG
Sin1myc

## Figure 8.

**Figure 8. Sin1 physically interacts with Gad8 to mediate the activity of TORC2 on Gad8.**
(A) The Sin1 subunit of TORC2 interacts with Gad8 in S. pombe cells. Cell lysates were prepared from sin1:myc gad8:FLAG, sin1:myc and gad8:FLAG stains. Gad8:FLAG was immunoprecipitated from the lysates with anti-FLAG affinity gel, and the precipitates were analyzed for co-precipitation of Sin1:myc by immunoblotting with anti-Myc antibodies.
(B) Small GTPases are regulated by guanidine exchanging factor (GEF) and GTPase-activating protein (GAP). GEF mediates the dissociation of GDP, thereby facilitating GTP loading which exists in 10 times excess of GDP in the cell. GAP mediates the hydrolysis of GTP to GDP. For the small GTPase Ryh1 of fission yeast, the TN mutation inhibits dissociation of GDP, while the QL mutation suppresses GTP hydrolysis.
(C) Expression of the GTP-locked form of Ryh1 promotes the interaction of Sin1 with Gad8. The gad8:FLAG sin1:myc strains carrying the expression plasmids of either GST alone (“–”), the GTP-locked form; GST-ryh1Q70L (“QL”), or the GDP-locked form; GST-ryh1T25N (“TN”) were grown in the absence of thiamine to induce the expression of each protein from nmt1 promoter. The cell lysates were subject to immunoprecipitation with anti-FLAG affinity gel, and co-precipitated Sin1:myc was detected with anti-myc antibodies.
(D) The effects of GST-Ryh1 over-expression on the cell proliferation. The sin1:myc gad8:FLAG cells were transformed with the expression vectors either of GST-Ryh1wt, GST-Ryh1QL, GST-Ryh1TN or GST alone as a negative control. The expressions of the plasmids under the control of nmt promoter were induced by culturing them in the absence of thiamine. The time points represent hours after the induction of the protein expression. Small fractions of the cell cultures were taken at the indicated time points during the time course (12-36hrs) and subject to the analysis of the cell density of the culture by measuring the optical density (OD) with UV spectrometer at 600nm to estimate the cell proliferation rate.
(E) GTP-locked form of Ryh1, but not the turnover of GTP/GDP may be important for the stabilization of the Sin1-Gad8 interaction. The expressions of GST-Ryh1wt as well as GST-Ryh1QL in the sin1:myc gad8:FLAG cells were induced as in (C). The samples taken at the indicated time points of 3hrs interval were subject to immunoprecipitation assay with anti-FLAG beads. The expressions of GST-Ryh1 were analyzed by immunobloting the cell lysates with anti-GST antibodies. The cell lysates were also subject to immunobloting analysis against Gad8:FLAG and Sin1myc. Co-precipitation of Sin1myc with Gad8FLAG was detected by probing the precipitated materials with anti-myc antibody and anti-FLAG antibody, respectively.

### 3.1.3. Sin1 interacts with Gad8 through a conserved central region (Gad8/Akt associating domain, GAD) within the CRIM domain

In order to identify the region of Sin1 that binds Gad8, a series of truncated Sin1 variants were tested for their ability to interact with Gad8 through yeast two-hybrid assays. This attempt successfully narrowed down the Gad8-interacting domain of Sin1 to 281-400 amino acid residues (Figure 9A, B), which are within the so-called CRIM (Conserved Region In the Middle) domain (Schroder et al., 2004). To confirm this result biochemically, plasmids were constructed to express the Sin1 fragment comprising residues 281-400 as well as two shorter fragments; one lacking N-terminal 20 residues and the other lacking C-terminal 20 residues. These fragments were expressed as GST-fusion proteins in a *gad8:FLAG* strain, and subsequently affinity-purified onto glutathione (GSH) beads to determine co-purification of Gad8 (Figure 9C). Gad8:FLAG was only detected in the purified fraction of the Sin1 281-400 fragment, but not in those of the other two shorter fragments, confirming that Gad8 interacts with the region of 281-400 residues in Sin1. Interestingly, yeast two-hybrid assays also showed that human SIN1 interacts with Akt through the corresponding region within the CRIM domain (Tatebe et al., 2017). According to these findings, the region comprised of residues 281-400 of *S. pombe* Sin1 is termed as Gad8/Akt associating domain (GAD) hereafter.

To further corroborate the above observations, a GST-fused Sin1GAD fragment or a GST alone as a control were expressed in a bacterial strain, and affinity-purified onto GSH beads. The GSH beads bound with GST-Sin1GAD or GST were then incubated with the *S. pombe* lysate derived from cells expressing Gad8:FLAG. After extensive wash, proteins bound to the GSH beads were probed with the antibodies against the FLAG-tag to detect Gad8:FLAG. The results showed that Gad8 was co-purified with GST-Sin1GAD but not with GST, providing supporting evidence for the physical interaction between Gad8 and Sin1 through Sin1GAD (Figure 9D).

I next investigated whether Gad8 binding to Sin1GAD is important for Gad8 phosphorylation by TORC2. A competition assay was employed to test whether over-expression of the Sin1GAD fragment interferes with the Sin1-Gad8 interaction and perturbs signaling from TORC2 to Gad8. In this experiment, either the Sin1GAD (281-400) fragment fused to GST or GST alone were over-expressed from plasmids using the inducible *nmt1* promoter. Two types of antibodies were used to monitor TORC2 signaling to Gad8; one recognizes the C-terminus of the Gad8 protein and the other recognizes the TORC2-dependent phosphorylation of Ser546 within the hydrophobic motif of Gad8 (Tatebe et al., 2010). Immunoblotting with these antibodies found that the Ser546 phosphorylation of Gad8 was significantly decreased when GST-Sin1GAD, but not GST alone, was over-expressed (Figure 9E). These results suggest that the interaction of Gad8 with Sin1 through Sin1GAD is indispensable for the phosphorylation of Gad8 by TORC2.

**Figure 9.**

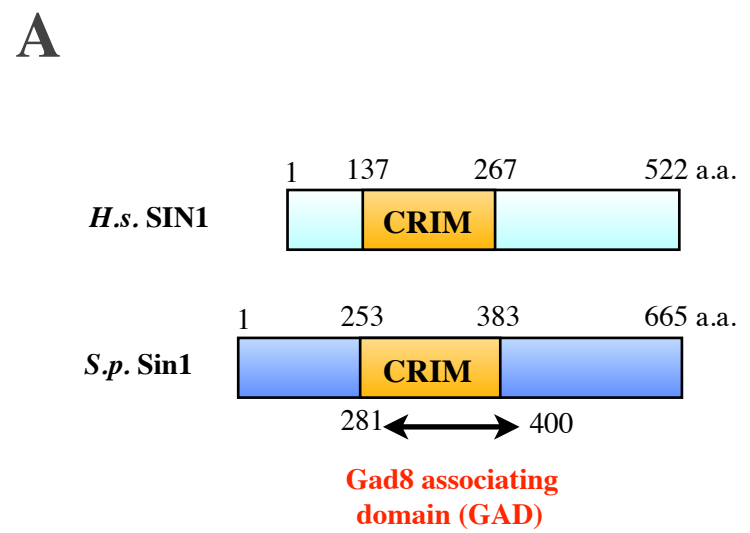
A
1
137
267
522 a.a.
H.s. SIN1
CRIM
1
253
383
665 a.a.
S.p. Sin1
CRIM
281
400
Gad8 associating domain (GAD)
B
Tor1
GAD
Sin1
Interact!
Gad8
P
C
GST-Sin1GAD:
281-400
301-400
247-380
GSH beads
GST-Sin1GAD
Gad8FLAG
Lysate

**Figure 9.**

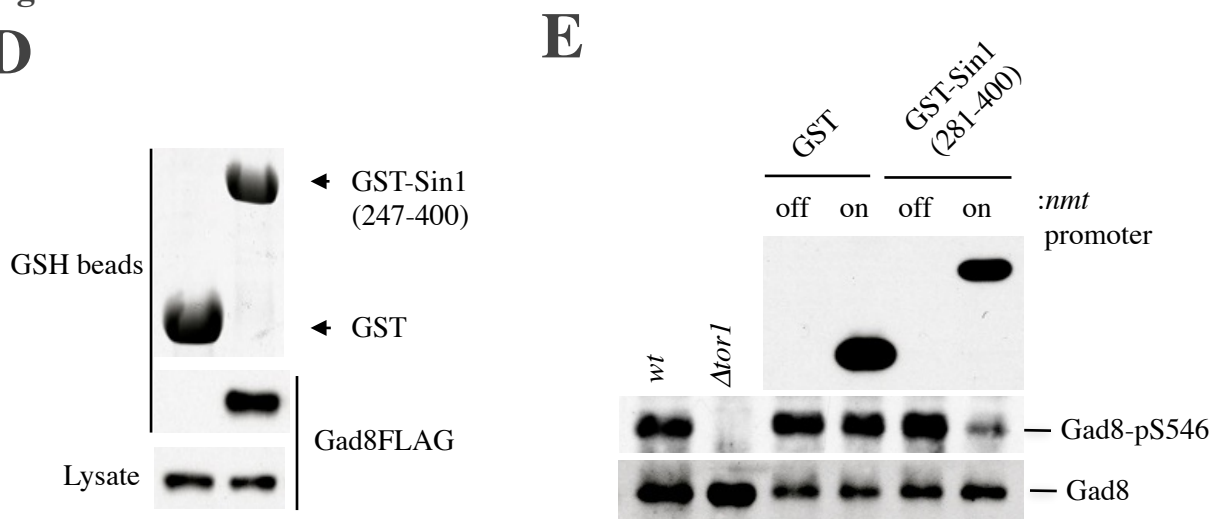


**Figure 9. Sin1 directly binds Gad8 through Gad8/Akt associating domain (GAD) that overlaps with the CRIM domain**

(A) Schematic representations of *Homo sapiens (H.s.)* and *Schizosaccharomyces pombe (S.p.)* Sin1 architectures. The Conserved Region in the Middle (CRIM) domain is defined as the region from 253 to 383 amino acid residues in *S. pombe* Sin1. The Gad8/Akt associating domain (GAD) was identified as the region from 281 to 400 amino acid residues which overlaps the most of the CRIM domain and further extended out towards the C-terminus of Sin1 (double-head arrow)

(B) A cartoon presents a view about how TORC2 interacts with Gad8 through the identified GAD region.

(C) Identification of the Gad8/Akt associating domain (GAD) of Sin1. The GST-Sin1 truncates of Sin1 central region with the indicated lengths were expressed from the *nmt* promoter. The cell lysates were incubated with glutathione (GSH)-Sepharose beads and the GST-Sin1 truncates were affinity purified onto the GSH beads. The co-purification of Gad8:FLAG were examined by immunoblotting with anti-FLAG antibodies.

(D) Physical interaction of Sin1GAD with Gad8. The expressions of GST-fused Sin1(247-400) along with GST alone control were induced in a *E. coli* strain, BL21 by growing the cells in IPTG (0.1mM) supplemented cultures at 16˚C for about 24hrs. GST and GST-Sin1 (247-400) were affinity purified onto GSH beads by incubating the beads with the bacterial cell lysates (GST-pulldown). The purified GSH beads were incubated with the lysates prepared from a Gad8:FLAG strain. The purified fractions were analyzed for the co-purification of Gad8:FLAG by immunobloting with anti-FLAG antibodies. GST and GST Sin1 (247-400) in the pulldown samples were visualized by Coomassie Brilliant Blue (CBB) staining.

(E) The overproduction of GST-Sin1GAD compromises Gad8 phosphorylation. The *S. pombe* cells carrying GST alone or GST-Sin1GAD expression plasmids under the control of the *nmt* promoter were grown either in the presence [off] or the absence [on] of thiamine. Crude cell lysates prepared with TCA extraction were analyzed by immunoblotting with antibodies against GST, phospho-Gad8 Ser546 and Gad8. The wild-type [*wt*] and tor1 knockout strain [*Δtor1*] served as a positive or negative control, respectively, for the phosphorylation of Gad8 at Ser546.

### 3.1.4. Sin1 is dispensable for the assembly of the other TORC2 subunits

In other organisms including humans, lack of the Sin1 subunit leads to disruption of TORC2 formation (Frias et al., 2006; Jacinto et al., 2006). It needs to be investigated if the fission yeast Sin1 might also be required for the integrity of TORC2. For this purpose, the strains that express FLAG:Tor1 from its chromosomal locus and one of the TORC2 subunits with Myc epitope-tag were constructed in wild-type as well as in the respective gene deletion backgrounds where each one of the TORC2 subunit genes was knocked out (Figure 10). These strains were subjected to immunoprecipitation assays using either anti-FLAG affinity gel to immunoprecipitate FLAG:Tor1 or anti-Myc affinity gel to immunoprecipitate each Myc-tagged TORC2 subunit. The immunoprecipitates with FLAG:Tor1 were probed by immunoblotting with anti-Myc antibodies to detect the co-precipitation of the subunit of interest, and the immunoprecipitates of each TORC2 subunit were subjected to immunoblotting to detect FLAG:Tor1. The association between Tor1 and Ste20 or between Tor1 and Wat1 (Pop3) were unaffected in all the deletion strains tested including the *Δsin1* strain (Figure 10A, B). The interaction between Tor1 and Bit61 was lost only in the absence of Ste20, consistent with the previous result indicating that Bit61 is specifically associated with Ste20 (Figure 10C) (Tatebe et al., 2010).

**Figure 10.**

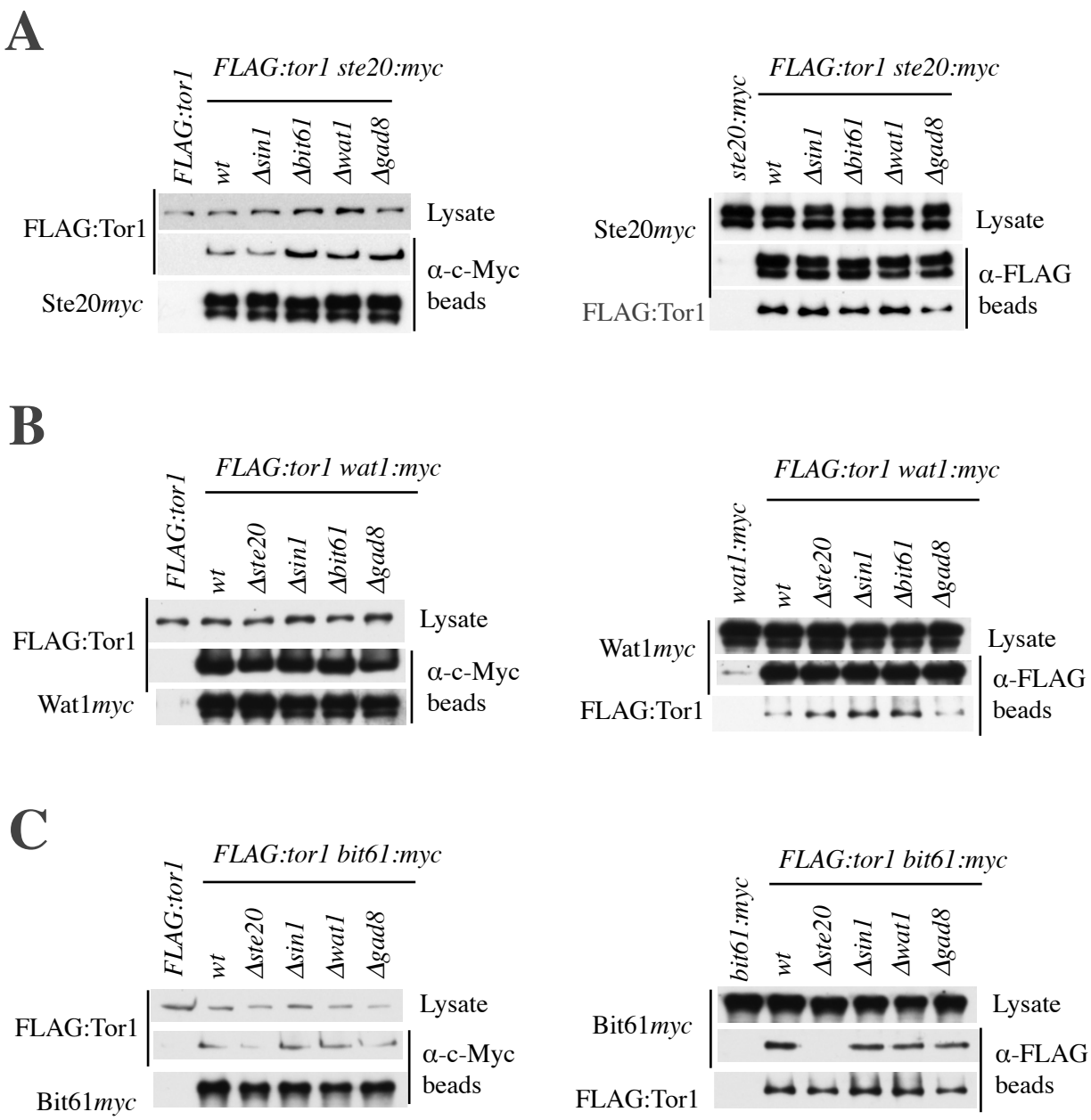


**Figure 10. The role of each subunit in maintaining the integrity of TOR Complex 2**

(A) Tor1-Ste20 interaction. Cell extracts prepared from *FLAG:tor1 ste20:myc* strains with the different genetic background of *wild-type (wt)*, *Δsin1*, *Δbit61*, *Δwat1* and *Δgad8* were incubated with anti-FLAG affinity gel (Left panel) or anti-c-Myc affinity gel (Right panel). The presence of the bait proteins in the pulldown samples were examined by immunobloting with antibodies against Ste20:myc (Left panel) or FLAG:Tor1 (Right panel). The precipitates were analyzed for co-precipitation of the prey proteins as well as the lysates for quantifying inputs, by immunobloting assay with antibodies against FLAG:Tor1 (Left panel) and Ste20:myc (Right panel)

(B) Tor1-Wat1 interaction. *FLAG:tor1 wat1:myc* strains with the different genetic background of *wt*, *Δste20*, *Δsin1*, *Δbit61*, and *Δgad8* were subject to immunoprecipitation assay as in (A).

(C) Tor1-Bit61 interaction. *FLAG:tor1 bit61:myc* strains with the different genetic background of *wt*, *Δste20*, *Δsin1*, *Δwat1*, and *Δgad8* were subject to immunoprecipitation assay as in (A).

### 3.1.5. Isolation of single amino acid substitutions within the Sin1GAD region that disrupt the interaction with Gad8

In order to further characterize the Gad8 interaction interface of Sin1GAD, it is attempted to isolate amino acid substitutions within Sin1GAD that disrupt the Sin1-Gad8 interaction. The GAD region was subjected to PCR-based random mutagenesis to produce the Sin1GAD fragments carrying amino acid substitutions. In a reverse yeast two-hybrid screen, the Sin1GAD variants that lost the interaction with Gad8 were selected, and the mutations were identified through DNA sequencing of the plasmids expressing theses variants. The successful interaction between prey and bait proteins will induce the *HIS3* reporter gene and thus, the production of histidine essential for yeast cell growth. The 3-amino-1,2,4-triazole (3AT) competitively inhibits the *HIS3*-gene product, disrupting histidine biosynthesis and therefore the addition of 3AT to the growth medium will allow to detect weak inhibition of yeast cell growth (Fields and Song, 1989). The mutations isolated without the 3AT supplementation can be considered to strongly inhibit *HIS3* expression and yeast cell growth, which are shown in red (Figure 11A). On the other hand, those substitutions that require the supplementation of 3AT to cause the complete inhibition of yeast cell growth can be classified into the weak inhibition group shown in blue. Some of these resultant amino acid substitutions were found on the residues conserved between fission yeast Sin1 and human SIN1. In order to test the interaction between the isolated Sin1GAD variants and Gad8 biochemically, the Sin1GAD variants with a single amino acid substitution were expressed as GST-fusion proteins in a *gad8:FLAG* strain. The cell lysate was incubated with GSH beads and after extensive wash, co-purification of Gad8 was analyzed. The amounts of Gad8 co-purified with any of the GST-Sin1GAD variants were significantly reduced compared to that with wild-type Sin1GAD (Figure 11B, C). These results demonstrate that the amino acid substitutions identified in this screen render the Sin1GAD unable to interact with Gad8.

The demonstration of binding between Gad8 and Sin1 alone is not sufficient to

exclude the possibility that the substrate might interact with the other parts of TORC2. If a single mutation in the entire TORC2 is sufficient to disrupt the TORC2-Gad8 interaction, and yet does not disrupt the TORC2 integrity, then the mutated residue is more likely to be directly responsible for Gad8 binding. In order to demonstrate that the Sin1 full-length variants are stably incorporated into TORC2, a *FLAG:tor1 Δ sin1* strain was transformed with plasmids expressing the Sin1 full-length variants isolated in the above screen along with a wild-type control. The Sin1 full-length variants were tested for their ability to interact with Tor1 in immunoprecipitation assays. The immunoprecipitates of FLAG:Tor1 with anti-FLAG beads were examined for the presence of the co-precipitated Sin1 full-length variants by immunobloting. Except for the partial reduction in the amount of co-precipitated Sin1 with the L348S substitution, the results showed that the rest of the Sin1 full-length variants were stably associated with the Tor1 kinase, comparable to wild-type Sin1 (Figure 11D). Thus, it is very likely that those Sin1 full-length variants were stably incorporated into TORC2. TORC2 that contains the Sin1 variant incapable of binding Gad8 is expected to be defective in phosphorylating Gad8, and would therefore not complement the stress sensitivity of TORC2 deficient cells. Investigation through immunobloting assays with anti-phopho-Ser546 and anti-Gad8 antibodies revealed that the Gad8 phosphorylation was abolished in *Δsin1* cells expressing the Sin1 full-length variants (Figure 11E). Furthermore, unlike the wild-type Sin1, the Sin1 variants could not rescue growth of *Δsin1* cells on agar plates with high osmostress or high calcium (Figure 11F). These experiments provide the evidence that the single amino acid substitutions in the Sin1 protein do not disrupt the integrity of TORC2 and are solely responsible for the compromised substrate recruitment.

The 3D structure information of the CRIM domain would provide deeper insights into the docking mode of the Sin1 protein. In collaboration with Dr. Chojiro Kojima, a NMR structure biologist, the solution structure of the *S. pombe* Sin1 CRIM was determined,

revealing a unique structure with a ubiquitin-like fold (Tatebe et al., 2017). In order to know if the amino acid residues identified in the above screen are actually exposed on the molecular surface for the direct physical interaction with Gad8, those residues are mapped on the NMR structure of Sin1 (Figure 11G). Although most of the residues whose substitution strongly inhibit the Sin1-Gad8 interaction are buried under the surface, many of the weak inhibitor mutations are found on the surface residues, implying that the strong inhibitor mutations disturb the folding of the Sin1 polypeptide. As shown in Figure 11G, residues F296, Y327, Q330, G355, G368 and S371 are almost wholly exposed, while residues L364 and F378 are half-buried on the molecular surface. Among them, only G355 is directly accessible to solvent (more than 25% surface accessible area). Because the residues other than G355 are not solvent accessible, it is less likely for them to be directly involved in the binding with Gad8. Yet, it remains possible that, after conformational changes upon the Sin1-Gad8 interaction, these residues are induced to form direct contact sites. Alternatively, they might support the nearby residues that act as the direct contact sites. For instance, residues I294 and F296 identified in the present screen flank Y295, which is solvent accessible and, in the later analysis, is shown to have a certain impact on the Sin1-Gad8 interaction. Collectively, these data as summarized in Table 3 reinforce the notion that the recruitment of Gad8 onto TORC2 through the Sin1GAD region is essential for the TORC2-dependent phosphorylation of Gad8.

**Figure 11.**

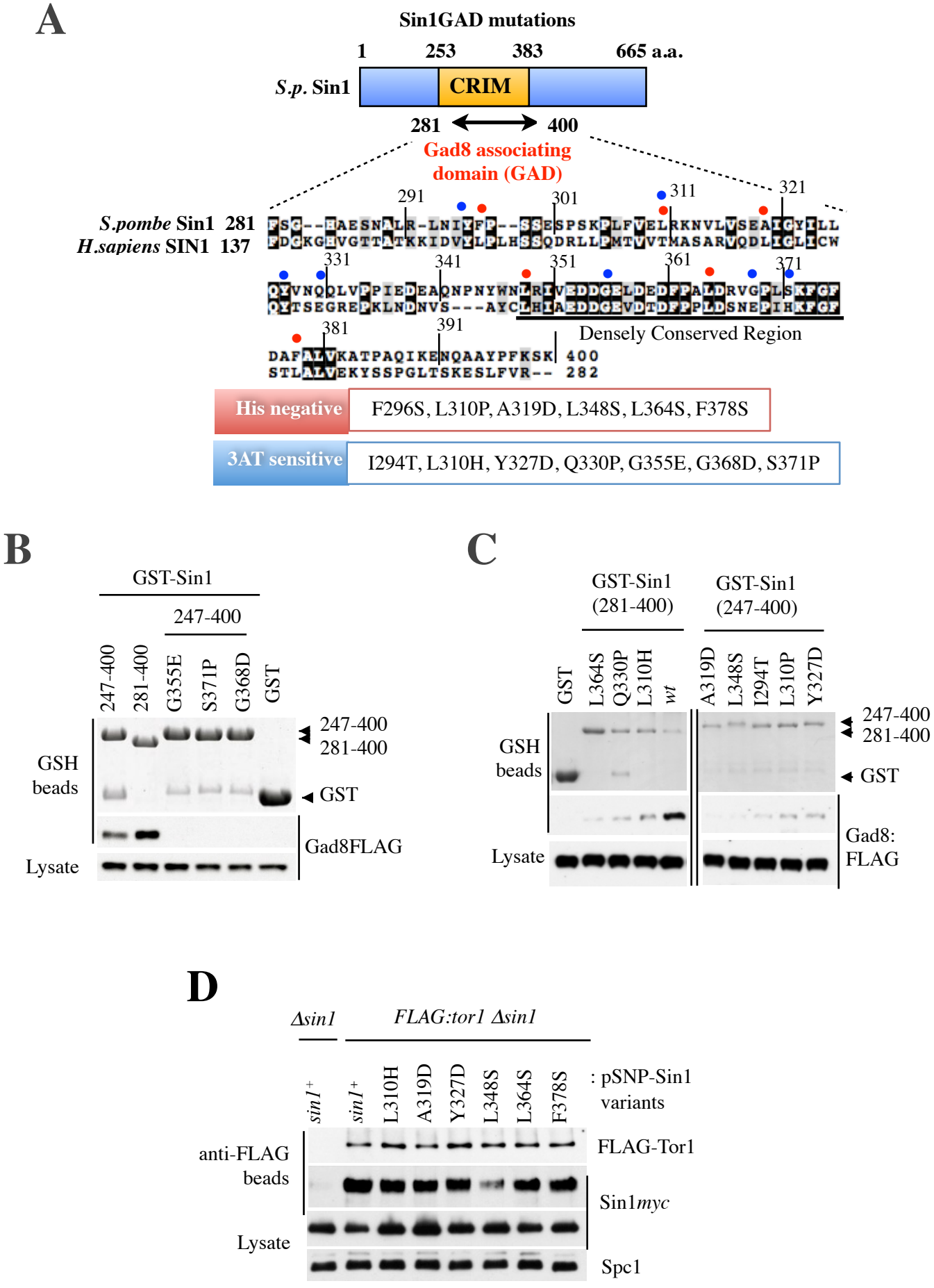
A
Sin1GAD mutations
1
253
383
665 a.a.
S.p. Sin1
CRIM
281
400
Gad8 associating domain (GAD)
S.pombe Sin1 281
H.sapiens SIN1 137
Densely Conserved Region
His negative
F296S, L310P, A319D, L348S, L364S, F378S
3AT sensitive
I294T, L310H, Y327D, Q330P, G355E, G368D, S371P
B
GST-Sin1
247-400
247-400
281-400
G355E
S371P
G368D
GST
GSH beads
Lysate
Gad8FLAG
C
GST-Sin1 (281-400)
GST-Sin1 (247-400)
GST
L364S
Q330P
L310H
wt
A319D
L348S
I294T
L310P
Y327D
GSH beads
Lysate
Gad8: FLAG
D
Δsin1
FLAG:tor1 Δsin1
sin1+
sin1+
L310H
A319D
Y327D
L348S
L364S
F378S
: pSNP-Sin1 variants
anti-FLAG beads
Lysate
FLAG-Tor1
Sin1myc
Spc1

**Figure 11.**

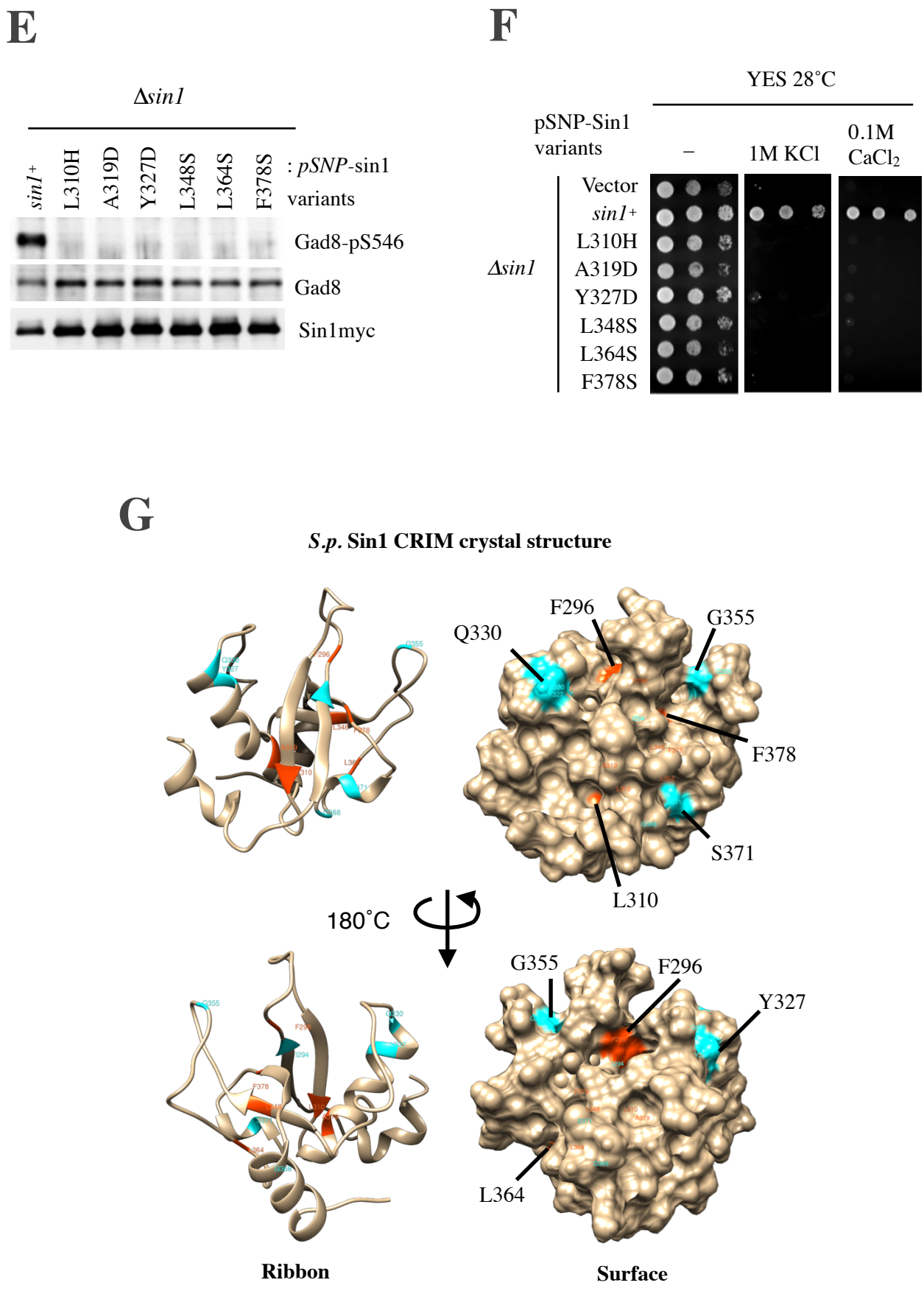
E
Δsin1
sin1+
L310H
A319D
Y327D
L348S
L364S
F378S
: pSNP-sin1 variants
Gad8-pS546
Gad8
Sin1myc
F
YES 28˚C
pSNP-Sin1 variants
–
1M KCl
0.1M CaCl2
Δsin1
Vector
sin1+
L310H
A319D
Y327D
L348S
L364S
F378S
G
S.p. Sin1 CRIM crystal structure
Q330
F296
G355
F378
S371
L310
180˚C
G355
F296
Y327
L364
Ribbon
Surface

## Figure 11.

**Figure 11. Isolation of single amino acid substitutions within the GAD region that disrupt the interaction with Gad8**

(A) The sequence alignment of *S. pombe* and *H. sapience* Sin1 GAD region and the locations of single amino acid substitutions. The GAD region corresponding to amino acid residues 281-400 in *S. pombe* Sin1 was aligned with the homologous region of *H. sapiens* SIN1 by Clustal W algorithm. Identical residues were shaded black and conserved residues were shaded grey at a 50% level of consensus. A red dot (His negative) indicates an amino acid change by which Sin1 GAD lost the interaction with Gad8 in Yeast Two-Hybrid assay (Y2H) in the medium lacking histidine. A blue dot (3AT sensitive) indicates an amino acid change by which Sin1GAD lost the interaction with Gad8 in Y2H assay in the medium lacking histidine and supplemented with 3 AT drug which titrates histidine.

(B), (C) Sin1GAD fragments (281-400 or 247-400 a.a.) with single point mutations lose the interaction with Gad8. GST-Sin1GAD fragments carrying single point mutations were expressed from the *nmt* promoter in *Δsin1 gad8:FLAG* cells, which were then affinity purified onto GSH beads by incubating the beads with the cell lysates. The purified GSH beads as well as crude cell lysates were subject to immunoblotting analysis with the anti-FLAG antibody against Gad8:FLAG. Although the figure in panel (C) was divided into two for the sake of a concise presentation, the samples were run on the same SDS-PAGE gel.

(D) Sin1 proteins with a single amino acid substitution are stably incorporated into TORC2. *FLAG:tor1 Δsin1* cells were transformed with the plasmids expressing a wild-type Sin1 (*sin1*$^+$) or Sin1 variants with a single amino acid substitution under the control of the Sin1 native promoter (pSNP-vector). The *Δsin1* cells expressing a wild-type Sin1:myc serve as a negative control. Cell lysates were incubated with anti-FLAG affinity gel to immunoprecipiate FLAG:Tor1. Immunoblotting analysis was performed to detect co-precipitated Sin1:myc in the precipitated fraction as well as Sin1:myc, FLAG:tor1 and Spc1 in crude cell lysates. Spc1 served as a loading control.

(E) The mutant Sin1 cannot mediate the phosphorylation of Gad8 by TORC2. Sin1 deficient cells (*Δsin1* cells) were transformed with pSNP-*sin1*$^+$ (wild-type) and *sin1* variants. Crude cell lysates prepared with TCA extraction were analyzed by immunoblotting with antibodies against phospho-Gad8 S546, Gad8, and Sin1:myc.

(F) The mutant Sin1 cannot complement the stress sensitivity of sin1 knockout strain (*Δsin1*). The *Δsin1* cells as in (B) were analyzed by spot tests where ten-fold serial dilutions of cell suspensions were spotted onto a control YES plate ("–") and the stress plates supplemented with 1M KCL, or 0.1M $CaCl_2$, which were incubated at 28˚C.

(G) Some of the amino acid residues important for the interaction with Gad8 are visible on molecular surface (differ from surface accessible area). The NMR structure of Sin1CRIM domain is depicted in both ribbon (left) and surface (right) form. The residues strongly inhibited the interaction when substituted are colored in red, while those that mildly inhibited the interaction are colored in blue.

**Table 3. Summary of the random mutagenesis study on the Sin1CRIM**

| Substitution*** [Fig. 10A] | pREP1-sin1:myc in Δsin1 cells | | | Conserved? [Fig. 10A] | Exposed on Molecular Surface* [Fig. 10H] | Y2H with Gad8 | Sin1 CRIM Fragment | pREP1-GST-Sin1 [Fig. 10B, C] | |
|---|---|---|---|---|---|---|---|---|---|
| | YES +1M KCL at 30˚C [Fig. 10G] | Phospho-S546 Gad8 [Fig. 10F] | Co-precipitation with FLAG:tor 1 [Fig. 10E] | | | | | Expression level | Gad8 pull-down** |
| *wt* | ++++ | YES | YES | N/A | N/A | YES | 281-400 | High | YES |
| A319D | – | No | YES | × | × | his⁻ | 247-400 | Low | None |
| Y327D | + | Very low | YES | ○ | ○ | 8mM 3AT sensitive | 247-400 | Low | Little |
| L348S | – | No | YES (weaker) | ○ | × | his⁻ (as double mutation) | 247-400 | Low | None |
| L310H | – | No | YES | × | × | 2mM 3AT sensitive | 281-400 | Low | Little |
| Q330P | ++ | Low | YES | △ | ○ | 2mM 3AT sensitive | 281-400 | Low | Little |
| L364S | – | No | YES | ○ | △ | his⁻ | 281-400 | Low | None |
| I294T | ++ | N/A | N/A | × | × | 8mM 3AT sensitive | 247-400 | Low | Little |
| F296S*** | ++++ | N/A | N/A | × | ○ | his⁻ | 281-400 | N/A | N/A |
| L310P | ++ | N/A | N/A | × | × | his⁻ | 281-400 | Low | Little |
| G355E | +++ | N/A | N/A | ○ | ○ | 8mM 3AT sensitive | 247-400 | High | None |
| G368D | + | N/A | N/A | × | ○ | 8mM 3AT sensitive | 247-400 | High | None |
| S371P | + | N/A | N/A | × | ○ | 8mM 3AT sensitive | 247-400 | High | None |
| F378S | + | No | YES | × | △ | his⁻(as double mutation) | 281-400 | N/A | N/A |

**Strong inhibition**, **Weak Inhibition**. YES+1M KCL (stress) at 30˚C: –, no growth even at the highest cell concentration; +, growth at 3 dilution factor; ++, growth at 2 dilution factor. +++, growth at 1 dilution factor. ++++, wild-type level growth. * Exposed on the molecular surface of Sin1 CRIM; ○=Exposed, △=Half-exposed, ×=Buried. ** Gad8 co-purified with GST-Sin1: None equals to the level of GST control. ***=Classification of strong and weak inhibition may not always be consistent with the results of Y2H. For example, F296S can be re-classified as the weak inhibitor based on the observation on the 1M KCl stress plate.

**Table 3. summarizes the data obtained from wide-range of analyses presented in Figure 10.**

### 3.1.6. NMR solution structure of the Sin1 CRIM domain reveals putative amino acid residues responsible for the physical interaction with Gad8

The amino acid residues identified by the random mutagenesis study are found rather dispersed throughout the GAD region and there is no indication as to which part of the GAD region is particularly important for the Sin1-Gad8 interaction. An examination of the 3D structure of a TORC2 substrate and its potential binding interface with Sin1 might give a further insight into the binding interface of the Sin1 CRIM. Being a human Gad8 counterpart, Akt may offer clues to predict the Sin1 binding site on Gad8, because the crystal structures of Akt are available. Inspections of the Akt crystal structures in the Protein Data Bank (PDB), both inactive (PDB ID:1MRV) (Huang et al., 2003) and active (PDB ID:1O6K) (Yang et al., 2002a) forms, revealed an apparent conformational change around the hydrophobic patch formed by residues F152, Y154 and L155; a pocket-like structure seen in the inactive form of Akt is absent from the active form of Akt (Figure 12A). In support of possible hydrophobic interaction between Gad8 and Sin1, these residues are conserved in Gad8 as L230 L232 and L233, and the interaction between Sin1 and Gad8 was increased in a salt-concentration dependent manner (Figure 12B). In addition, this hydrophobic patch in Akt accompanies a shallow dent formed by a basic residue cluster, which could be involved in additional electrostatic interaction (Figure 12A). It can, therefore, be hypothesized that this basic dent region with the hydrophobic pocket-like structure as a primary candidate for the Sin1 binding-site on Akt/Gad8. A careful examination of the solution structure of Sin1 CRIM identified a few acidic clusters including a serine-rich region, which has been shown to be heavily phosphorylated by a phospho-proteome analysis are exposed on surface, and readily found in both human and fission yeast (Figure 12C, D) (Hayashi et al., 2007). In addition, some of the amino acid residues identified in the random mutagenesis study actually locate near or inside of these acidic clusters. It is possible that any one of the prominent acidic clusters on the

surface of Sin1 CRIM is responsible for the docking with the basic dent region on Akt/Gad8. There are several hydrophobic residues exposed on the surface of Sin1 including Y295, L357, F361, F373, and F375 (Figure 12C, D). It is therefore highly probable that some of exposed hydrophobic residues contribute to the Sin1-Gad8/Akt interaction. Of note, these acidic protrusions and hydrophobic residues of Sin1 CRIM are well conserved among species, not just exposed on the surface. However, the information was lacking in order to determine the contributions of these acidic clusters for the Sin1-Gad8 interaction. Thus, I set out to determine if these candidate sites of Sin1 GAD are responsible for the direct physical interaction with Gad8 by employing site-directed mutagenesis. The candidate sites include acidic protrusions such as Acidic region1 (Acid1); EDE (337-339 a.a.), Acidic region 2 (Acid2); EDDGELDEDF (352-361 a.a.), and also the Serine rich region SSES (298-301 a.a.) which can be acidic when phosphorylated. These acidic amino acid residues along with hydrophobic surface residues; Y295, L357, F361, F373, and F375 were subjected to analysis by site-directed mutagenesis (Figure 12D, E). In the mutagenesis study, target residues were replaced as in Figure 12D. In Figure 12E, the model on the left shows the distribution of the candidate amino acid residues on the surface of Sin1 CRIM. In the right model, it can be seen that the densely conserved cluster in the CRIM region (residues 348-375) forms a hollow-like structure composed of the hydrophobic residues that are found in the acidic loop (Acid2) as well as the KFGF motif. The Sin1GAD variants carrying these amino acid substitutions were expressed in bacteria as GST-fusion proteins and purified onto GSH beads. After extensive wash, the GSH beads were incubated with crude yeast cell lysates derived from *Δsin1 gad8:FLAG* cells. The loss of the Sin1-Gad8 interaction as a result of the mutagenesis was quantified by the amount of Gad8 co-purified with the GST-Sin1GAD variants. As shown in Figure 12F, almost complete loss of Gad8 co-purification was observed with the Acid2, Acid2double, and F373A F375A variants. The Acid2hydro substitution also significantly

reduced Gad8 co-purification. A single substitution of the hydrophobic residue of F375 alone significantly compromised co-purification of Gad8. On the other hand, the amounts of Gad8 co-purified with Acid1 or S301Q variants were comparable to that with wild-type Sin1GAD, suggesting that these residues are not important for the Sin1-Gad8 interaction. The results from the yeast two-hybrid assays were consistent with the above findings (Figure 12G).

**Figure 12.**

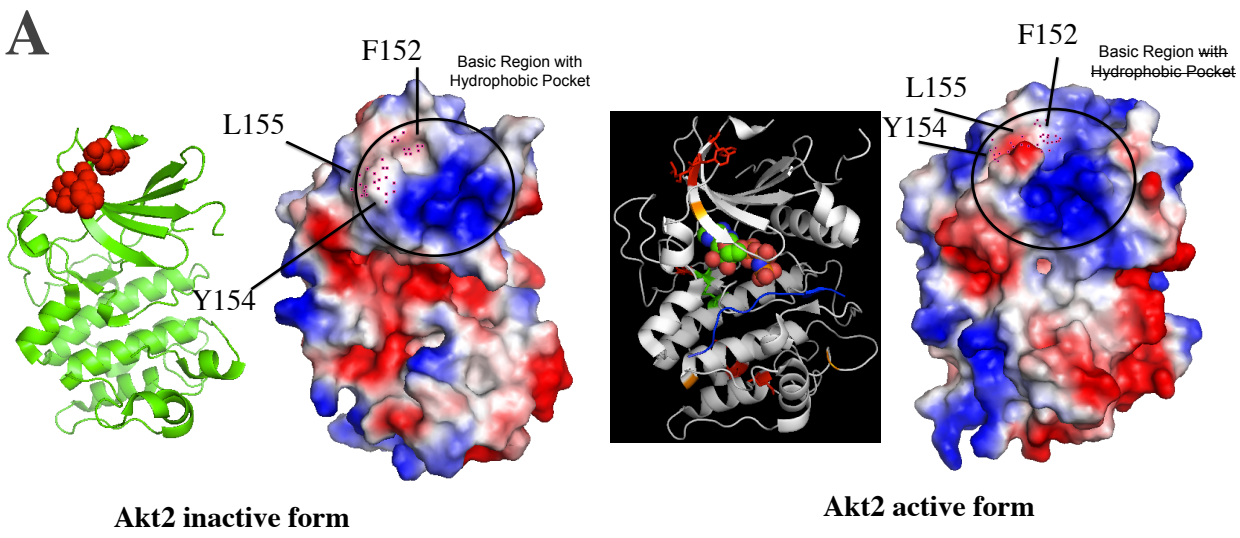
A
F152
Basic Region with Hydrophobic Pocket
L155
Y154
F152
Basic Region with Hydrophobic Pocket
L155
Y154
Akt2 inactive form
Akt2 active form

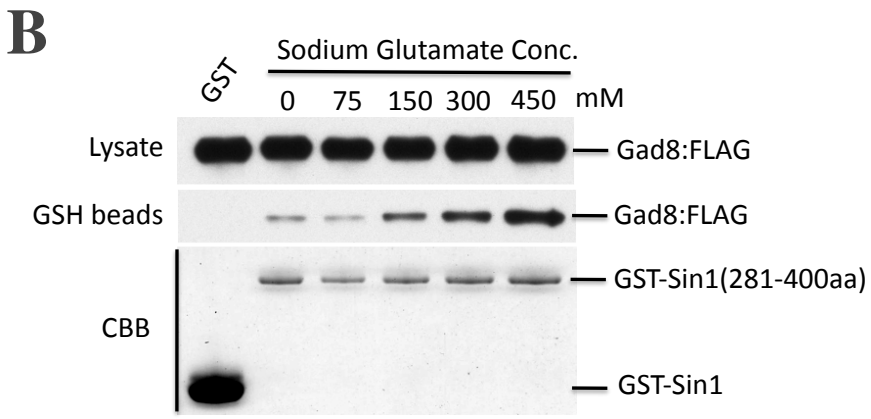
B
Sodium Glutamate Conc.
GST
0 75 150 300 450 mM
Lysate
GSH beads
CBB
Gad8:FLAG
Gad8:FLAG
GST-Sin1(281-400aa)
GST-Sin1

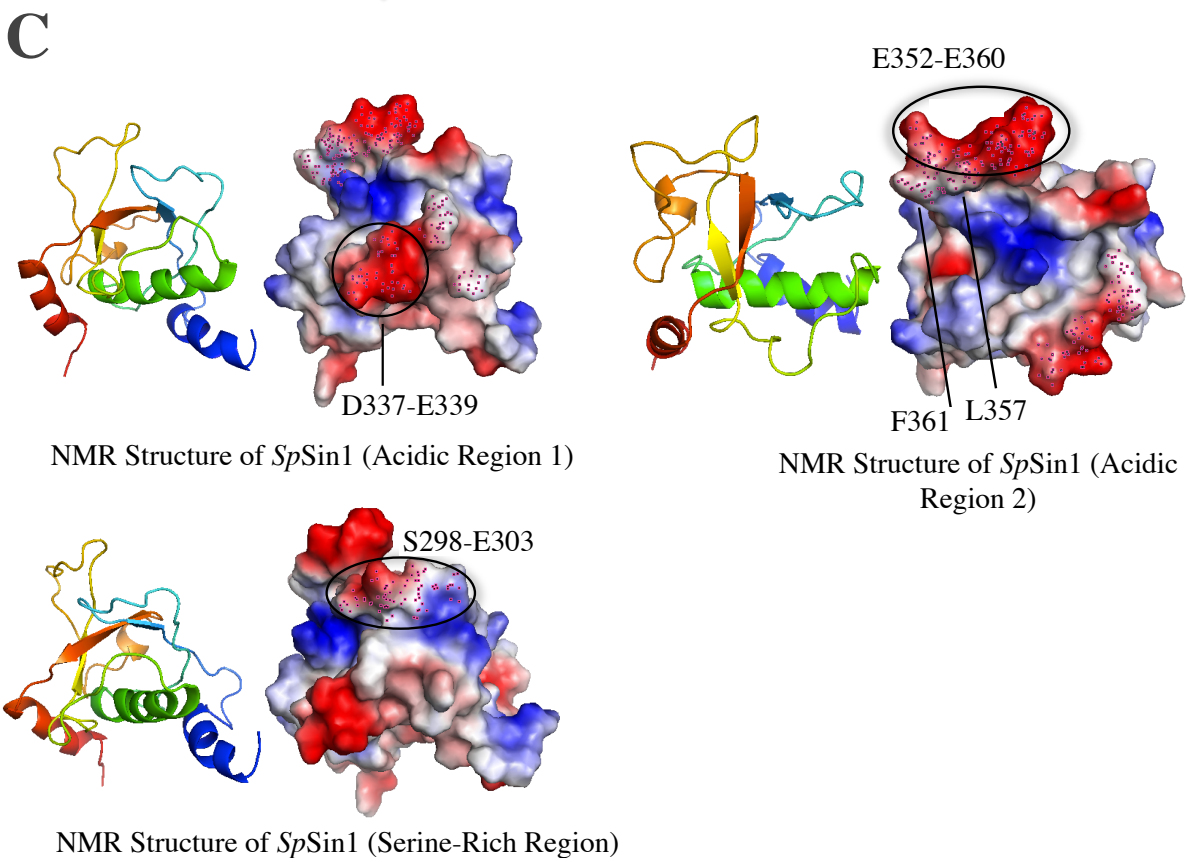
C
D337-E339
NMR Structure of SpSin1 (Acidic Region 1)
E352-E360
F361
L357
NMR Structure of SpSin1 (Acidic Region 2)
S298-E303
NMR Structure of SpSin1 (Serine-Rich Region)

Figure 12.

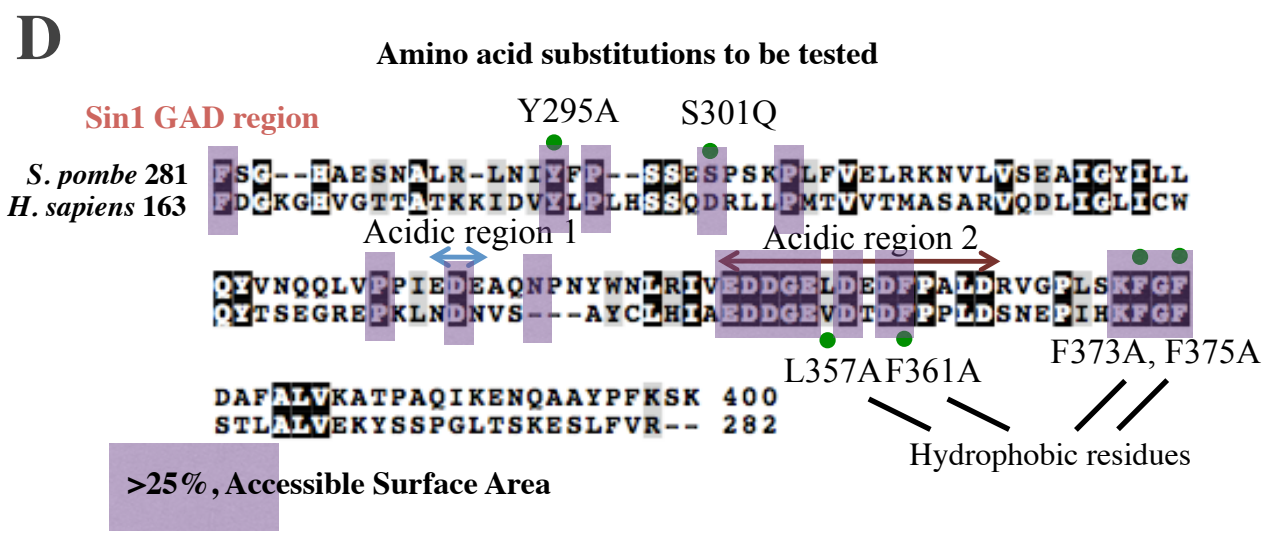


**Acidic region 1 = 337-EDE-339**
Acid1 → QNQ
Y295A
S301Q
F375A
F373A, F375A

**Acidic region 2 = 352-EDDGELDEDF-361**
Acid2 → -QNNGQLNQNF-
L357A, F361A→ -EDDGEADEDA-
Acid2double → -QNNGQANQN-
Poly K → -KKKGKLKKKF-

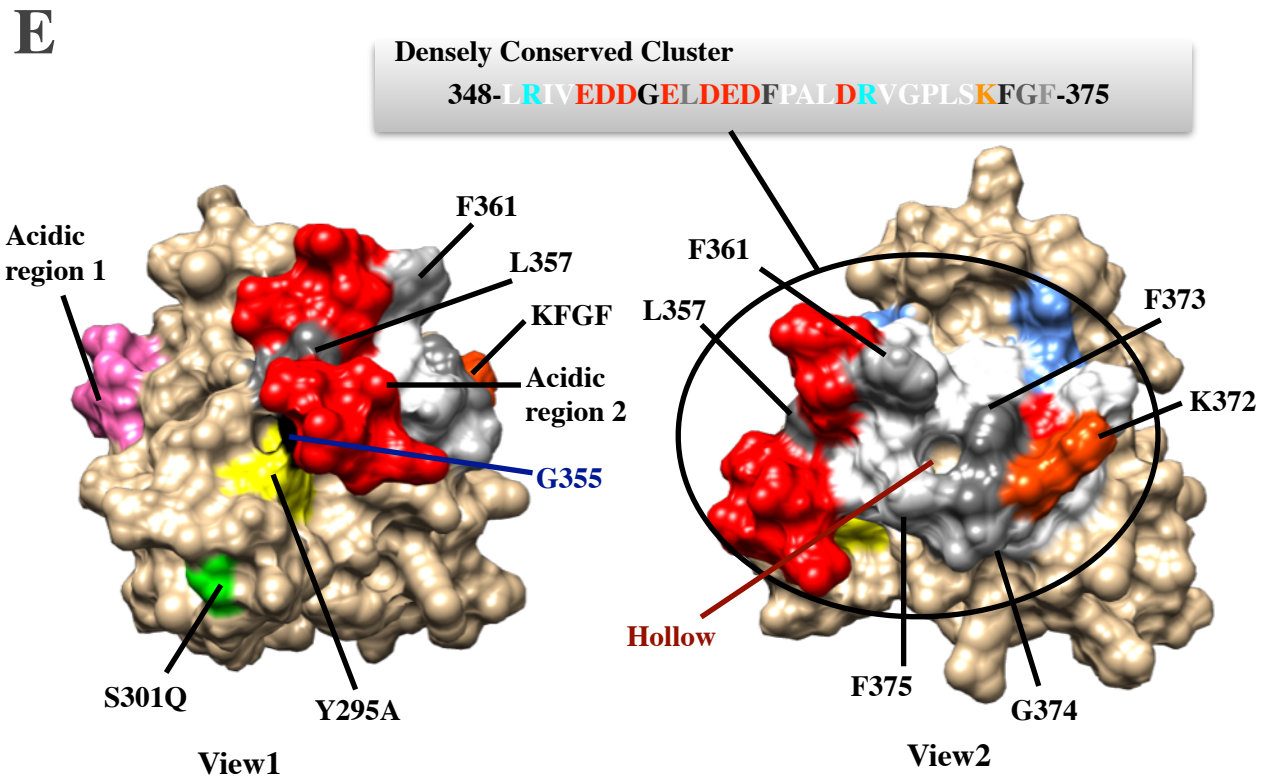


*Sp*Sin1 CRIM

**Figure 12.**

**F**

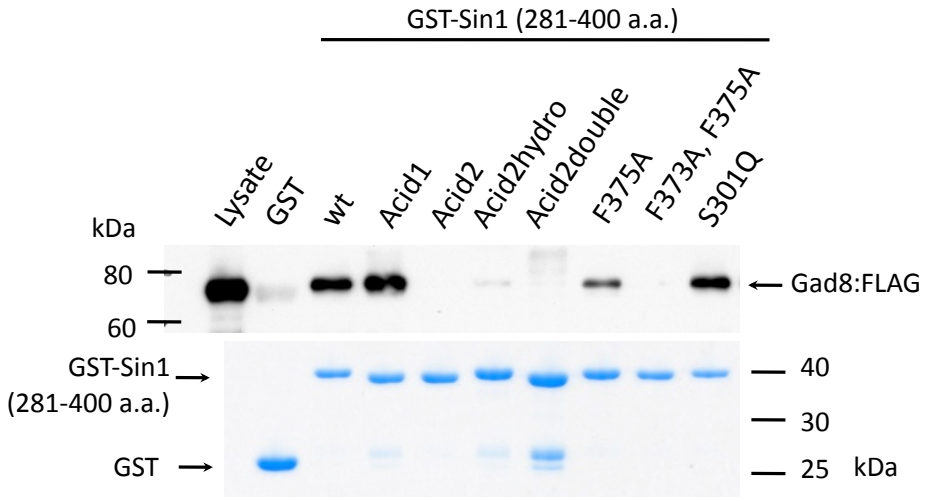


**G**

| | pGBT | pGADGH |
|---|---|---|
| 1 | Gad8⁺ | – |
| 2 | – | Empty |
| 3 | Gad8⁺ | Empty |
| 4 | Gad8⁺ | Sin1$^{(281\text{-}400aa)}$ |
| 5 | Gad8⁺ | Acid1 |
| 6 | Gad8⁺ | Acid2 |
| 7 | Gad8⁺ | Acid2hydro |
| 8 | Gad8⁺ | Acid2double |
| 9 | Gad8⁺ | F375A |
| 10 | Gad8⁺ | F373A F375A |
| 11 | Gad8⁺ | S301Q |

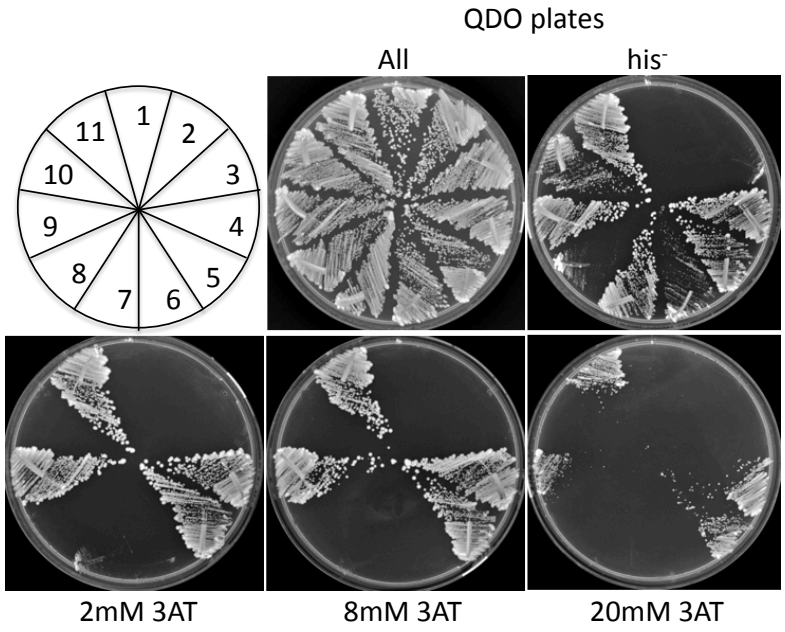

## Figure 12.

**Figure 12. Identifying the amino acid residues that are responsible for the direct physical interaction with Gad8 based on the NMR structure of Sin1 CRIM (1)**

(A) Comparison of an inactive and an active from of Akt2 reveals the hydrophobic pocket-like structure in the inactive form of Akt, which disappears in the active form of Akt (Ribbon & Surface forms of the crystal structure of Akt2 is prepared by Dr. Kojima). F152, Y154, and L155 residues of Akt2 which form a hydrophobic pocket-like structure in its inactivation form corresponds to Gad8 L230, L232, and L233 residues.

(B) Hydrophobic interaction between Sin1 and Gad8. GST or GST-Sin1 (281-400 a.a.) recombinant protein was affinity-purified onto GSH beads from bacterial cell lysates. The GSH beads are then incubated with yeast cell lysates which chromosomally expresses Gad8:FLAG. The amount of Gad8:FLAG co-purified with GST-Sin1 (281-400 a.a.) or GST was measured by immunobloting with anti-FLAG antibody against Gad8:FLAG in the increasing degree of salt (sodium glutamate) concentration.

(C) NMR structure of *s. pombe* Sin1 CRIM solved by Dr. Kojima reveals putative amino acid residues that would be responsible for the direct physical interaction with Gad8. The putative amino acids are chosen on the following selection criteria; (1) conserved between *S. pompe* and *H. sapiens*, (2) exposed on the solvent surface, (3) hydorophobic and/or Acidic residues

(D) The putative amino acid residues are substituted as indicated in the figure to be tested for the loss of interaction with Gad8, shown along with the amino acid sequence alignment between *H. sapiens* and *S. pombe*.

(E) The putative amino acid residues that may be responsible for the interaction with Gad8 are mapped on the NMR crystal structure of *S.p*.Sin1CRIM. View1 shows all the putative amino acid residues, while View2 reveals the arrangement of the amino acid residues consisting of the densely conserved region. In View2, the amino acid sequence of the densely conserved region is shown and each residue is exhibited with matching color to that of the 3D model.

(F) The Sin1 variants carrying the amino acid substations interact with Gad8 in differential degree and ratio depending on the substituted residues. The GHS beads bound with bacterially purified recombinant GST-fused Sin1 variants along with Sin1 wilds-type and GST alone controls were incubated with the yeast cell lysate that chromosomally expresses Gad8:FLAG. The amounts of Gad8:FLAG co-purified with the recombinant proteins were quantified by immunoblotting with anti-FLAG antibody.

(G) Yeast two-hybrid assay confirmed the results from the GST-pulldown assay. Gad8 protein, which was expressed from the bait plasmid (pGBT), was tested for its ability to interact with the indicated Sin1 variants expressed from the prey plasmid (pGADGH). In this system, the degree of histidine production is dependent on the interaction between prey and bait, which determines the cellular growth rate on the plate without histidine. Audiobasisin (3AT) suppresses the production of histidine, enhancing the growth suppression of the cells failed to produce histidine.

In the second round of the verification assays, the Y295A, L357A, F361A, and F373A substitutions as well as the PolyK substitution, in which acidic residues of Acid region 2 were replaced by the positively charged residues (KKKGKLKKKF), were included and compared with the others (Figure 12D, Figure 13A). These amino acid residues were selected based on both their surface exposure rate and hydrophobicity, with the assumption that surface hydrophobic residues would play a role in substrate binding. In this second round of the assays, the results of the first-round assays for Acid2, Acid2hydro, Acid2double, F375A and F373A F375A (double) substitutions were reproduced in both the GST-pulldown and the yeast two-hybrid assays (Figure 13A, B). Alanine-substitution of Y295, which is flanked by residues I294 and F296 identified in the random mutagenesis study, was found to diminish the interaction with Gad8 (Figure 13A), and a more prominent inhibitory effect was seen in the yeast two-hybrid assay (Figure 13B). The Acid2hydro substitutions were separated into single substitutions of L357A and F361A and they were tested individually. While the L357A variant still maintains the interaction with Sin1 to some extent, the F361A variant seems to lose the most of interacting potency with Sin1 (Figure 13A). On the contrary, both L357A and F361A variants still seem to retain the interaction with Sin1 in the yeast two-hybrid assays (Figure 13B). The F373A variant seems less potent in binding to Gad8 compared to the F375A variant, as more of the F373A variant was found on GSH beads than the F375A variant (Figure 13A). An additive effect of the F373A and F375A substitutions was observed; no detectable amount of Gad8 was co-purified with the F373A F375A variant. Consistent with the results from the GST-pulldown assay, the Gad8 phosphorylation at Ser546 was undetectable in the strain expressing Sin1 with the Acid2hydro substitution (L357A, F361A) (Figure 13C). Despite a complete loss of the Ser546 phosphorylation in the PolyK substitution (Figure 13C), a weak interaction between the GST-PolyK variant fusion and Gad8 was observed (Figure 13A). Some Sin1 variants such as F361A and F375A still allowed a certain

level of the Ser546 phosphorylation, despite their loss of the interaction with Gad8 in the GST-pulldown assays (Figure 13A, C), suggesting that compromised, weak interaction is sufficient to bring about the Ser546 phosphorylation in some cases. A higher level of the Gad8 phosphorylation was observed with the F375A variant than F373A, reflecting the results from both the GST-pulldown assays and the yeast two-hybrid assays (Figure 13A, B, C). Stress sensitivity of *Δsin1* cells expressing the Sin1 variants provides estimation of the Gad8 activity mediated by these Sin1 variants. Indeed, their cell growth on the stress plates paralleled the phosphorylation status of Gad8 (Figure 13D). Of note, cells expressing the Y295A variant was found to be highly sensitive to the elevated temperature of 37°C.

To confirm if the Sin1 full-length variants expressed in *Δsin1* cells are stably incorporated into TORC2, in other words, if the amino acid substitutions do not compromise the structural integrity of TORC2, the interaction between the Sin1 variants and Tor1 was tested through an immunoprecipitation assay. The FLAG:Tor1 kinase was immunoprecipitated with anti-FLAG beads and the co-precipitations of the Sin1 variants with Myc-tag were probed by immunoblotting (Figure 13E). Most of the Sin1 variants showed the comparable interaction with the Tor1 kinase to that of wild-type Sin1. Although the polyK variant showed a significantly reduced expression level, the unchanged interaction rate was evident because the reduced level of co-precipitation was matched to the expression level of the PolyK variant. Quantification and a simple calculation gave the numbers summarized in Table 4. Notably, when normalized to the wild-type level, the interaction rates of the Sin1 variants with Tor1 were almost equal to that of wild-type Sin1 (Figure 13E, Table 4). These results indicate that, while amino acid substitutions may affect the protein stability or the expression levels of the Sin1 variants in a few cases, the capabilities of the Sin1 variants to be incorporated into TORC2 are not affected significantly.

To summarize, the surface composition of Acidic Region 2 most readily fulfils the

requirements predicted from the surface composition of the putative Sin1 binding-site of the human Gad8 counterpart Akt; a cluster of acidic residues with several hydrophobic residues around, which are not only conserved but also exposed on the surface (Figure 12C). The mutational analysis of Acidic Region 2 demonstrated that the charged residues play a significant role in the interaction with Gad8, with the hydrophobic residues involved in a lesser extent, although the alanine replacement of F361 alone disrupted the interaction to a significant degree. Y295 was also implicated in the interaction with Gad8, and this residue takes a unique position among already described residues I294, F296, G355 and Acidic Residue 2. Hydrophobic residues in the KFGF motif were also found to play an important role in the interaction with Gad8. In the NMR structure of Sin1 CRIM, Acidic Region 2 and the KFGF motif create a unique spatial arrangement by facing each other across the hollow-like structure. This unique positioning may be important for docking of the substrate to the Sin1 protein.

**Figure 13.**

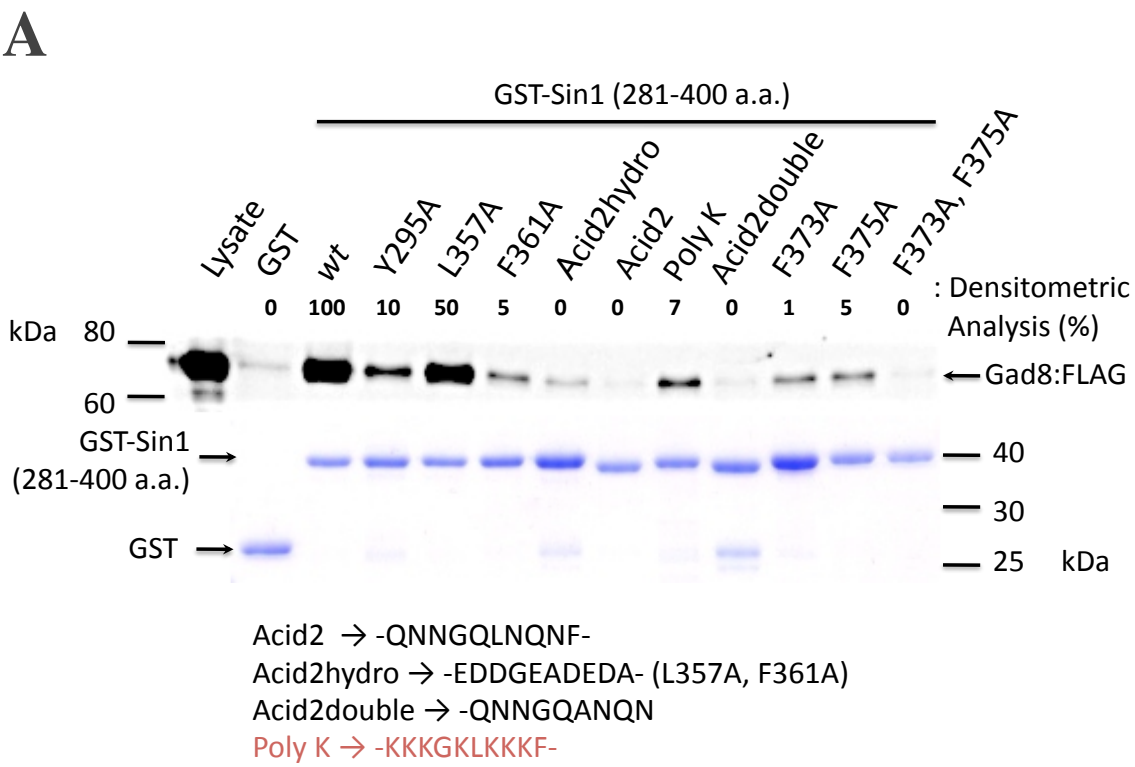


**B**

| | pGBT | pGADGH |
|---|---|---|
| 1 | Gad8⁺ | Empty |
| 2 | Gad8⁺ | Sin1$^{(281-400aa)}$ |
| 3 | Gad8⁺ | Y295A |
| 4 | Gad8⁺ | L357A |
| 5 | Gad8⁺ | F361A |
| 6 | Gad8⁺ | Acid2hydro |
| 7 | Gad8⁺ | Acid2 |
| 8 | Gad8⁺ | PolyK |
| 9 | Gad8⁺ | Acid2double |
| 10 | Gad8⁺ | F373A |
| 11 | Gad8⁺ | F375A |
| 12 | Gad8⁺ | F373A F375A |

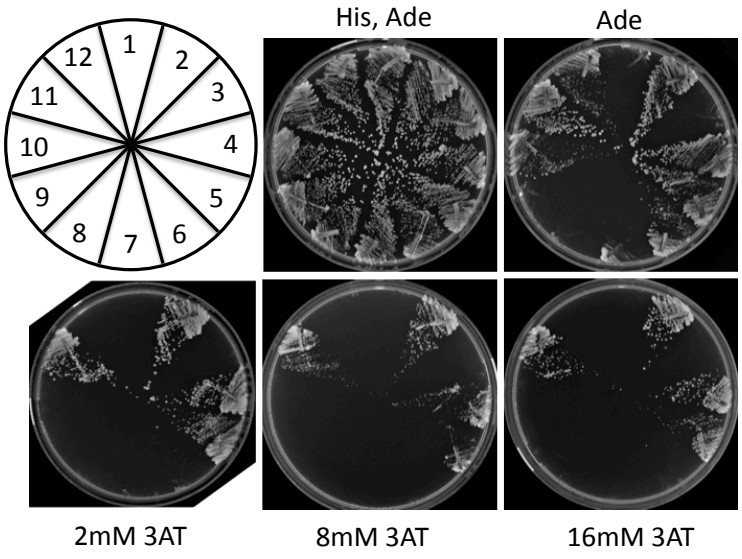

**Figure 13.**

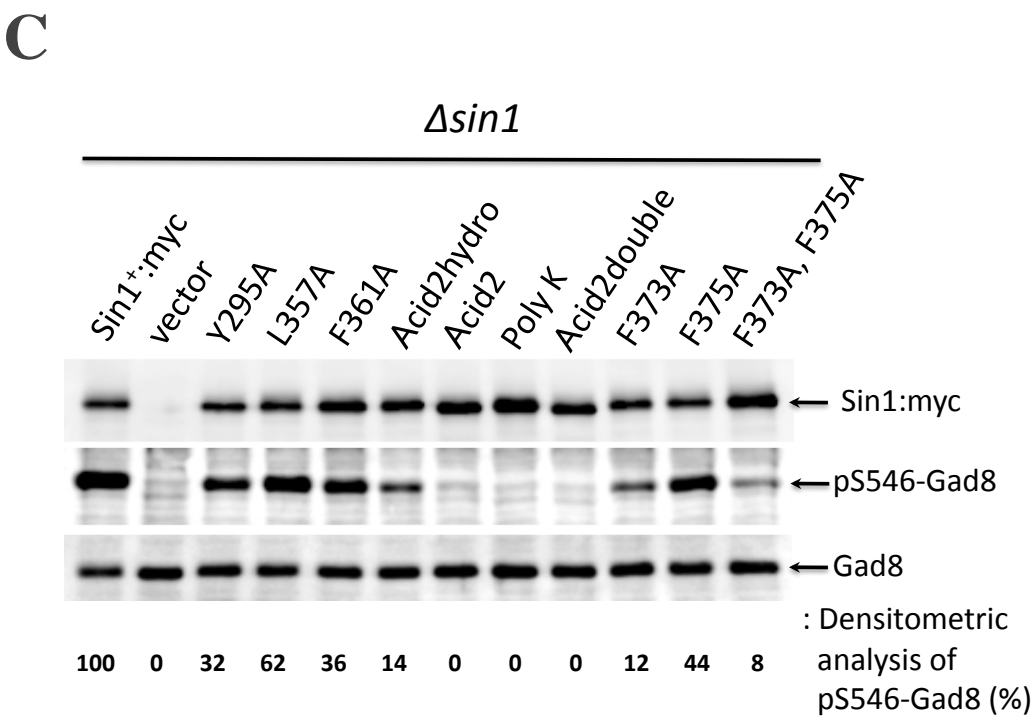
C
Δsin1
Sin1+:myc
vector
Y295A
L357A
F361A
Acid2hydro
Acid2
Poly K
Acid2double
F373A
F375A
F373A, F375A
Sin1:myc
pS546-Gad8
Gad8
100 0 32 62 36 14 0 0 0 12 44 8
: Densitometric analysis of pS546-Gad8 (%)

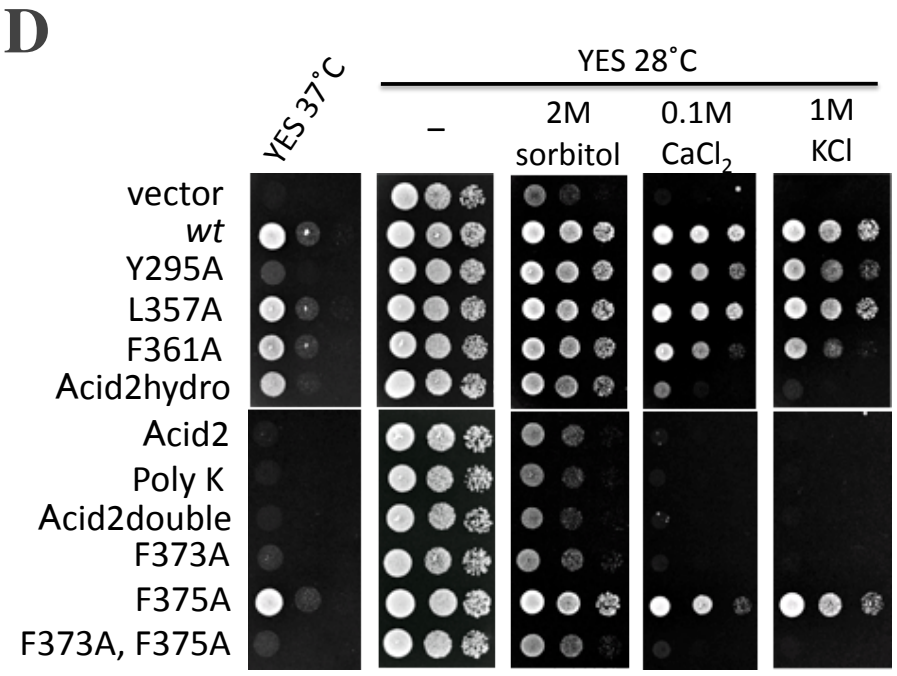
D
YES 37˚C
YES 28˚C
–
2M sorbitol
0.1M CaCl2
1M KCl
vector
wt
Y295A
L357A
F361A
Acid2hydro
Acid2
Poly K
Acid2double
F373A
F375A
F373A, F375A

**Figure 13.**

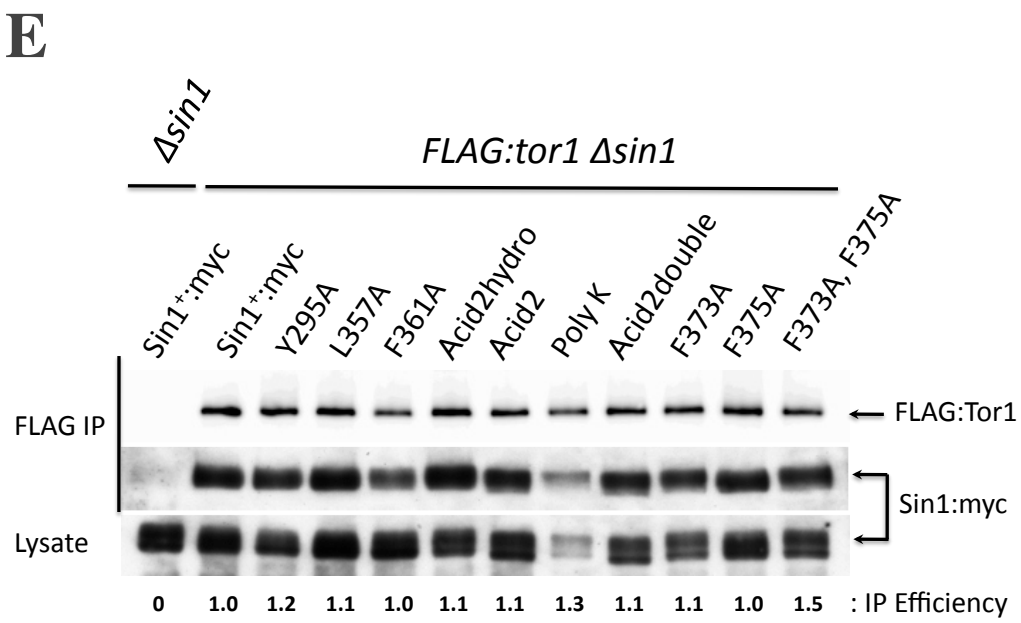


**Figure 13. Identifying the amino acid residues that are responsible for the direct physical interaction with Gad8 based on the NMR structure of Sin1 CRIM (2)**

**Second round assay**

(A) GST-pulldown assay with the second set of Sin1 variants was carried out as in (E). The normalization using densitometry data was done with {[co-precipitated Gad8:FLAG]/[GST-Sin1 in precipitate]}x100

(B) Yeast two-hybrid assay with the second set of Sin1 variants was carried out as in (F).

(C) The effect of the amino acid substitutions in the Sin1GAD on the phophorylation status of Gad8 by TORC2. The Sin1 variants were expressed in the *Δsin1* cells and the TORC2-dependent phosphorylation level of Gad8 was examined by immunoblotting. The normalization was done with {[phospho-S546]/[Gad8]x[Sin1Myc]}x100.

(D) The effects of the amino acid substitutions on the cellular tolerance to the various stresses. The *Δsin1* cells expressing the Sin1 variants were tested for their ability to survive the various stresses by spotting serially diluted cell suspension onto a control YES plate ("–") and the stress plates include the one that was incubated at 37˚C or those supplemented with 2M sorbitol, 1M KCL, or 0.1M $CaCl_2$, which were incubated at 28˚C.

(E) The ratios of the Sin1 variants at which interact with Tor1 were almost unchanged. Sin1 variants with myc-tag on its C-terminus were expressed in the *FLAG:tor1 Δsin1* cells. FLAG:Tor1 was immunoprecipitated by anti-FLAG-beads from the cell lysates and co-precipitation of the Sin1 variants were detected by immunoblotting using anti-myc antibody. The level of the co-purified Gad8 was normalized against the GST-Sin1GAD variants present in the precipitated GSH beads. The Gad8 phosphorylations at Ser546 were normalized against the Gad8 expression levels. The amounts of the co-precipitated Sin1 was affected by the amounts of the precipitated Tor1 and the expression levels of Sin1. Therefore, the normalization using Densitometry data was carried out as expressed by the equation of {[co-precipitated Sin1Myc]/[FLAG:Tor1(precipitate)]x[Sin1Myc(Lysate)]}x100, which represents the interaction rate.

**Table 4. Summary of the mutagenesis study based on the Sin1CRIM NMR structure**

| Sin1 Variants [Fig 11D] | Y2H[1] [Fig. 12B] | Co-purified Gad8 with GST-Sin1GAD (%)[2] [Fig. 12A] | pS546-Gad8 (%)[3] [Fig. 12C] | 1M KCl[4] [Fig. 12D] | F:Tor1 IP[5] [Fig. 12E] |
|---|---|---|---|---|---|
| –ve cont. | His – | 0 | 0 | – | 0 |
| Sin1$^{(281\text{-}400aa)}$ | + | 100 | 100 | +++ | 1.0 |
| Y295A | His – | 10 | 32 | +++ | 1.2 |
| L357A | + | 50 | 62 | +++ | 1.1 |
| F361A | + | 5 | 36 | ++ | 1.0 |
| Acid2hydro | 3AT – | 0 | 14 | + | 1.1 |
| Acid2 | His – | 0 | 0 | – | 1.1 |
| PolyK | His – | 7 | 0 | – | 1.3 |
| Acid2double | His – | 0 | 0 | – | 1.1 |
| F373A | 3AT – | 1 | 12 | – | 1.1 |
| F375A | + | 5 | 44 | +++ | 1.0 |
| F373A, F375A | 3AT – | 0 | 8 | – | 1.5 |

1 = Y2H: Yeast Two-Hybrid Assay [His– = No growth on histidine negative plate, 3AT– = No growin in the presence of 3AT, 3-AT is a selective inhibitor of histidine synthase]

2 = Gad8 co-purified with GST-Sin1GAD; normalized to the level of GST control.

3 = pS546 = TORC2-dependent phosphorylation level at S546

4 = YES+1M KCL (stress) at 30˚C: –, no growth even at the highest cell concentration; +, growth at 2 dilution factor; ++, growth at 1 dilution factor. +++, wild-type level growth.

5 = The ratio of the Sin1 variants at which interact with Tor1.

**Table 4 summarizes the data in Figure10 that are deduced and calculated by quantifying the mutagenesis study based on the Sin1 NMR structure.**

### 3.1.7. Gad8 recruitment onto TORC2 takes place through the Sin1GAD domain

If the recruitment of Gad8 occurs only through the Sin1GAD domain, but not the other parts of the Sin1 protein, the CRIM/GAD fragment alone instead of full-length Sin1 in TORC2 should be sufficient to recruit Gad8 onto TORC2 and induce the phosphorylation of Gad8. To test this possibility, the N-terminal end of the Sin1CRIM was fused to the C-terminal end of Ste20, another essential subunit of TORC2; its budding yeast counterpart Avo3 has been described as a scaffold protein within TORC2 (Ho et al., 2005; Wullschleger et al., 2005). The constructed Ste20-Sin1CRIM fusion protein (FLAG-Ste20*Sin1*) successfully complemented the defect of the *Δste20* strain in the Gad8 phosphorylation at Ser546 compared to an empty vector control (Figure 14A). This observation indicates that the Ste20 function is not compromised by being fused with Sin1CRIM. The Ste20-Sin1CRIM (247-400 a.a.) *wt* fusion protein as well as those carrying the L348S or L364S substitutions within Sin1CRIM were then expressed in the *Δsin1* strain and compared for their capabilities of inducing the TORC2-dependent phosphorylation of Gad8 at Ser546 (Figure 14B). Immunobloting with antibodies against Gad8 as well as phospho-Ser546 revealed that the wild-type Ste20-Sin1CRIM fusion protein could induce a significant level of the Gad8 phosphorylation (Figure 14A). On the other hand, the mutant Ste20-Sin1CRIM L348S or L364S fusion proteins or Ste20 with the Myc tag failed to induce the Gad8 phosphorylation. Correspondingly, *Δsin1* cells expressing the wild-type Ste20-Sin1CRIM fusion protein, but not the L348S or L364S variant forms, were able to grow on the stress plates (Figure 14C). Taken together, my findings are consistent with the notion that Gad8 recruitment onto TORC2 takes place through the Sin1CRIM/GAD; an essential event for TORC2 to phosphorylate Gad8 at Ser546.

**Figure 14.**

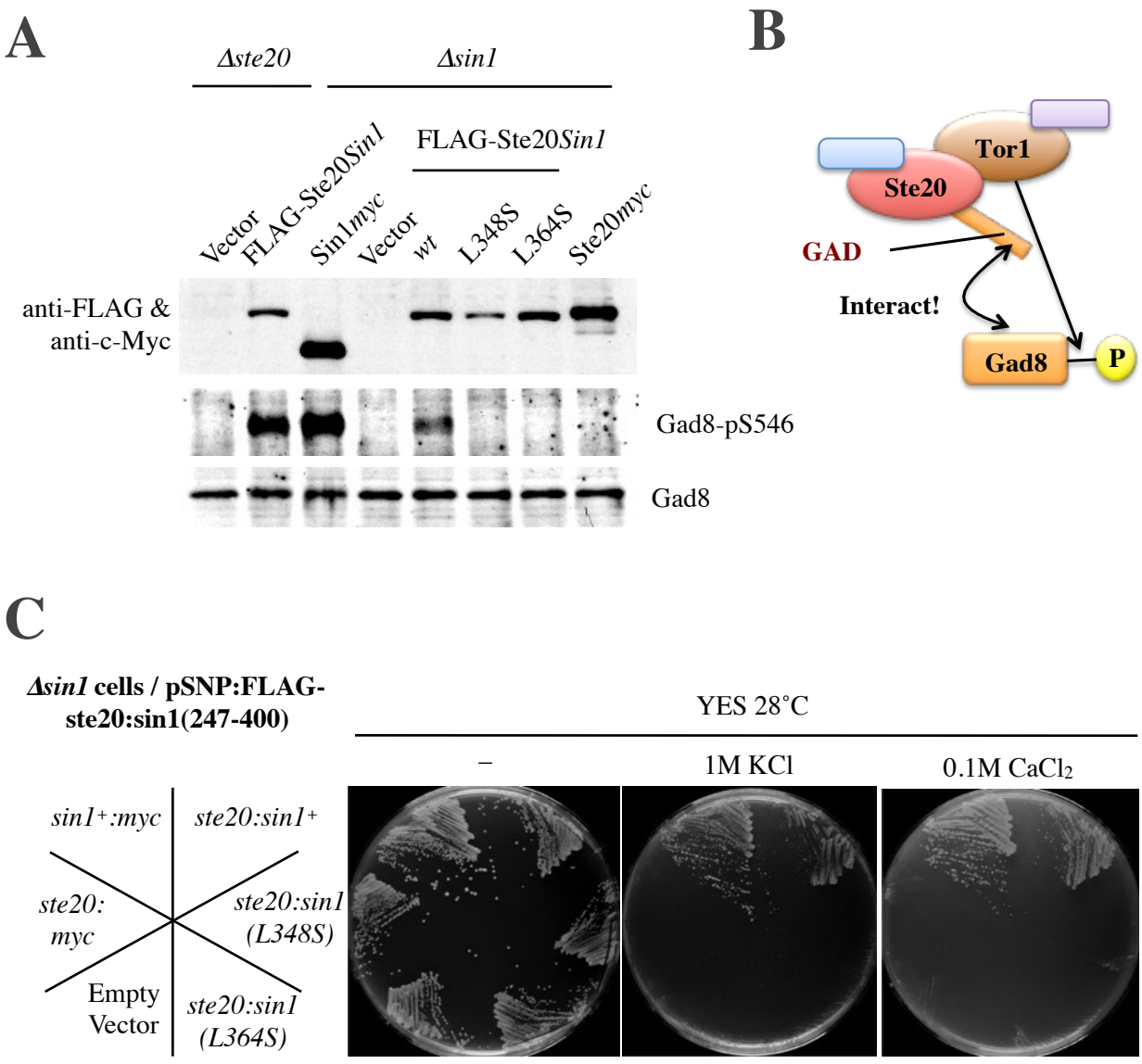


**Figure 14. The Ste20-Sin1GAD fragment fusion protein can recruit Gad8 onto TORC2**

(A) The Ste20-Sin1 GAD fusion protein can induce Gad8 Ser-546 phosphorylation. FLAG tagged Ste20-Sin1GAD fusion protein (FLAG-Ste20*Sin1*) where the Sin1 fragment of 247-400 amino acid residues fused to Ste20 was expressed along with an empty vector in *Δste20* or in *Δsin1* cells from pSNP vector under the control of Sin1 native promoter. The Ste20-Sin1GAD fusion protein with the amino acid change (L348S and L364S) as well as Sin1:myc and Ste20:myc were also expressed in *Δsin1* cells. Crude cell lysates were prepared with TCA extraction and subject to immunobloting analysis with anti-FLAG and anti-c-Myc antibody cocktail, as well as with anti-Gad8 and anti-phospo-Gad8 Ser546 antibodies.

(B) A cartoon shows how the Ste20-Sin1GAD recruits Gad8 onto TORC2

(C) The Ste20-Sin1GAD fusion protein can complement the stress-sensitive phenotype of *Δsin1* cells. The *Δsin1* cells expressing indicated proteins as in (A) were streaked onto a control YES plate ("–") and the stress plates supplemented with 1M KCL, or 0.1M $CaCl_2$ , which were incubated at 28˚C.

### 3.1.8. Tor1-Gad8 direct physical association can bring about the Gad8 phosphorylation at Ser546

The observations above strongly suggest that Sin1CRIM is required for the TORC2-dependent phosphorylation of Gad8, most likely through recruitment of Gad8 by direct physical interaction. However, the possibility remains that Sin1CRIM is also required for the kinase catalytic activity of Tor1. To test this possibility, a Ste20-Gad8 fusion protein was constructed by fusing the N-terminal end of Gad8 with the C-terminal end of Ste20. If the Tor1 kinase is fully functional even in the absence of Sin1, then a direct presentation of the substrate Gad8 to Tor1 by fusing to the Ste20 subunit would be sufficient to induce phosphorylation of Gad8 at Ser546. Therefore, the Ste20-Gad8 fusion protein was expressed in *Δste20 Δsin1* cells and *Δste20* cells. As a negative control, the *tor1D2137A* mutant strain that expresses catalytically inactive Tor1 was employed. Immunobloting analysis with anti-phospho-Ser546 and anti-Gad8 antibodies revealed that the Gad8 part of the fusion protein in *Δste20 Δsin1* cells was phosphorylated at Ser546 as in *Δste20* cells (Figure 15A), indicating that Tor1 is active even in the absence of Sin1. Furthermore, it was investigated if the absence of Wat1, another subunit of TORC2, could affect the intrinsic kinase activity of Tor1. According to the report on the 3D structure of mTORC1 including mLST8, the mammalian counterpart of Wat1 (Yang et al., 2013), Wat1 is expected to form a stable complex with both Tor2 and Tor1, participating in both TORC1 and TORC2. However, Wat1 has been shown to only affect the function of TORC2, but not TORC1, reducing the Gad8 phosphorylation level by more than half when Wat1 is absent (Ikeda et al., 2008; Nakashima et al., 2012), and yet its precise role in TORC2 remains elusive. The Ste20-Gad8 fusion protein was expressed in *Δsin1 Δwat1* cells and *Δsin1* cells as well as in *tor1DA* cells as a negative control. As shown in Figure 15B, the phosphorylation level of the Gad8 part at Ser546 in *Δsin1 Δwat1* cells was comparable to that in *Δsin1* cells. This observation implies that Wat1 is not essential for the

intrinsic Tor1 kinase activity, although the absence of Wat1 results in the compromised function of TORC2 (Ikeda et al., 2008). These data demonstrate that the direct recruitment of Gad8 onto the proximity of the Tor1 kinase brings about the Gad8 phosphorylation without the Sin1 and Wat1 subunits, indicating that Sin1 and Wat1 are not essential for the catalytic activity of the Tor1 kinase.

It was also tested if the Ste20-Gad8 fusion protein can complement the stress sensitivity of *Δsin1 Δste20* cells. The Ste20-Gad8 fusion proteins carrying the Gad8-K128E or Gad8-D153A mutations were also included in this assay for comparison. Gad8 carrying these substitutions bypass the TORC2 requirement for activation and is constitutively active, as described in the following section (Figure 18). Whilst *Δsin1 Δste20* cells expressing the K128E or D153A mutant Ste20-Gad8 fusion proteins grew very well on the stress plates of high osmolarity or high calcium contents, those expressing the wild-type Ste20-Gad8 fusion protein failed to do so (Figure 15C). An interpretation of this observation was summarized in a diagram (Figure 15D). The phosphorylation at Ser546 of the wild-type Ste20-Gad8 fusion is essential for the full activation of the Gad8 part. In *Δsin1 Δste20* cells, this phosphorylation occurs only when the fusion protein is stably incorporated into TORC2; the free fusion protein will not be phosphorylated and inactive. If Gad8 needs to be released into the cytosol or moved to a particular cellular location to phosphorylate its effectors after being activated by TORC2, the fusion protein stably integrated in TORC2 cannot carry out the substrate phosphorylation. Indeed, as shown in Figure 10, the interaction between Ste20 and Tor1 is very stable, suggesting that the Ste20-Gad8 fusion protein is likely to be trapped in the TORC2 complex. On the other hand, being active on its own, the “free” Ste20-Gad8 K128E or D153A mutant proteins can probably exert their functions and activate the effectors of Gad8 elsewhere, resulting in the complementation of the stress sensitivities of the *Δsin1 Δste20* mutant.

**Figure 15.**

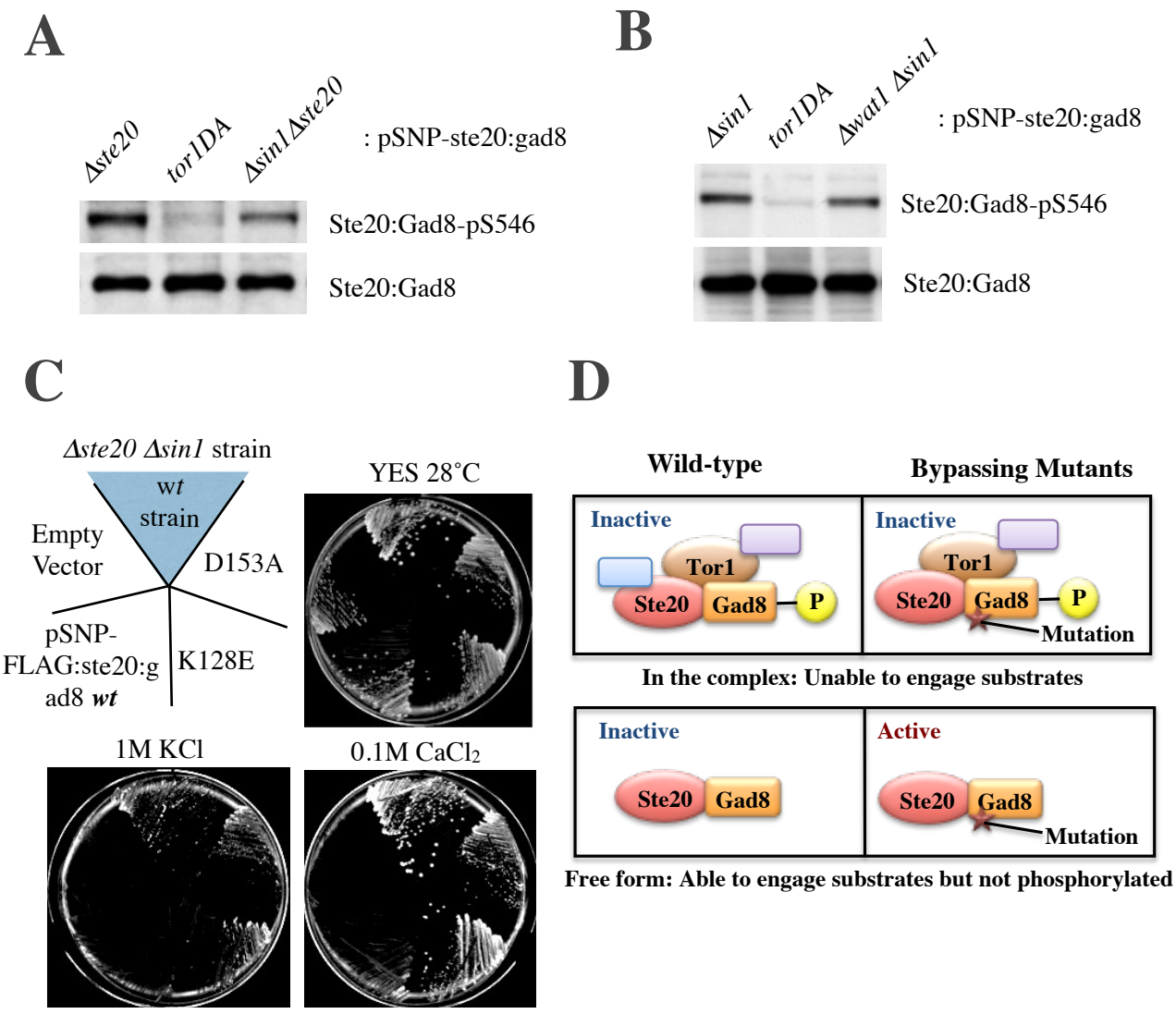


**Figure 15. Tor1 directly phoshphorylates the Gad8 part of the Ste20-Gad8 fusion protein in the absence of Sin1**

(A) The absence of Sin1 dose not affect Tor1 kinase activity; Tor1 phosphorylates Gad8 that is fused to Ste20. The Ste20-Gad8 fusion protein was expressed in *Δste20*, *tor1DA* and *Δsin1 Δste20* strains. Crude cell lysates prepared with TCA extraction were analyzed by immunobloting with antibodies against phospho-Ser546 and Gad8.

(B) Ste20-Gad8 fusion protein cannot efficiently complement the stress sensitivity. The *Δsin1 Δste20* cells expressing wild-type Ste20-Gad8 (*wt*) and those with a single amino acid change (K128E or D153A) on the Gad8 protein were spotted onto YES control plate "–" and those containing 1M KCl and 0.1M $CaCl_2$.

(C) Another TORC2 subunit Wat1 is also dispensable for Tor1 kinase activity. Ste20-Gad8 fusion protein was expressed in *Δsin1 Δste20*, *tor1DA* and *Δwat1 Δsin1 Δste20* strains. Samples were prepared and analyzed as in (A).

(D) Diagram shows the activation status of the fusion proteins inside or outside of TORC2. The fusion protein is unable to engage substrates in the complex due to mislocalisation. Although the free form of the fusion protein can engage substrates, it is not phosphorylated, and unphosphorylated wild-type is inactive, while the variant form is active independent of the phosphorylation status.

### 3.1.9. Glucose signaling and Ryh1 may act through different pathways to regulate TORC2-Gad8 signaling

It is now well established that TORC2 plays critical roles in Akt activation in response to growth factors (Guertin et al., 2006; Sarbassov et al., 2005). Yeasts do not possess the receptor tyrosine kinase system; instead, the phosphorylation status of Gad8 at Ser546 reflects glucose availability and TORC2 activates Gad8 in response to glucose (Cohen et al., 2014; Hatano et al., 2015). However, how glucose availability is coupled with TORC2-Gad8 signaling is not known. Previously, it has been reported that a Rab-family small GTPase, Ryh1 regulates Gad8 activity; while the GTP-bound form of Ryh1 up-regulates Gad8, the GDP-bound form down-regulates Gad8 (Tatebe et al., 2010). Moreover, the data imply that Ryh1 regulates the Gad8 activity by modulating the Sin1-Gad8 interaction, but not the Tor1 kinase activity itself. By employing the Ste20-Gad8 fusion protein, it is easy to evaluate the intrinsic kinase activity of Tor1 within TORC2. In order to examine the intrinsic Tor1 kinase activity in the presence of the active and inactive forms of Ryh1, the Ste20-Gad8 fusion protein was expressed in *Δste20* or *Δsin1* cells expressing GTP-locked Ryh1Q70L or GDP-locked Ryh1T25N from the chromosomal *ryh1* locus. In both *Δste20* and *Δsin1* backgrounds, the GTP-bound form of Ryh1 failed to augment the phosphorylation of the Gad8 part at Ser546 (Figure 16A). In the *ryh1TN* cells, a significant level of the Ser546 phosphorylation can be observed compared to that in *tor1DA* cells. These observations are consistent with the previous report showing that Ryh1 does not affect the catalytic activity of Tor1 in *in-vitro* kinase assays (Tatebe et al., 2010). It can be speculated that, if only Ryh1 mediates glucose signaling to TORC2, glucose availability would not affect the intrinsic kinase activity of Tor1. To probe the intrinsic kinase activity of Tor1 in response to glucose availability, the Ste20-Gad8 fusion protein was expressed in *Δsin1* cells, which were then subjected to glucose starvation. Upon glucose withdrawal, the Gad8 phosphorylation level at Ser546 of the fusion protein began to decline, reaching the lowest level around 20 min (right), as was the case with

the unfused Gad8 (left) (Figure 16B). This observation indicates that glucose availability can modulate the intrinsic kinase activity of Tor1.

There are several things to note in these experiments. First, the expression of the Ste20-Gad8 fusion protein seemed to prevent endogenous Gad8 from being hyper-phosphorylated in *ryh1QL* cells, indicating that the fusion protein might interfere with the process where Ryh1 modulates TORC2. Second, the presence of endogenous Ste20 would prevent the incorporation of the Ste20-Gad8 fusion protein into TORC2. Hence, it is not surprising that the Gad8 phosphorylation level in *Δsin1* cells as well as in *ryh1TN* cells was lower than that in *Δste20* cells; although Gad8 was phosphorylated at Ser546 in *ryh1TN* cells when compared to *tor1DA* cells, the phosphorylation level was not so significant considering the expression level of the fusion protein. Third, considering the expression levels of the Ste20-Gad8 fusion proteins in the *Δste20* and *Δste20 ryh1QL* as well as *Δsin1* and *Δsin1 ryh1QL* strains, the intrinsic kinase activity of Tor1 can be considered to be compromised in the presence of the GTP-bound from of Ryh1. Forth, whilst the Ser546 phosphorylation of wild-type Gad8 started to be recovered at 20min reaching the maximal phosphorylation level at 30min after glucose withdrawal, the Ser546 phosphorylation of the Ste20-Gad8 fusion protein remained low even at 30min after glucose depletion. This forth observation indicates that the intrinsic kinase activity of Tor1 is not recovered in glucose starvation and points towards the possibility that the recovery of the Gad8 phosphorylation at Ser546 can be caused either by another protein kinase or by the unavailability of phosphatases as a result of the glucose starvation.

**Figure 16.**

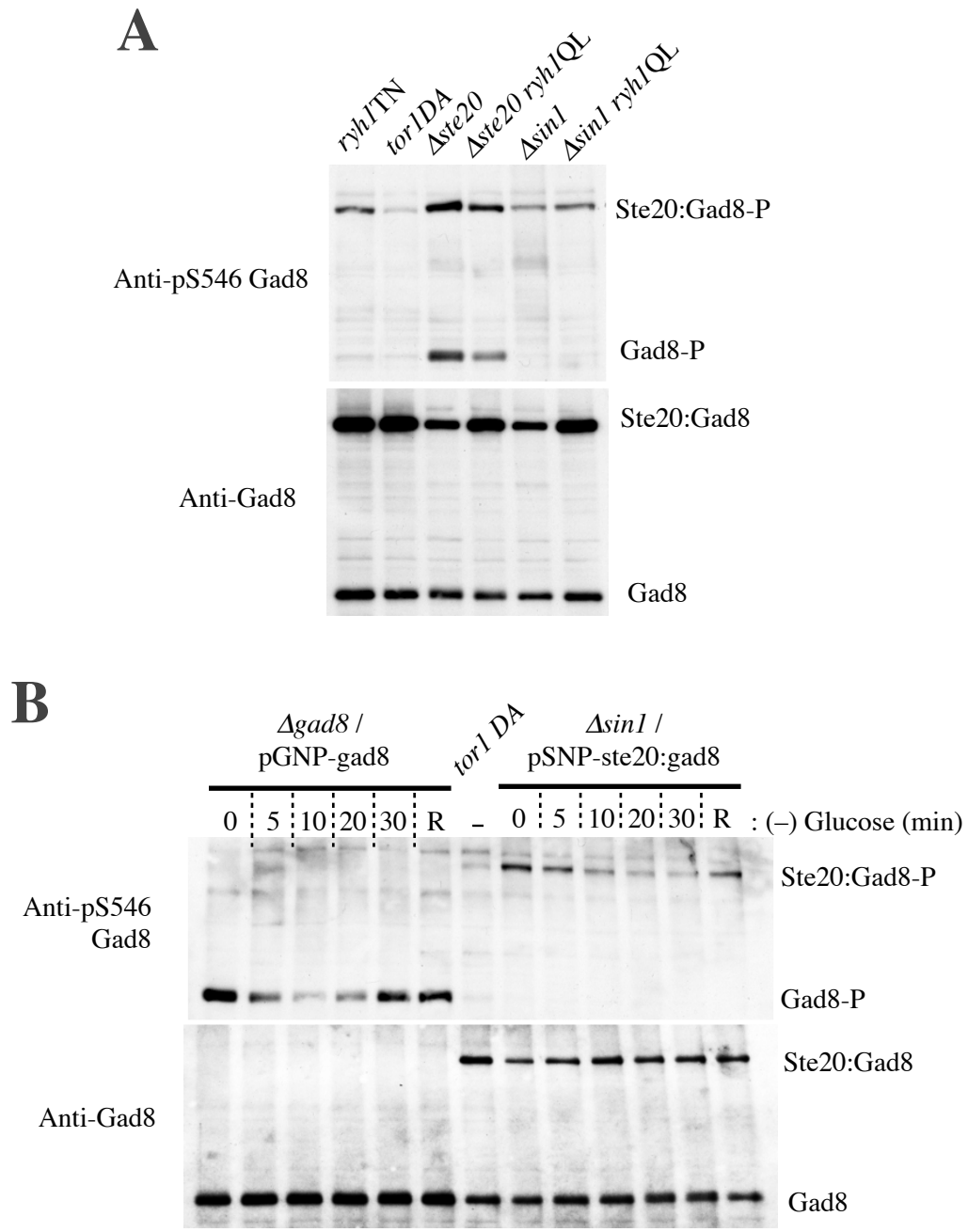


**Figure 16. Tor1 kinase activity responds to glucose starvation, but not to GTP-locked form of Rhy1**

(A) The GTP-bound form of Ryh1 does not affect Tor1 kinase activity. The Ste20-Gad8 fusion protein was expressed in indicated cell strains; *ryh1QL* strain produces GTP-locked form of Ryh1, while *ryh1TN* strain produces GDP-locked form of Ryh1 . The resultant cell lysates were subject to immunoblotting against the phospho-Ser546 of Gad8 or Gad8.

(B) Glucose withdrawal reduces Tor1 kinase activity. The Ste20-Gad8 fusion protein was expressed from plasmids under the control of Sin1 native promoter in *Δsin1* cells as well as *tor1DA* cells as a negative control. Gad8 protein was expressed from plasmids under the control of Gad8 native promoter in *Δgad8* cells for comparison. The resultant cell lysates were subject to immunoblotting against phospho-Ser546 of Gad8 or Gad8.

### 3.1.10. Intrinsic Tor kinase activity has no specificity against Gad8

Through the study of Sin1 in the previous sections, the notion has been reinforced that the substrate specificity of TORC2 is conferred by a specific subunit. This points to the possibility that the Tor kinases themselves cannot distinguish their substrates. Here, I extend the fusion-protein approach to investigate if the Tor2 kinase that forms TORC1 together with the Mip1 subunit can phosphorylate Gad8, when Gad8 is presented to Tor2. A plasmid was constructed to express the Mip1-Gad8 fusion protein, in which the N-terminus of Gad8 was fused to the C-terminus of Mip1. TORC1 loses its activity in response to nitrogen starvation, as evidenced by the phosphorylation status of its substrate, the Psk1 kinase, as well as the Psk1 substrate S6 (Nakashima et al., 2012). Thus, if the Mip1-Gad8 fusion protein is phosphorylated at Ser546 of the Gad8 part in a Tor2-dependent manner, then the phosphorylation level should be declined in response to nitrogen withdrawal. To exclude the possible phosphorylation of Mip1-Gad8 by TORC2, the experiment was performed with *Δtor1Δsin1* cells. As shown in Figure 17A, the phosphorylation level at Ser546 of the Mip-Gad8 fusion dramatically dropped just 5min after nitrogen withdrawal. It would be of note that the phosphorylation levels of Psk1 and S6 started to drop from later time points.

To confirm that the observed Ser546 phosphorylation of the Mip1-Gad8 fusion protein is specifically regulated by Tor2, the temperature-sensitive *tor2* mutant strain was employed. As in Figure 17B, the Ser546 phosphorylation level of the Mip-Gad8 fusion protein in a wild-type strain (*tor2*$^{+}$) was unchanged after a temperature shift from 25˚C to 35˚C. On the other hand, the Ser546 phosphorylation level of the fusion protein in the *tor2*$^{ts}$ mutant strain was dramatically reduced by 70% after the temperature shift-up to the restrictive temperature. These experiments demonstrate that Tor2 can phosphorylate Ser546 in the hydrophobic-motif of Gad8 when Gad8 is brought to the proximity to Tor2, demonstrating that the substrate specificity of Tor2 kinase itself is not so stringent; at least, the Tor2 kinase seems to be unable

to distinguish Gad8 from its canonical substrate, Psk1.

**Figure 17.**

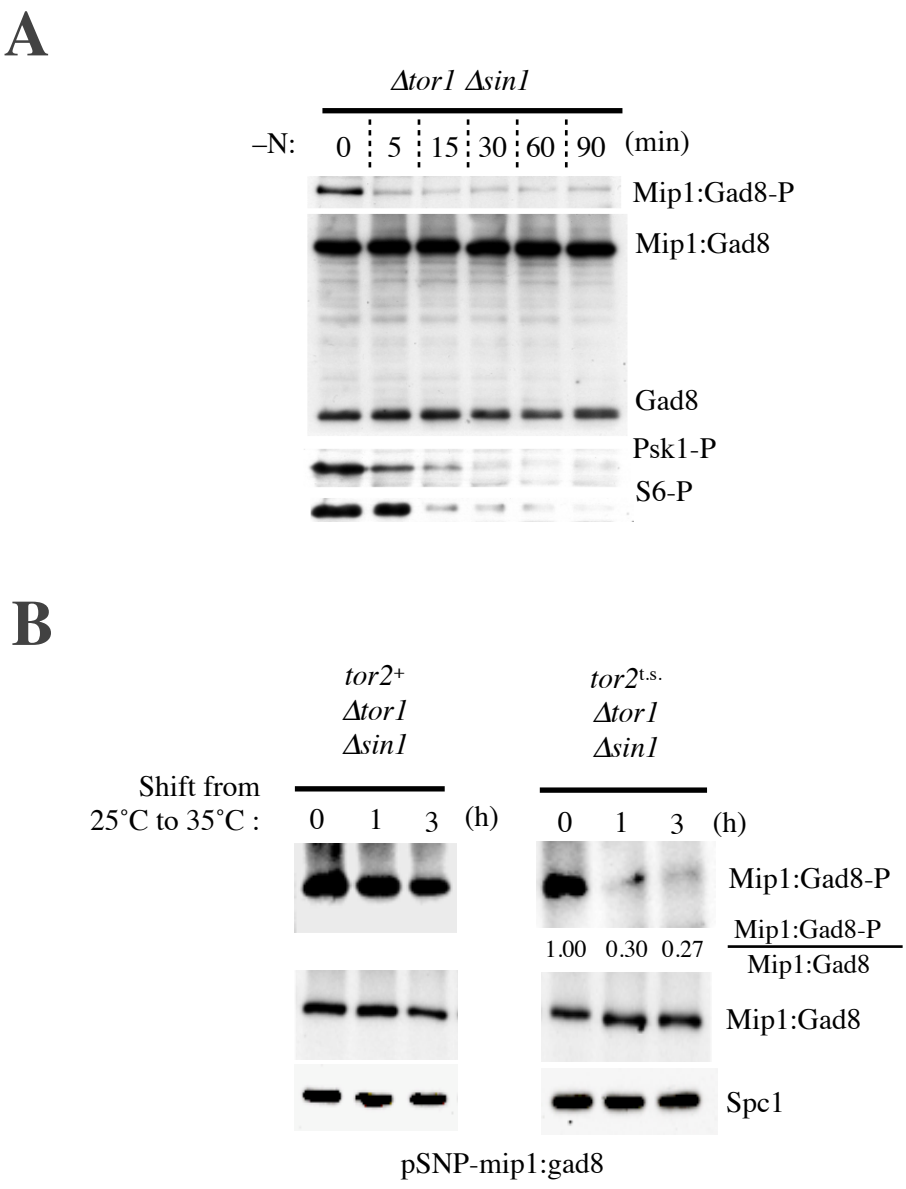


**Figure 17. Artificial presentation of Gad8 to Tor2 kinase induces Tor2-dependent phosphorylation of Gad8**

(A) Nitrogen withdrawal causes the reduction of the phosphorylation on the C-terminal hydrophobic motif of Gad8 that is fused to Mip1. Mip1-Gad8 fusion protein was expressed in the *Δsin1 Δtor1* cells. After withdrawal of nitrogen source, the cells were sampled at the indicated time points (*R refers to re-additon of nitrogen source). The resultant cell lysates were subject to immunoblotting by the antibodies against either the phosphorylated HM site of Gad8 or Gad8 as well as phosphorylated form of Psk1 (the direct substrate of TORC1) and phosphorylated S6 (the substrate of Psk1). Gad8 blot serves as a loading control.

(B) Gad8 phosphorylation level of Mip1-Gad8 fusion protein is significantly reduced upon temperature shift in temperature-sensitive *tor2* strain. Mip1-Gad8 fusion protein was expressed in either *Δtor1 Δsin1* cells or *tor2* ts *Δtor1 Δsin1* cells. After shift-up to 35˚C, cells were collected at the indicated time points. The resultant cell lysates were subject to immunoblotting against the phospho-Ser546 Gad8 or Gad8 as well as Spc1 (for a loading control). The Ser546 phosphorylation levels of Mip1-Gad8 normalized against Mip1:Gad8 were presented as numerical expressions.

## 3.2. Identification and characterization of Sin1 binding site within Gad8

### 3.2.1. Gad8 N-terminal variants can bypass TORC2-dependent phosphorylation for their activation

In order to further characterize the protein-protein interaction interface between Sin1 and Gad8, the Gad8 variants carrying one or two amino acid substitutions were generated by a PCR-based random mutagenesis. These Gad8 variants were subjected to a reverse yeast two-hybrid screen where those unable to interact with Sin1 were isolated. For PCR mutagenesis, Gad8 was divided into three regions; the N-terminal non-catalytic domain (residues 1-203), the N-lobe of the kinase domain (residues 162-384), and the rest of the protein (from the C-lobe of the kinase domain to the C-terminus), which was not covered in this study as it does not interact with Sin1 (see Figure 21G). Mutagenesis of the Gad8 N-terminal portion (residues 1-203) successfully isolated single amino acid substitutions that disrupt the Sin1-Gad8 interaction (Figure 18A). Using the budding yeast Gad8 ortholog, Ypk2, Kamada *et al*., previously reported that an alanine substitution of residue D239 resulted in constitutive activation of Ypk2, by bypassing the requirement of TORC2 for the activation of Ypk2 (Kamada et al., 2005). Ypk2 D239 corresponds to D153 in Gad8 and, in consistent with the observation with Ypk2, the D153G substitution has been identified in the above screen. The isolated Gad8 N-terminal variants including D153G were expressed in *Δtor1 Δgad8* cells from the Gad8 native promoter (GNP) and their cell lysates were subjected to *in-vitro* binding assays with GST-Sin1GAD. None of the Gad8 N-terminal variants were co-purified with GST-Sin1GAD, whereas a stable interaction can be seen with wild-type Gad8 (Figure 18B). In order to evaluate the TORC2-independent activities of the Gad8 N-terminal variants, I first confirmed that the Gad8 N-terminal variants were not phosphorylated at Ser546 in the absence of TORC2, by immunobloting against phopho-Ser546. None of the Gad8 N-terminal variants were phosphorylated at Ser546 in the *Δtor1 Δgad8* background (Figure 18C). The

TORC2-independent activities of the Gad8 N-terminal variants were then evaluated by the complementation of the stress-sensitive phenotypes of a *Δtor1 Δgad8* strain. The expression of some of the Gad8 variants suppressed the hypersensitive phenotype of the *Δtor1 Δgad8* strain to high osmolarity and high calcium concentration; prominent effects were seen with the K128E, D153A and D153G variants (Figure 18D). Thus, these Gad8 N-terminal variants appear to be functional in the absence of the TORC2-dependent phosphorylation. However, the Gad8 N-terminal variants expressed in the TORC2-active cells were found to be phosphorylated at Ser546 (Figure 18E; upper panel). This phosphorylation occurs in a Sin1-dependent manner because the phosphorylation at Ser546 was abolished when the Gad8 N-terminal variants were expressed in *Δsin1* cells (Figure 18E; lower panel), implying that these Gad8 N-terminal variants still have a weak affinity for Sin1. Consistent with these results, the complementation ability of the Gad8 N-terminal variants were by far greater when functional TORC2 was present (compare *Δtor1* and *Δgad8* cells in Figure 18F), indicating that the Gad8 N-terminal variants can be activated in a TORC2-dependent fashion. Table 5 summarizes the observations of the isolated Gad8 N-terminal variants.

**Figure 18.**

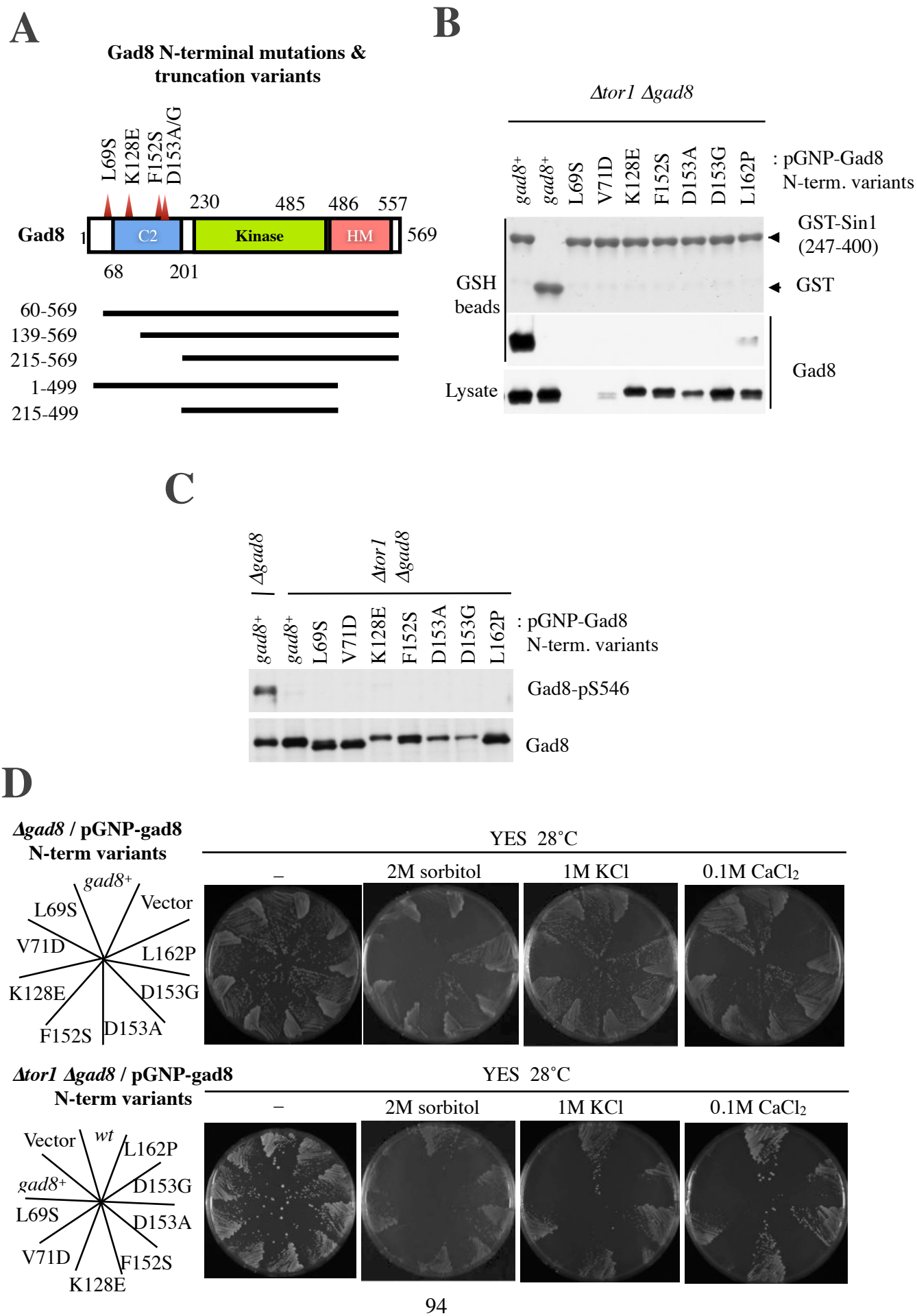
A
Gad8 N-terminal mutations & truncation variants
L69S
K128E
F152S
D153A/G
230
485
486
557
Gad8
1
C2
Kinase
HM
569
68
201
60-569
139-569
215-569
1-499
215-499
B
Δtor1 Δgad8
gad8+
gad8+
L69S
V71D
K128E
F152S
D153A
D153G
L162P
: pGNP-Gad8 N-term. variants
GST-Sin1 (247-400)
GST
GSH beads
Gad8
Lysate
C
Δgad8
Δtor1 Δgad8
gad8+
gad8+
L69S
V71D
K128E
F152S
D153A
D153G
L162P
: pGNP-Gad8 N-term. variants
Gad8-pS546
Gad8
D
Δgad8 / pGNP-gad8 N-term variants
YES 28°C
–
2M sorbitol
1M KCl
0.1M CaCl2
gad8+
Vector
L69S
V71D
L162P
K128E
D153G
F152S
D153A
Δtor1 Δgad8 / pGNP-gad8 N-term variants
YES 28°C
–
2M sorbitol
1M KCl
0.1M CaCl2
Vector
wt
L162P
gad8+
D153G
L69S
D153A
V71D
F152S
K128E

**Figure 18.**

**E**

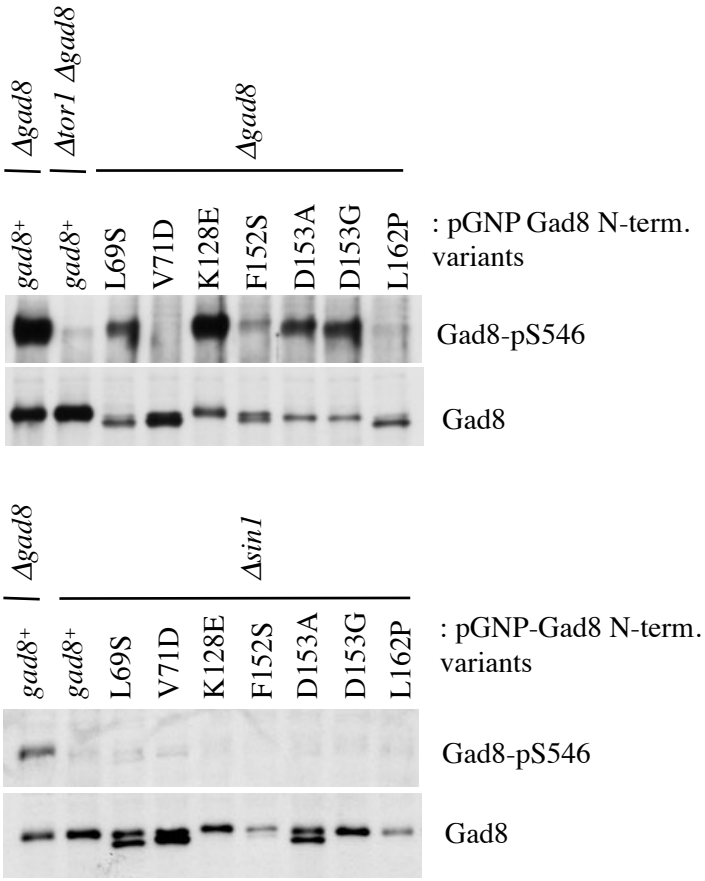
Δgad8
Δtor1 Δgad8
Δgad8
gad8+
gad8+
L69S
V71D
K128E
F152S
D153A
D153G
L162P
: pGNP Gad8 N-term. variants
Gad8-pS546
Gad8
Δgad8
Δsin1
gad8+
gad8+
L69S
V71D
K128E
F152S
D153A
D153G
L162P
: pGNP-Gad8 N-term. variants
Gad8-pS546
Gad8

**F**

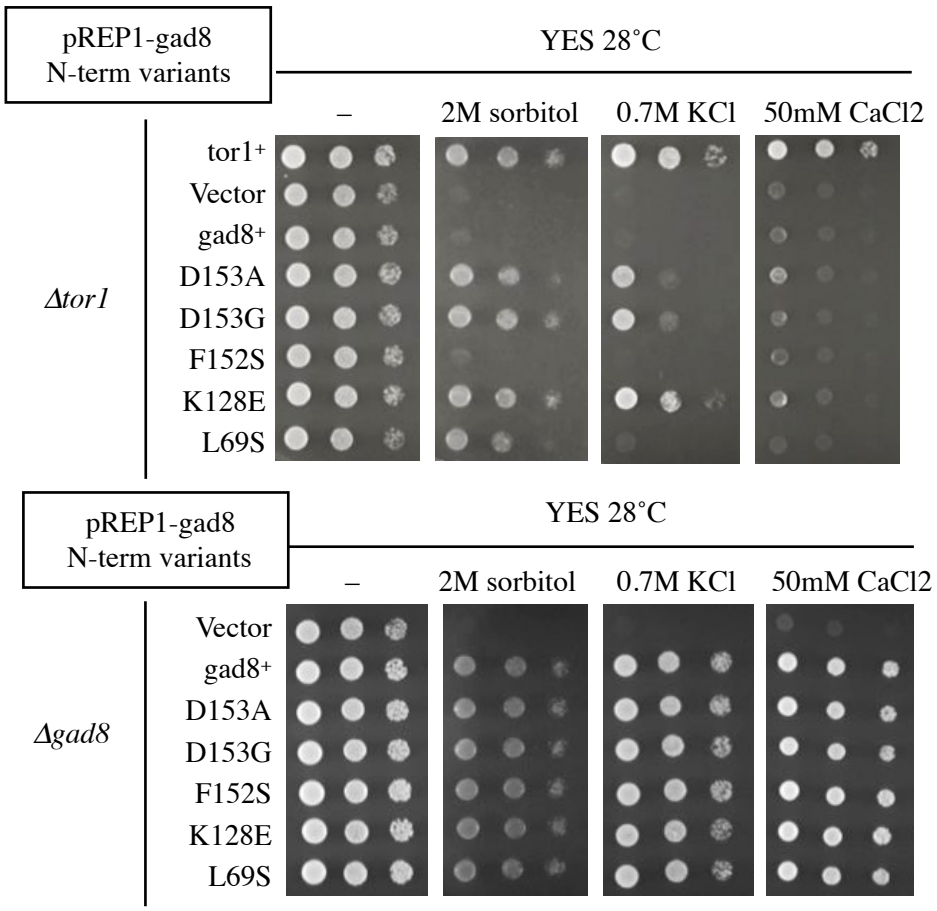
pREP1-gad8 N-term variants
YES 28˚C
–
2M sorbitol
0.7M KCl
50mM CaCl2
Δtor1
tor1+
Vector
gad8+
D153A
D153G
F152S
K128E
L69S
pREP1-gad8 N-term variants
YES 28˚C
–
2M sorbitol
0.7M KCl
50mM CaCl2
Δgad8
Vector
gad8+
D153A
D153G
F152S
K128E
L69S

## Figure 18.

**Figure 18. Amino acid substitutions that cancel the *cis*-inhibitory effect imposed by the Gad8 N-terminal portion enable Gad8 to bypass the regulation by TORC2**

(A) Deletion and mutagenic analysis of Gad8. Schematic diagram represents the architecture of Gad8 protein showing the positions of isolated amino acid substitutions that disrupt the interaction of the Gad8 variants with Sin1 in the yeast two-hybrid assay along with Gad8 truncation variants. C2 = C2 domain, Kinase = Kinase domain, HM = Hydrophobic motif.

(B) Disruption of the Sin1-Gad8 interaction by single amino acid substitutions in Gad8 N-terminal potion. Purified GST and GST-Sin1 (247-400) on GSH beads were prepared by incubating the beads with the BL21 bacterial lysates expressing each. The Gad8 variants with the single amino acid changes were expressed in *Δtor1 Δ gad8* cells from Gad8 native promoter. The cell lysates were incubated with GST-Sin1 (247-400) or GST alone for wild-type Gad8. The precipitated fraction as well as crude cell lysate were analyzed by immunoblotting with anti-Gad8 antibody. GST and GST-Sin1 (247-400) in the pulldown samples were visualized by CBB staining. The Gad8 variants with L69S and V71D substitution were very unstable and degraded during the preparation of the crude lysate.

(C) Mutant Gad8 are not phosphorylated in a *Δtor1* background. The *Δtor1 Δ gad8* cells expressing the Gad8 variants as in (B) were TCA-extracted and the samples were subject to Western-blotting analysis with antibodies against phospho-Ser546 and Gad8.

(D) Some of the Gad8 variants can complement the stress sensitivity of the *Δtor1 Δgad8* strain. The *Δtor1 Δ gad8* cells expressing the Gad8 variants as in (B) were streaked onto a control YES plate ("–") as well as the YES plates containing 2M sorbitol, 1M KCl and 0.1M $CaCl_2$.

(E) Mutant Gad8 are phosphorylated in TORC2 dependent manner. The *Δsin1* and *Δgad8* were transformed with pGNP-vector expressing Gad8 variants along with wild-type Gad8 as in (B). The *Δtor1 Δgad8* cells expressing wild-type Gad8 served as a negative control for phospho-Gad8 blot. The samples were prepared and analyzed as in (C).

(F) The Gad8 N-terminal variants can still further be activated through the phosphorylation by TORC2. The *Δtor1* as well as *Δgad8* cells were transformed with pREP-vector expressing the Gad8 variants that were found phosphorylated in (E) along with wild-type Gad8 and an empty vector under the control of the *nmt* promoter. The expression of the plasmids were maintained minimum as YES medium contains thiamine. Ten-fold serial dilutions of cell suspensions were spotted onto a control YES plate ("–") along with those containing 2M sorbitol, 0.7M KCl and 50mM $CaCl_2$.

**Table 5. Summary of the data for the Gad8 N-terminal variants presented in Figure 18.**

| gene: gad8 [Fig. 17A] | Interaction with Sin1CRIM[1] [Fig. | Δgad8[2] [Fig. 17E] | Δtor1 Δgad8[2] [Fig. 17C] | Δgad8[3] | Δtor1 Δgad8[3] | Sensitivity test at 0.7-1M KCL: Δgad8[4] | | Δtor1 Δgad8[4] | | Surface[5] [Supp. Fig. 1] | Comments |
|---|---|---|---|---|---|---|---|---|---|---|---|
| **Substitution** | **GST-Sin1 (247-400)** | **pS546 (%)*** | **pS546 (%)*** | **Exp. Level (%)*** [Fig. 17D, F] | | **Streak** [Fig. 17D] | **Spot *** [Fig. 17F] | **Streak** [Fig. 17D] | **Spot *** [Fig. 17F] | **Surface Exposure** | **Comments on the expression-suppressive activity of Gad8** |
| L69S | N/A | 52 | 0 | 49 | 121 | ++ | ++++ | + | ++ | Buried | Minimum activity in the absence of TORC2. Can be fully activated by TORC2. |
| **V71D** | N/A | 0 | 0 | 97 | 114 | — | N/A | — | N/A | Buried | Cannot be activated by TORC2 and disfunctional |
| **K128E** | None | 91 | 0 | 55 | 62 | ++ | ++++ | ++ | ++++ | Surface | Active even in the absence of TORC2 |
| **F152S** | None | 16 | 0 | 47 | 106 | ++ | ++++ | + | — | Surface | Minimum activity in the absence of TORC2. Can be fully activated by TORC2. The phosphorylated/active form is unstable. |
| **D153A** | None | 55 | 0 | 31 | 55 | ++ | ++++ | ++ | +++ | Surface | Active even in the absence of TORC2 |
| **D153G** | None | 101 | 0 | 27 | 35 | ++ | ++++ | ++ | +++ | Surface | Active even in the absence of TORC2 |
| **L162P** | little | 5 | 0 | 50 | 170 | ++ | N/A | — | N/A | Buried | No activity in the absence of TORC2, and yet can be fully activated by TORC2. The phosphorylated/active form is unstable. |

*Signal quantification was done using imageJ (100% = wt)

**Expressed from pGNP(Gad8 Native Promoter)

***Expressed from pREP1

1 = Gad8 variants co-purified with GST-Sin1CRIM: None equals to the level of GST control.

2 = TORC2-dependent phosphorylation level at S546 in *Δgad8* or *Δtor1 Δgad8*

3 = The expression levels of the Gad8 variants in *Δgad8* or *Δtor1 Δgad8*

4 = YES+1M KCL (stress) at 30˚C: –, no growth even at the highest cell concentration; +, growth at 3 dilution factor; ++, growth at 2 dilution factor. +++, growth at 1 dilution factor. ++++, wild-type level growth.

5 = The surface exposure of the amino acid residues on the molecular surface of the Gad8 N-terminal region judged using the theoretical 3D structure of the Gad8 N-terminal region.

**Table 5. lists the test results for the Gad8 N-terminal variants, which are then classified as shown in comments according to their deduced features.**

the TORC2-dependent phosphorylation of the C-terminal hydrophobic motif (Kamada et al., 2005). Therefore, a series of N-terminal deletion variants of Gad8 was generated and examined for their ability to complement the stress sensitivity of *Δtor1* and *Δgad8* cells. The spot assays revealed that the truncation variant (residues 215-569) lacking most of the N-terminal non-catalytic domain (residues 1-229) rescued the growth defect of *Δtor1* cells on the stress plates (Figure 19A; left panel). In *Δgad8* cells where functional TORC2 presents, the Gad8 215-569 variant seems to be further activated, markedly suppressing the growth defect on the stress plates (Figure 19A; right panel). These observations suggest that the Gad8 215-569 variant still interacts with TORC2. Indeed, the Gad8 230-569 variant was co-purified with the recombinant fusion protein of MBP-Sin1 in an *in-vitro* binding assay (Figure 19B). However, compared to wild-type Gad8 (left panel), the binding affinity of the N-terminally truncated Gad8 with Sin1 (right panel) was significantly reduced. Together with the results of the point mutations (Table 5), these results imply that the N-terminal region of Gad8 may be required for the proper formation of the Sin1-docking site.

In general, a kinase binds its substrate and, once phosphorylation reaction is completed, it releases the substrate so that the activated substrate can work on its downstream effector(s) (Ubersax and Ferrell, 2007). Indeed, as shown in Figure 15C & D, the Ste20-Gad8 fusion trapped in TORC2 could not complement the growth defects of *Δsin1 Δste20* cells under stress conditions, illustrating the need for a release of activated Gad8. To investigate if Sin1 preferentially binds to the inactive form of Gad8, the Sin1-Gad8 interaction was compared between the TORC2 hyper-activating strain, *ryh1QL,* and the TORC2-inactivating strain, *ryh1TN* along with a *tor1DA* strain as a negative control. Immunoblotting with anti-phospho-Ser546 antibodies confirmed that the Gad8 phosphorylation at Ser546 in *ryh1QL* cells was prominent in the cell lysate (Figure 19D). The cell lysates derived from each strain were incubated with GSH beads bound with either GST alone or GST-Sin1GAD. The amount

of Gad8 co-purified with GST-Sin1GAD from *ryh1QL* cells was significantly reduced compared to that from *ryh1TN* and *tor1DA* cells (Figure 19D). These results imply that Sin1 preferentially binds to an inactive form of Gad8.

**Figure 19.**

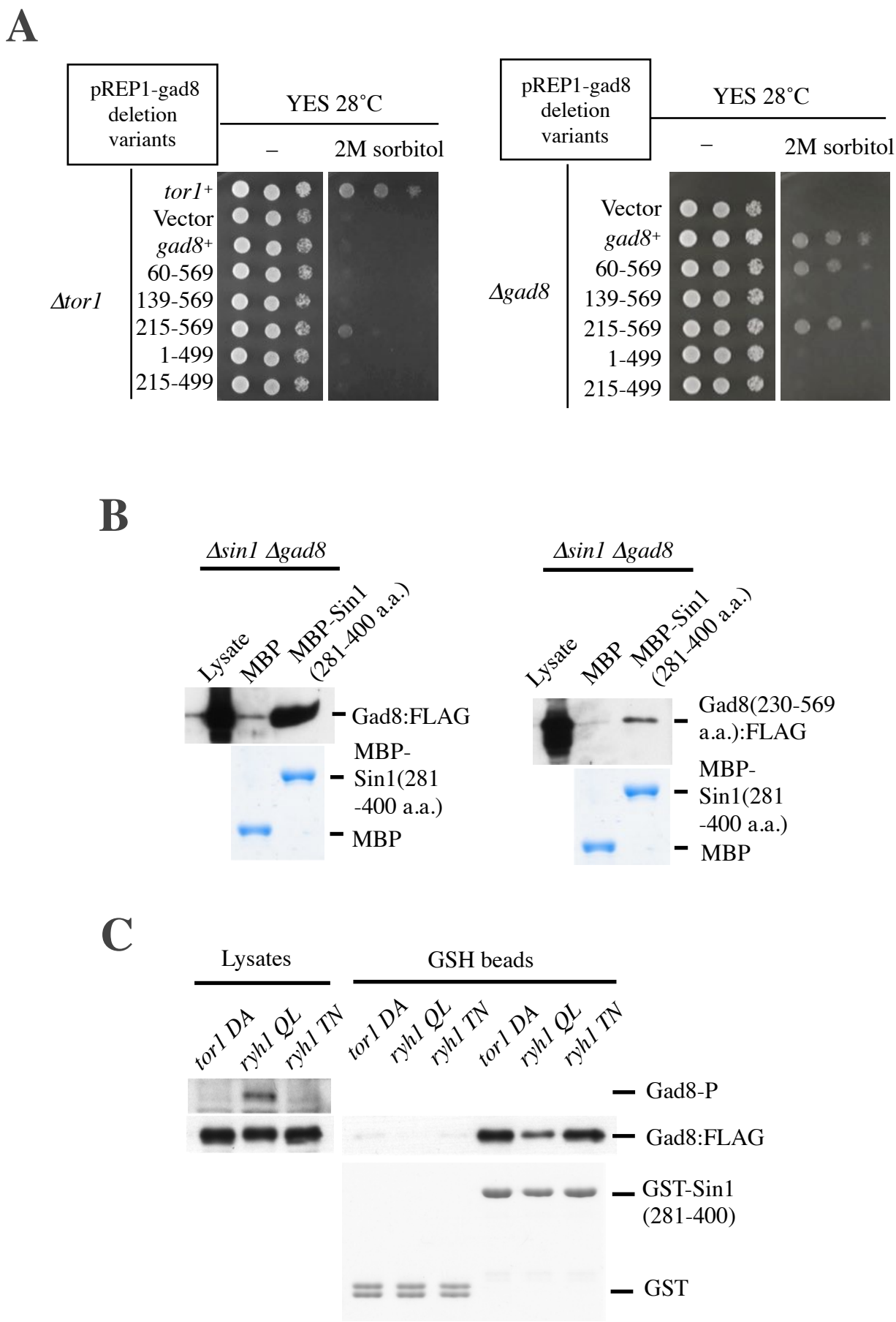
A
pREP1-gad8 deletion variants
YES 28˚C
–
2M sorbitol
Δtor1
tor1+
Vector
gad8+
60-569
139-569
215-569
1-499
215-499
Δgad8
B
Δsin1 Δgad8
Lysate
MBP
MBP-Sin1 (281-400 a.a.)
Gad8:FLAG
MBP-Sin1(281-400 a.a.)
MBP
Gad8(230-569 a.a.):FLAG
C
Lysates
GSH beads
tor1 DA
ryh1 QL
ryh1 TN
Gad8-P
Gad8:FLAG
GST-Sin1 (281-400)
GST

## Figure 19.

**Figure 19. The N-terminal non-catalytic portion of Gad8 play an important role in Gad8 activation, which might be modulated by the interaction with Sin1**

(A) Deletion of the N-terminal portion partially restores the kinase activity of the mutant Gad8 independently of TORC2 regulation. The Gad8 deletion constructs described in (A) were transformed into *Δtor1* and *Δgad8* strains along with wild-type tor1, gad8 and empty vector as controls. Serially diluted cells as in (F) were spotted onto YES plate ("–") as well as YES 2M sorbitol plate.

(B) Sin1GAD binds to the Gad8 variant deleted for its N-terminal portion. Gad8:FLAG as well as Gad8 (230-569 a.a.):FLAG were expressed under the control of Gad8 native promoter (GNP) from plasmids in *Δsin1 Δgad8* cells. The cell lysates were subject to incubation with either MBP-Sin1 (281-400 a.a.) or MBP alone bound amylose resins. Precipitated resins were probed for co-purification of Gad8:FLAG or Gad8 (230-569 a.a.):FLAG by immunoblotting with anti-FLAG antibody.

(C) Sin1 CRIM selectively binds to unphosphorylated/inactive form of Gad8. The cell lysates prepared from *ryh1QL*, *ryh1TN* and *tor1DA* cells expressing Gad8:FLAG were incubated with the GSH beads bound with wither GST alone or GST-Sin1 (281-400 a.a.). Co-purification of Gad8:FLAG was detected by immunoblotting with anti-FLAG antibody.

### 3.2.2. Characterizing the single amino acid substitutions in the Gad8 kinase domain that disrupt the interaction with Sin1

In an effort to characterize the Sin1-Gad8 interface, the reverse yeast two-hybrid screen has also been applied to the N-lobe of the Gad8 kinase domain to isolate amino acid substitutions that disrupt the interaction with Sin1 (Figure 20A). The isolated amino acid substitutions were classified into two classes, depending on the degree of the inhibitions of growth on the yeast two-hybrid assay plates; those shown in red color represent strong inhibitions, while weak inhibitions are in blue. I focused on the strong inhibitory mutations in the following biochemical assays. The Gad8 kinase variants carrying those amino acid substitutions failed to be co-purified with GST-Sin1GAD from the cell lysates (Figure 20B). Correspondingly, the TORC2-dependent phosphorylation at Ser546 was abolished in the most of the Gad8 kinase variants except for T252A and L303P (Figure 20C). However, the stress sensitivity tests revealed that most of the Gad8 kinase variants were still under the regulation of TORC2; they were able to grow on the stress plates when TORC2 was active, but not when TORC2 was inactive (Figure 20D). One exception to this was the T252A variant which was able to induce growth of the TORC2-deficient cells under stress conditions, like the K128E and D153A variants described in the previous section (Table 5). The other exception was the L303P variant that was unable to complement the stress sensitivity, even when phosphorylated at Ser546 in *Δgad8* cells. Table 6 summarizes the observations in Figure 20, together with the solvent surface accessibilities of the identified residues. It is quite probable that an amino acid substitution to the kinase domain alters its conformation, resulting in the reduced kinase activity. Therefore, it is important to know if the identified residues are available on the molecular surface of Gad8 for direct interaction with Sin1. For this purpose, a theoretical model of Gad8 was constructed through homology modeling based on the crystal structures of the inactive form of Akt2 (PDB ID: 1MRV)(Figure 20E, Table 6). From this model, residues T252 and L303 are predicted to be exposed, while the mutations to the buried

residues are likely to result in the disruption of the folding of the kinase domain (Figure 20E). Further evidence is required to determine whether residues T252 and L303 are involved in the direct binding to Sin1.

Interestingly, Gad8 L303 corresponds to L225 in Akt2 (L223 in Akt1; Figure 20A), which plays an important role in guiding the phosphorylated hydrophobic-motif in between the αB and αC helices (Calleja et al., 2009; Yang et al., 2002b). While the N-terminal domain binds to the kinase domain when Akt is inactive, the hydrophobic-motif on the C-terminal loop is tethered into the pocket formed between the αB and αC helices when Akt is activated (Calleja et al., 2009; 2007; Huang et al., 2011; Yang et al., 2002b). The theoretical 3D structure of the active form of Gad8 demonstrated that the side-chain of L303 is flanked by the side-chains of the F542 and F545 in the hydrophobic-motif, resulting in docking of the aromatic ring of F542 to the pocket formed by αB and αC helices (Supplemental Figure 1). Diagrams in Figure 20F explain a possible molecular mechanism for the effect of the L303P substitution, which prevents the C-terminal hydrophobic-motif from binding properly to the N-lobe of the kinase domain through the structured αB and αC helices. Limited interaction of the Gad8 L303P variant with TORC2 probably allows the observed phosphorylation at Ser546 (Figure 20C), though the L303P variant is not functional *in vivo* (Figure 20D).

Figure 20.

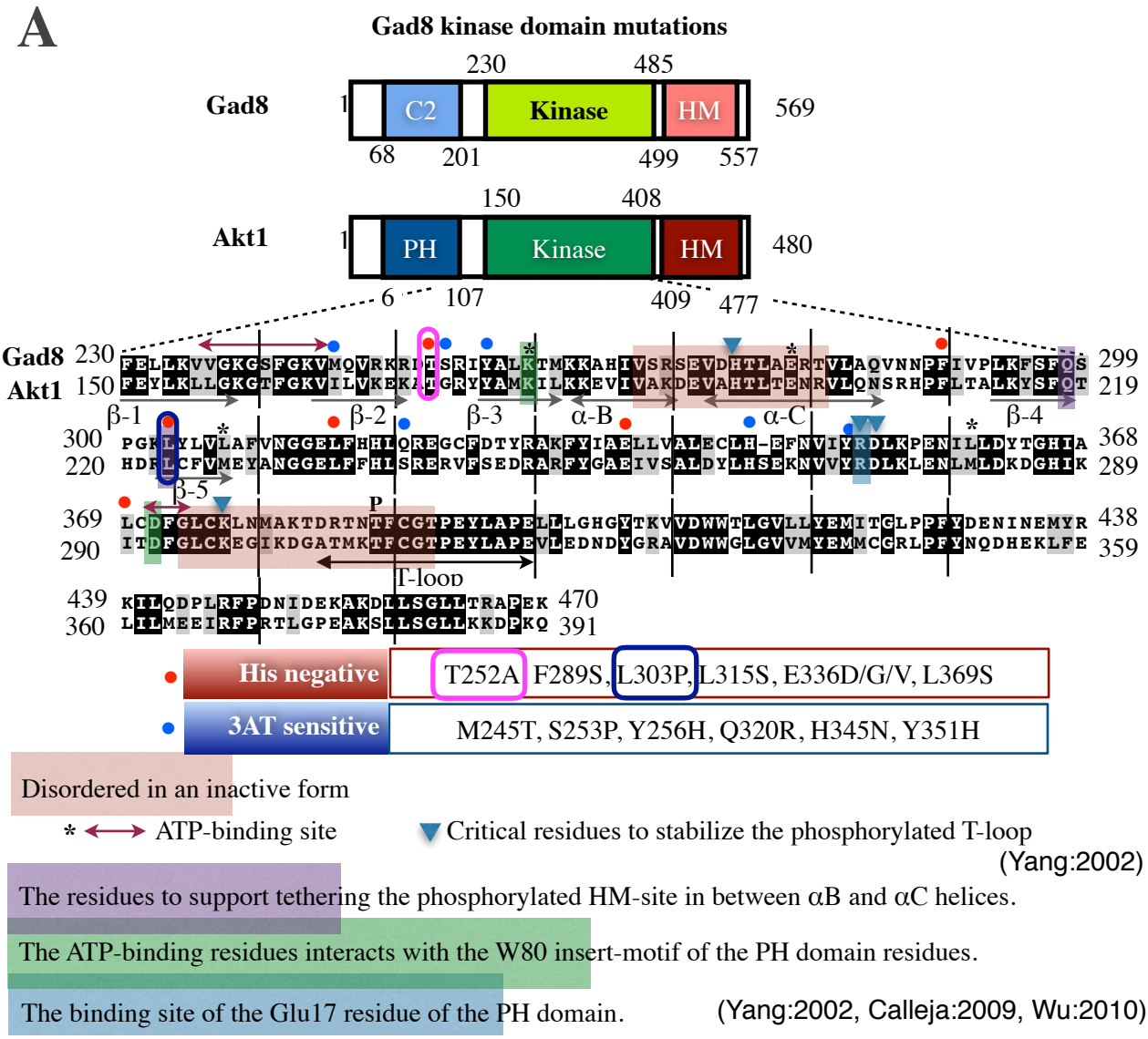
A
Gad8 kinase domain mutations
Gad8
230
485
1
C2
Kinase
HM
569
68
201
499
557
Akt1
150
408
1
PH
Kinase
HM
480
6
107
409
477
Gad8 230 FELLKVVGKGSFGKVMQVRKRDTSRIYALKTMKKAHIVSRSEVDHTLAERTVLAQVNNPFIVPLKFSFQS 299
Akt1 150 FEYLKLLGKGTFGKVILVKEKATGRYYAMKILKKEVIVAKDEVAHTLTENRVLQNSRHPFLTALKYSFQT 219
β-1 β-2 β-3 α-B α-C β-4
300 PGKLYLVLAFVNGGELFHHLQREGCFDTYRAKFYIAELLVALECLH-EFNVIYRDLKPENILLDYTGHIA 368
220 HDRLCFVMEYANGGELFFHLSRERVFSEDRARFYGAEIVSALDYLHSEKNVVYRDLKLENLMLDKDGHIK 289
β-5
P
369 LCDFGLCKLNMAKTDRTNTFCGTPEYLAPELLLGHGYTKVVDWWTLGVLLYEMITGLPPFYDENINEMYR 438
290 ITDFGLCKEGIKDGATMKTFCGTPEYLAPEVLEDNDYGRAVDWWGLGVVMYEMMCGRLPFYNQDHEKLFE 359
T-loop
439 KILQDPLRFPDNIDEKAKDLLSGLLTRAPEK 470
360 LILMEEIRFPRTLGPEAKSLLSGLLKKDPKQ 391
His negative
T252A F289S, L303P, L315S, E336D/G/V, L369S
3AT sensitive
M245T, S253P, Y256H, Q320R, H345N, Y351H
Disordered in an inactive form
* ATP-binding site
Critical residues to stabilize the phosphorylated T-loop
(Yang:2002)
The residues to support tethering the phosphorylated HM-site in between αB and αC helices.
The ATP-binding residues interacts with the W80 insert-motif of the PH domain residues.
The binding site of the Glu17 residue of the PH domain.
(Yang:2002, Calleja:2009, Wu:2010)
B
Δtor1 Δgad8
: pGNP-Gad8 Kinase Domain variants
gad8+ gad8+ T252A F289L L303P L315S E336D E336G E336V L369S
GSH beads
GST-Sin1 (247-400)
GST
Gad8
Lysate
C
Δgad8 Δtor1 Δgad8
: pGNP-Gad8 Kinase Domain variants
gad8+ gad8+ T252A F289L L303P L315S E336D E336G E336V L369S
Gad8-pS546
Gad8
Δgad8 Δtor1 Δgad8
: pGNP-Gad8 Kinase Domain variants
gad8+ gad8+ T252A F289L L303P L315S E336D E336G E336V L369S
Gad8-pS546
Gad8

**Figure 20.**

**D**

***Δgad8* / pGNP-gad8 Kinase Domain variants**

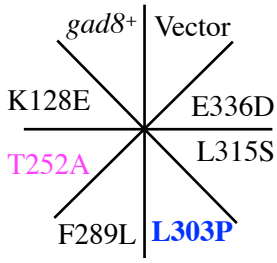


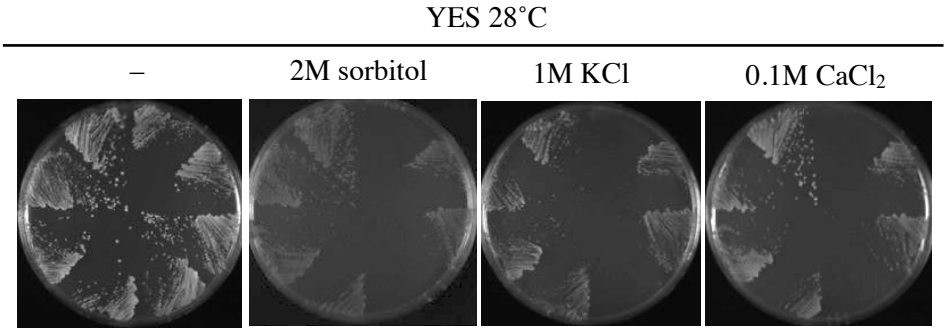


***Δtor1 Δgad8* / pGNP-gad8 Kinase Domain variants**

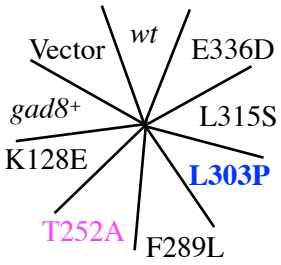


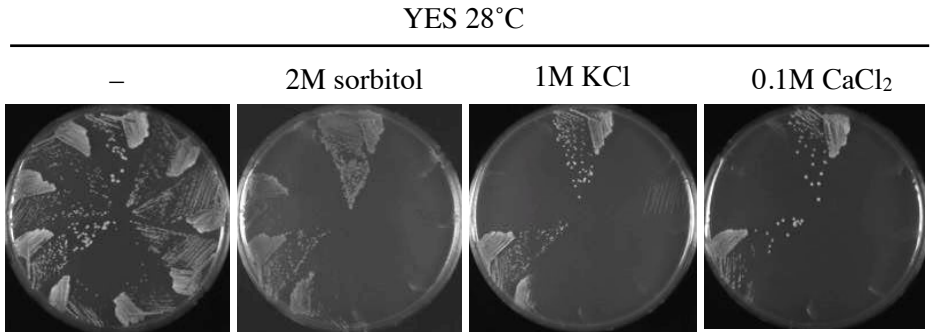


**E** **Gad8 (Theoretical model based on the inactive form of Akt2: 1MRV)**

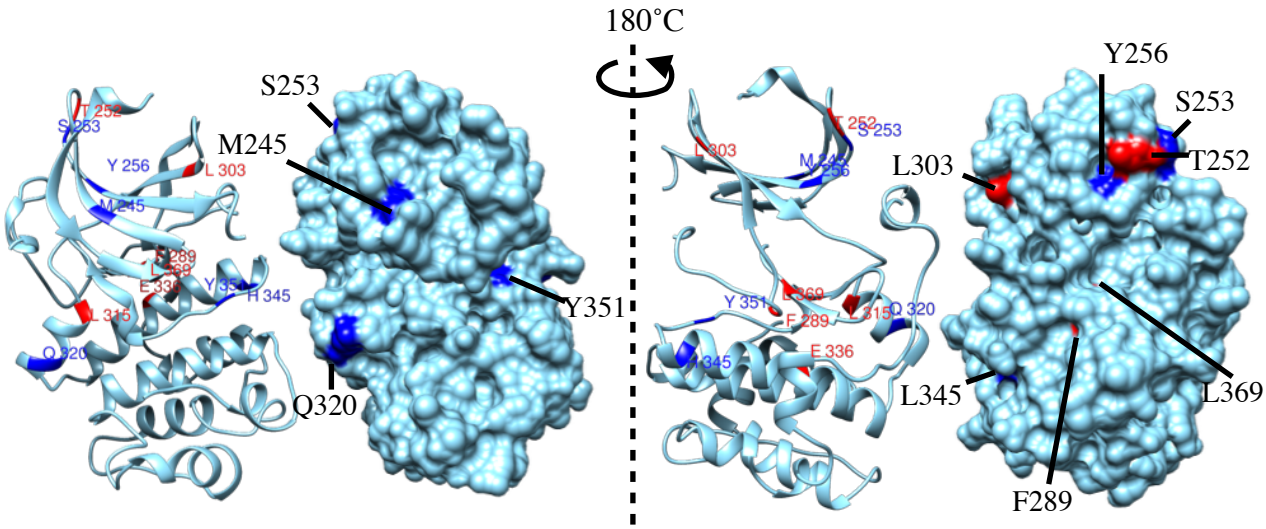


**F**

- **An inferred model that accounts for the mode of action of the Gad8 L303P variant**

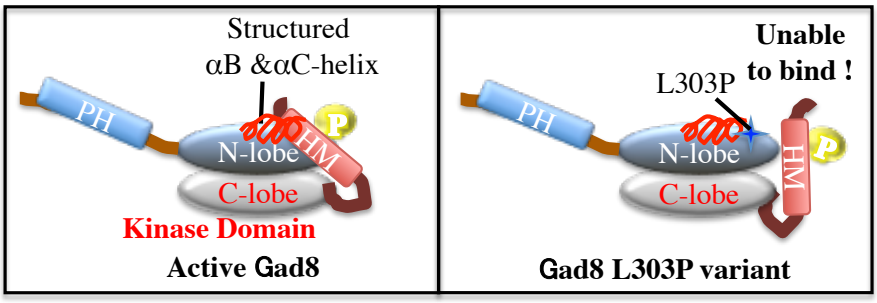

## Figure 20.

**Figure 20. Characterization of the Gad8 variants carrying the amino acid substitutions on its kinase domain that disrupt the interaction with Sin1**

(A) Deletion and mutagenic analysis of Gad8 on its N-lobe of the kinase domain. Schematic diagram represents the architecture of Gad8 and human Akt1. The pairwise sequence alignment by NEEDLE shows conserved amino acid residues; Identical residues are shaded black and conserved residues are shaded grey at a 50% level of consensus. The alignment also shows the the positions of isolated amino acid substitutions in Gad8 kinase domain. The mutagenesis was performed on the region of 162-384 a.a., the N-lobe of Gad8 kinase domain. A red dot (His negative) indicates an amino acid change by which Sin1 GAD lost the interaction with the Gad8 variants in Y2H assay on the plates lacking histidine. A blue dot (3AT sensitive) indicates an amino acid change by which Sin1GAD lost the interaction with the Gad8 variants in Y2H assay on the plates lacking histidine and supplemented with 3 AT drug which titrates histidine. The substituted residues are listed in red and blue boxes. The red double headed arrows and * shows ATP-binding site and the green shaded residue is suggested to be the binding site of W80 on the PH domain of Akt N-terminal portion. The purple shaded residues represent the site to interact with the C-terminal hydrophobic motif as previously reported {Wu:2010cw}. C2 = C2 domain, PH = Pleckstrin homology domain, Kinase = Kinase domain.

(B) Disruption of the Sin1-Gad8 interaction by single amino acid substitutions in Gad8 kinase domain. The interactions of the Gad8 kinase domain (KD) variants with Sin1CRIM were tested in GST-pulldown assay. The GST-Sin1 (247-400) was affinity-purified onto GSH beads along with GST alone negative control. The GSH beads were incubated with the cell lysates derived from the *Δtor1 Δgad8* cells expressing the Gad8 KD variants as well as wild-type Gad8 as controls. The purified GSH beads were examined for the co-purified Gad8 KD variants or Gad8 *wt*.

(C) The phosphorylation of the Gad8 KD variants are significantly compromised in the presence or absence of functional TORC2, except for a few exceptions. The *Δgad8* cells as well as the *Δtor1 Δgad8* cells expressing the Gad8 KD variants as in (B) were TCA-extracted and the samples were subject to Western analysis with antibodies against phopho-Ser546 or Gad8.

(D) The Gad8 KD variants did not manifest a significant bypassing effects and still seem to be under the regulation of TORC2, except for a few exceptions. The *Δgad8* cells as well as the *Δtor1 Δgad8* cells expressing the kinase domain Gad8 variants were streaked onto a control YES plate ("–") as well as the YES plates containing 2M sorbitol, 1M KCl and 0.1M $CaCl_2$. The K128E variant serves as a positive control.

(E) The theoretical model of a crystal structure of Gad8 (230-569 a.a.) was constructed based on the inactive form of Akt2 (AKT2_HUMAN: 1mrv) through homology modeling using UCSF Chimera and Modeller. The isolated mutations through this study is plotted on the ribbon and the surface representations of the theoretical model of Gad8. This mapping of mutation residues reveal which mutation sites are on the molecular surface and which sites are buried inside the protein folding. The classification with red and blue color are in accord with the results from Y2H (A).

(F) The diagram illustrates an inferred model that accounts for how L303P substitution might disrupt the formation of the bonding between the HM site and the αB and αC-helices.

**Table 6. Summary of the data for Gad8 kinase variants presented in Figure 18.**

| **gene: gad8** [Fig. 19A] | **Interaction with Sin1 CRIM** [Fig. 19B] | ***Δgad8*** *[Fig. 19C]* | ***Δtor1 Δgad8*** *[Fig. 19C]* | ***Δgad8*** *[Fig. 19D]* | ***Δtor1 Δgad8*** *[Fig. 19D]* | **Exposed on Molecular Surface** [Fig. 19E] |
|---|---|---|---|---|---|---|
| **Substitution** | **GST-Sin1 (247-400)** | **pS546 (%)*** | **pS546 (%)*** | **Streak**** | **Streak**** | **(accessible surface area, >25%)** |
| T252A | None | 10 | 0 | ++ | + | ○ (○) |
| F289L | None | 10 | 0 | ++ | — | × (×) |
| L303P | None | 50 | 0 | — | — | ○ (○) |
| L315S | None | 10 | 0 | ++ | — | × (×) |
| E336D | None | 0 | 0 | ++ | — | × (×) |
| E336G | None | 0 | 0 | ++ | — | × (×) |
| E336V | None | 0 | 0 | + | — | × (×) |
| L369S | None | 0 | 0 | ++ | — | △ (×) |
| M245T | N/A | N/A | N/A | N/A | N/A | ○ (×) |
| S253P | N/A | N/A | N/A | N/A | N/A | ○ (△) |
| Y256H | N/A | N/A | N/A | N/A | N/A | ○ (×) |
| Q320R | N/A | N/A | N/A | N/A | N/A | ○ (○) |
| H345N | N/A | N/A | N/A | N/A | N/A | ○ (×) |
| Y351H | N/A | N/A | N/A | N/A | N/A | ○ (○) |

*Signal quantification was done using imageJ (100% = wt)

**Expressed from pGNP(Gad8 Native Promoter)

**Table 6. summarizes the data obtained from the analysis of the Gad8 kinase domain variants isolated through the random mutagenesis study in Figure 18.**

The first column lists amino acid substitutions introduced to each Gad8 variant (Figure 19A). The classification with red and blue color are based on the degree of the growth suppression in the Y2H assay (Figure 19A). The second column lists the results of the GST-pulldown assay from Figure 19B (ND = Not Detected). In the third and fourth columns, the results of Figure 19 C are quantified and and expressed in % when compared to the wild-type as 100%. The fifth and sixth columns lists the results from the sensitivity tests (Figure 19D)[++ denotes the wild-type level growth rate, + denotes the growth rate less than half of that to wild-type. - denotes no growth]. The last column shows if the target amino acid residue is exposed on the molecular surface [○ = exposed, △ = half-exposed, X = not exposed, judged by the analysis of the theoretical 3D structure of Gad8 constructed based on Akt inactive form (PDB ID=1mrv).] Inside parenthesis shows if the accessible surface area of the amino acid residues are more than 25%, which can be judged as exposed from the molecular surface[○ = >25%, X = <25%]

### 3.2.3. Single amino acid substitutions of the predicted Sin1 binding-site on Gad8 result in the loss of the interaction with Sin1

Protein folding is enabled by hydrophobic interactions that expel water molecules by assembling hydrophobic side-chains close together (Huggins, 2016; Tanford, 1997). When hydrophobic residues are located on a protein surface and hence solvent accessible, hydrophobic side-chains are expected to participate in substantial hydrophobic interactions, generating a strong affinity between the interacting proteins (Tiwary et al., 2015). As described in Section 5 above, the inactive form of Akt2 has a hydrophobic pocket-like structure composed of residues F152, Y154 and L155 on its molecular surface, but this characteristic structure is no longer prominent in the active form of Akt2 (Figure 12A). Corresponding residues are readily found in Gad8 as F230, L232 and L233, among which F230 is conserved at the N-termini of all the catalytic domains of AGC-family kinases (Figure 21A). Intriguingly, the surface exposure ratio of one of the residues that form this pocket-like structure, Y154, is dramatically dropped between the inactive (PDB ID:1MRV) and active (PDB ID:1O6K) forms of Akt (Figure 21A). If TORC2 preferentially binds inactive Akt/Gad8 for phosphorylation and activation, the hydrophobic pocket-like structure present only in the inactive form seems to be a good candidate for the Sin1-binding site. Indeed, the acidic protrusion of Sin1 GAD (Acidic Region 2), which has been implicated in Gad8 binding, harbors two essential hydrophobic residues (Figure 12). Thus, I carry out site-directed mutagenesis studies on the three hydrophobic residues of Gad8, F230, L232 and L233, to reveal their possible role in the interaction with Sin1. While the L232A and L233A variants retained the interaction with Sin1 to some extent in yeast two-hybrid assays (Figure 21B), Gad8 carrying the alanine substitutions of F230, L232 and L233 failed to be co-purified with MBP-fused Sin1GAD (Figure 21C). Correspondingly, the phosphorylation by TORC2 was abolished with the F230A variant, whereas the L232A or L233A variants were phosphorylated similarly to wild-type Gad8 (Figure 21D); limited interactions of the L232A

or L233A variants with Sin1 may be sufficient to bring about the Ser546 phosphorylation. The F230 residue corresponds to Akt2 F152, which is rather buried and almost inaccessible from the outside (the table in Figure 21A), implying that F230 might be deeply involved in the folding of Gad8. Indeed, the expression level of the F230A variant was reduced to one third of that of wild-type Gad8, indicating the instability of the F230A variant. On the other hand, the L232A and L233A substitutions do not seem to affect the stable expression of the variant proteins. Moreover, L232 is predicted to more prominently protrude from the surface than L233, making residue L232 an ideal candidate for Sin1 docking.

To further confirm that Sin1 actually binds to the N-lobe of the Gad8 kinase domain, the truncated variants of Gad8 shown in Figure 21E were subjected to *in-vitro* co-purification assays using the GST-Sin1GAD recombinant protein. Firstly, it was clearly shown that Sin1 binds to the Gad8 1-498 variant lacking the C-terminal region, though the strength of the interaction seemed to be reduced compared to wild-type Gad8 (Figure 21F). In Figure 21G, the Gad8 230-498 variant as well as the 1-369 variant were shown to retain the binding activity against GST-Sin1GAD. On the other hand, the Gad8 370-569 variant that represents the C-terminal half of the protein was unable to bind to GST-Sin1GAD. These experiments suggest that the N-lobe of the Gad8 kinase domain plays a critical role in the interaction with Sin1, supporting the notion that the hydrophobic pocket-like structure within the N-lobe contributes to the Sin1-Gad8 interaction.

**Figure 21.**

**A**

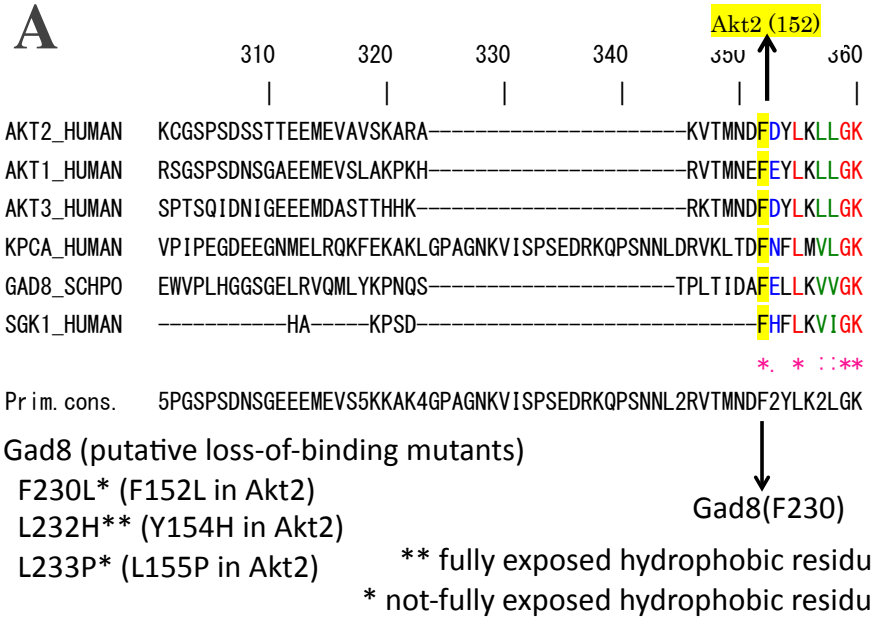


Gad8 (putative loss-of-binding mutants)
F230L* (F152L in Akt2)
L232H** (Y154H in Akt2)
L233P* (L155P in Akt2)

** fully exposed hydrophobic residue
* not-fully exposed hydrophobic residue

| Exposure Ratio (%) | | |
|---|---|---|
| | 1MRV | 1O6K |
| F152 | 2.0 | 0.0 |
| Y154 | 63.7 | 25.9 |
| L155 | 23.5 | 20.0 |

**B**

| | pGBT | pGADGH |
|---|---|---|
| 1 | Empty | Sin1$^{(281\text{-}400aa)}$ |
| 2 | Gad8$^{+}$ | Sin1$^{(281\text{-}400aa)}$ |
| 3 | Gad8 F230A | Sin1$^{(281\text{-}400aa)}$ |
| 4 | Gad8 L232A | Sin1$^{(281\text{-}400aa)}$ |
| 5 | Gad8 L233A | Sin1$^{(281\text{-}400aa)}$ |

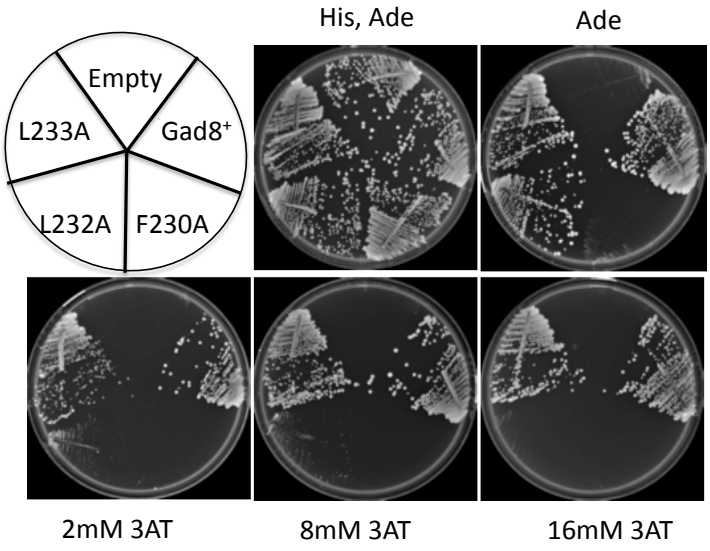


**C**

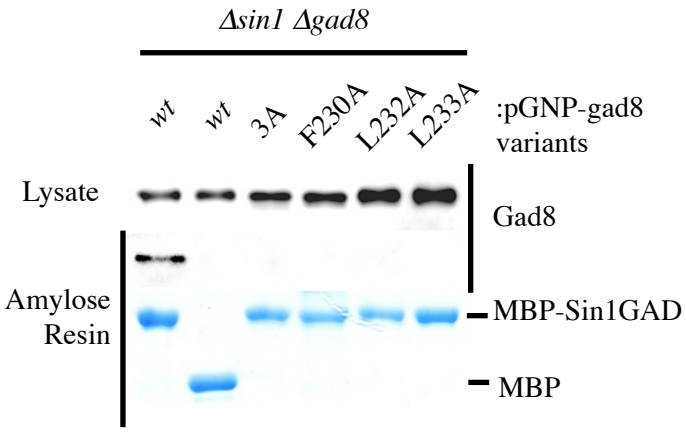


3A = F230A, L232A, L233A

**D**

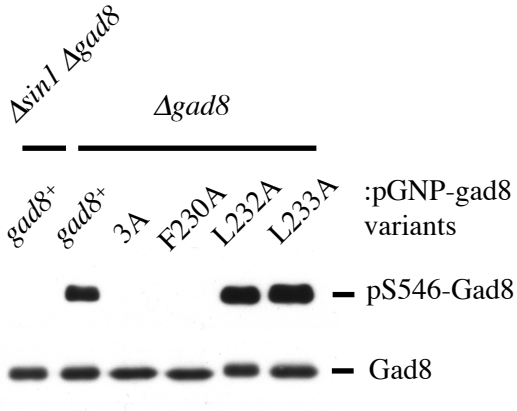

**Figure 21.**

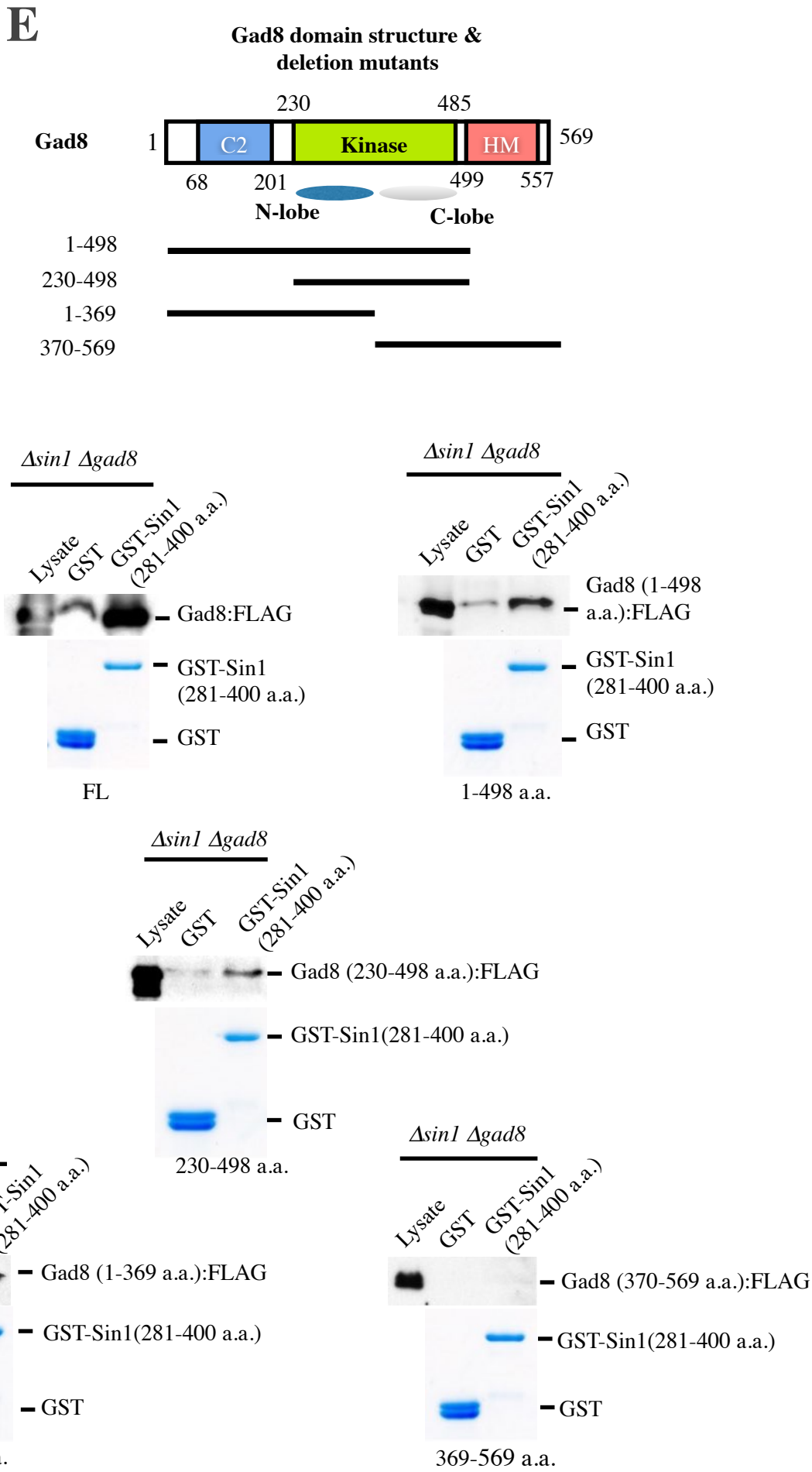
E
Gad8 domain structure &
deletion mutants
230
485
Gad8
1
C2
Kinase
HM
569
68
201
499
557
N-lobe
C-lobe
1-498
230-498
1-369
370-569
F
Δsin1 Δgad8
Lysate
GST
GST-Sin1
(281-400 a.a.)
Gad8:FLAG
GST-Sin1
(281-400 a.a.)
GST
FL
Δsin1 Δgad8
Lysate
GST
GST-Sin1
(281-400 a.a.)
Gad8 (1-498
a.a.):FLAG
GST-Sin1
(281-400 a.a.)
GST
1-498 a.a.
G
Δsin1 Δgad8
Lysate
GST
GST-Sin1
(281-400 a.a.)
Gad8 (230-498 a.a.):FLAG
GST-Sin1(281-400 a.a.)
GST
230-498 a.a.
Δsin1 Δgad8
Lysate
GST
GST-Sin1
(281-400 a.a.)
Gad8 (1-369 a.a.):FLAG
GST-Sin1(281-400 a.a.)
GST
1-369 a.a.
Δsin1 Δgad8
Lysate
GST
GST-Sin1
(281-400 a.a.)
Gad8 (370-569 a.a.):FLAG
GST-Sin1(281-400 a.a.)
GST
369-569 a.a.

## Figure 21.

**Figure 21. Characterizing the putative amino acid residues on Gad8 that form a hydrophobic pocket maybe responsible for the interaction with the Sin1 CRIM**

(A) F152, Y154, and L155 of Akt2 which form a hydrophobic pocket in an inactive form of Akt corresponds to Gad8 F230, L232, and L233. The results of the data analysis is provided by Dr. Kojima. The sequences of Human Akt, PKA, and SGK1 are aligned with that of the fission yeast counterpart Gad8. The putative loss of interaction mutants of Akt2 isolated from the reverse Y2H assay between Akt2 and Sin1, and the counterpart residues of Gad8 are shown. The hydrophobic pocket composed of F152, Y154 and L155 of Akt2 are mapped on the crystal structures of the inactive and active forms of Akt2 (1MRV and 1O6K, respectively). The surface exposure rates of the three residues in the inactive and active forms of Akt2 are summarized in the table. F152, Y154, and L155 residues of Akt2 which form a hydrophobic pocket-like structure in its inactivation form corresponds to Gad8 L230, L232, and L233 residues.

(B) The interaction between Gad8 variants and Sin1 were also examined in yeast two-hybrid assay. The Gad8 variants expressed from the bait plasmid (pGBT) were tested for their ability to interact with Sin1GAD (281-400 a.a.) expressed from the prey plasmid (pGADGH).

(C) The Gad8 variants carrying indicated amino acid substitutions are tested for its ability to interact with Sin1. The Gad8 variants were expressed in *Δsin1 Δgad8* cells from the plasmids under the control of Gad8 native promoter. The cell lysates were incubated with amylose resins which were coated with MBP-Sin1GAD (281-400a.a.) fusion protein or MBP alone as a negative control. After washing and spinning down the amylose resins, the resultant precipitates were probed with anti-Gad8 antibody to detect Gad8 co-purification.

(D) Evaluating TORC2-dependent phosphorylation status of the Gad8 variants. The F230A, L232A, and L233A Gad8 variants were expressed in *Δgad8* cells from the plasmids under the control of Gad8 native promoter. The phosphorylation level of the Gad8 variants were quantified by immunoblotting against phosphorylated form of Gad8 as well as Gad8 as a loading control. Three times more amount of the sample than that of the others was loaded for the F230A variant as the expression level of this variant was significantly reduced.

(E) Deletion analysis of Gad8. Schematic diagram represents the architecture of Gad8 protein showing Gad8 truncation variants tested for their ability to interact with Sin1GAD. C2 = C2 domain, Kinase = Kinase domain, HM = Hydrophobic motif.

(F) Sin1GAD does not directly bind to Gad8 hydrophobic motif (HM) on its C-terminal region. Gad8:FLAG as well as Gad8 variant lacking its C-terminal region containing the HM-site (1-498 a.a.) were fused to Flag tag at the C-terminal end and were expressed from the plasmids under the control of Gad8 native promoter (GNP) in *Δsin1 Δgad8* cells. The cell lysates were subject to incubation with GST-Sin1 (281-400 a.a.) or GST bound GSH beads. Precipitated beads were probed for co-purification of Gad8:FLAG or Gad8 (1-498 a.a.):FLAG by immunoblotting with anti-FLAG antibody

(G) Sin1GAD binds to the N-lobe of Gad8 kinase domain. The Gad8 deletion variants fused to FLAG tag at the C-terminal end were expressed from the plasmids under the control of Gad8 native promoter (GNP) in the *Δsin1 Δgad8* cells. Samples were prepared and analyzed as in (F).

**Table 7. Summary of the data for Gad8 kinase variants presented in Figure 20**

| gene: gad8 | Interaction with Sin1 CRIM | Y2H | *Δgad8* | *Δtor1 Δgad8* | *Δgad8* | Exposed on Molecular Surface |
|---|---|---|---|---|---|---|
| **Substitution** | **GST-Sin1 (247-400)** | | **pS546 (%)*** | **pS546 (%)*** | **Streak**** | **(accessible surface area, >25%)** |
| F230A | None | - | 0 | 0 | – | × (×) |
| L232A | None | + | 100 | 0 | + | ○ (○) |
| L233A | None | ++++ | 100 | 0 | ++ | △ (×) |

*Signal quantification was done using imageJ (100% = wt)

**Expressed from pGNP(Gad8 Native Promoter)

**Table 7. summarizes the data obtained from the analysis of the Gad8 kinase domain variants generated by site-directed mutagenesis study in Figure 20.**

The first column lists amino acid substitutions introduced to each Gad8 variant (Figure 20A). The second column lists the GST-pulldown assay from Figure 20B (None = Not Detected). The third column lists the results of Y2H in Figure 20C. In the fourth and fifth columns, the results of Figure 20D are quantified and and expressed in % when compared to the wild-type as 100%. The sixth columns lists the results from the sensitivity tests [++ denotes the wild-type level growth rate, + denotes the growth rate less than half of that to wild-type. - denotes no growth]. The last column shows if the target amino acid residue is exposed on the molecular surface [○ = exposed, △ = half-exposed, X = not exposed, judged by the analysis of the theoretical 3D structure of Gad8 constructed based on Akt inactive form (PDB ID=1mrv).] Inside parenthesis shows if the accessible surface area of the amino acid residues are more than 25%, which can be judged as exposed from the molecular surface[○ = >25%, X = <25%](Figure 20A).

## 3.3. Identification and characterization of Tor1 associating domain (TAD) within Sin1

### 3.3.1. Tor1 associating domain (TAD) of Sin1 is mapped on the region including the N-terminus of the CRIM domain

In general, the more critical is the domain for the essential function of the protein, the more of the constituent amino acid residues are likely to be conserved (Glaser et al., 2003; Pupko et al., 2002). The function of Sin1 to associate with Tor1, Ste20 and Wat1 would be critical for TORC2 assembly. This notion raises the question of which parts of Sin1 actually mediate the incorporation of Sin1 into TORC2. Therefore, as a first step, I set out to determine Tor1 associating domain (TAD) on Sin1, by testing whether the Sin1 variants shown in Figure 22A can still interact with Tor1. These Sin1 truncated variants as well as full-length Sin1 were expressed as Myc-tag fusions in *FLAG:tor1 Δsin1* cells, while untagged wild-type Sin1 was expressed in *Δsin1* cells as a negative control. The expression levels differed among the variants; the N-terminal half (1-340) and the Sin1ΔGAD variants were both strongly expressed, whereas the full-length Sin1 was at a much reduced level and the C-terminal half variant was detectable only as a faint band. These Sin1 variants were subjected to immunoprecipitation assays with anti-FLAG beads, and the precipitates were probed for the co-purification of the Sin1 variants with anti-Myc antibodies. A significant amount of the Sin1ΔGAD variant was present in the precipitated beads comparable to that of full-length Sin1 (Figure 22B). Considering the more of the Sin1ΔGAD variant expressed in the crude cell lysate, the interaction of the Sin1ΔGAD variant with Tor1 might have been compromised to some extent, but not so significantly. For the C-terminal half fragment of Sin1, not a trace amount was observed in the FLAG:Tor1 precipitate. On the other hand, a small amount of the N-terminal Sin1 variant was detected in the immunoprecipitated beads. These results indicate that Sin1 might interact with Tor1 probably through its N-terminal region.

In order to further narrow down the Sin1 domain responsible for the interaction with the Tor1 kinase, the GST-fused Sin1 truncated variants listed in Figure 22C were expressed in *E. coli* cells and affinity-purified onto GSH beads. The recombinant Sin1 proteins produced in *E. coli* were found to be less susceptible to degradation. The purified proteins on GSH beads were incubated with the cell lysate of a *FLAG:tor1 Δsin1* strain. After extensive wash, the precipitated GSH beads were probed for the co-purified FLAG:Tor1 by immunoblotting. With the exception of Sin1 289-665, the Tor1 kinase was co-purified with all the other Sin1 fragments tested, including the Sin1 171-665 and 1-290 variants (Figure 22D). Consistent with this observation, only the Sin1 289-665 variant failed to rescue growth of *Δsin1* cells under stress conditions (Figure 22E). No significant difference in the manner of the Tor1 co-purification was observed in the presence and the absence of the Ste20 subunit (Figure 22F). Taken together, these data clearly demonstrate that a region spanning residues 171-288 in the N-terminal portion of Sin1 is required for the interaction with the Tor1 kinase.

The interactions between Ste20 and the Sin1 variants were also tested, aiming to locate the Ste20 associating domain (SAD) on Sin1. Unexpectedly, Ste20 was co-purified with all the Sin1 truncated variants tested (Figure 22G). However, the amount of Ste20 co-precipitated with the Sin1 variants were markedly reduced compared to that with full-length Sin1, except for the Sin1ΔGAD variant, suggesting that Ste20 interacts with multiple sites in the Sin1 protein; one candidate may be the 1-85 region and the other may be the 390-530 region which overlaps with the putative Ras Binding Domain (RBD).

The report from Wilkinson *et al*. (1999) states that the Sin1 lacking the C-terminal 164 amino acid residues could not complement the stress sensitivity of *Δsin1* cells (Wilkinson et al., 1999). It has been noticed that the Sin1 gene fragment that they had employed lacks the N-terminal 15 amino acid residues when compared to the gene registered in the database PomBase, may be because they failed to identify the first intron in the 5'-end region of the

*sin1*$^{+}$ gene. Interestingly, the Sin1 C-terminal deletion variant (residues 1-390) containing the intact N-terminus was capable of complementing the stress sensitivity of *Δsin1* cells (Figure 22E), in contrast to the result by Wilkinson *et al*. Therefore, it is possible that the Sin1 fragment (16-501) reported by Wilkinson *et al*. (1999) lacks both Ste20-binding sites, the N-terminal tip and the C-terminal RBD overlapping region. Figure 22H shows the primary structure of Sin1 from 1 to 85 amino acid residues along with the predicted secondary structure and the solvent accessibility of each residue. The N-terminal tip can be judged as a rather exposed area with loop structure, which may be available for the access from another protein such as Ste20.

**Figure 22.**

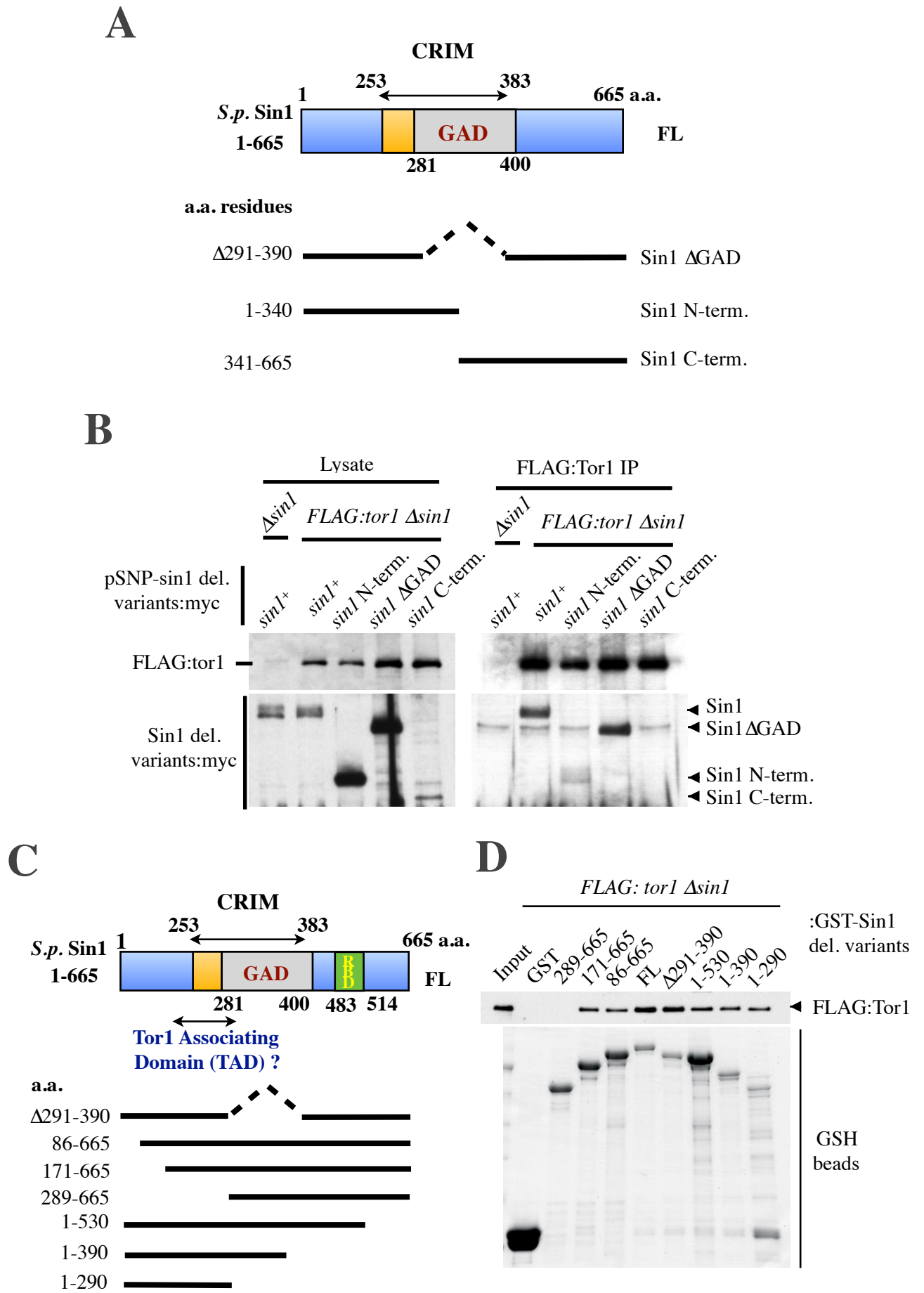
A
CRIM
253
383
1
665 a.a.
S.p. Sin1
1-665
GAD
FL
281
400
a.a. residues
Δ291-390
Sin1 ΔGAD
1-340
Sin1 N-term.
341-665
Sin1 C-term.
B
Lysate
FLAG:Tor1 IP
Δsin1
FLAG:tor1 Δsin1
pSNP-sin1 del. variants:myc
sin1+
sin1 N-term.
sin1 ΔGAD
sin1 C-term.
FLAG:tor1
Sin1 del. variants:myc
Sin1
Sin1 ΔGAD
Sin1 N-term.
Sin1 C-term.
C
CRIM
253
383
1
665 a.a.
S.p. Sin1
1-665
GAD
FL
281
400
483
514
Tor1 Associating Domain (TAD) ?
a.a.
Δ291-390
86-665
171-665
289-665
1-530
1-390
1-290
D
FLAG: tor1 Δsin1
:GST-Sin1 del. variants
Input
GST
289-665
171-665
86-665
FL
Δ291-390
1-530
1-390
1-290
FLAG:Tor1
GSH beads

**Figure 22.**

**E**

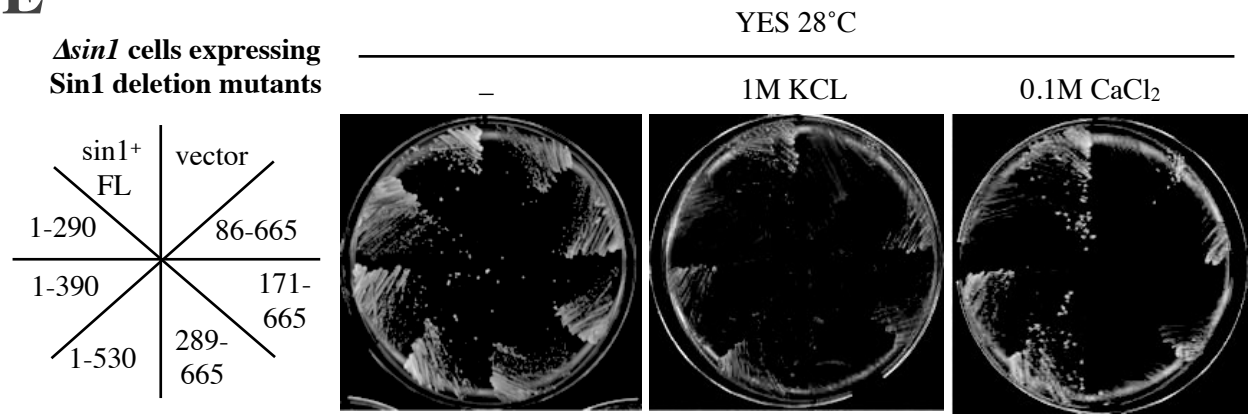


**F**

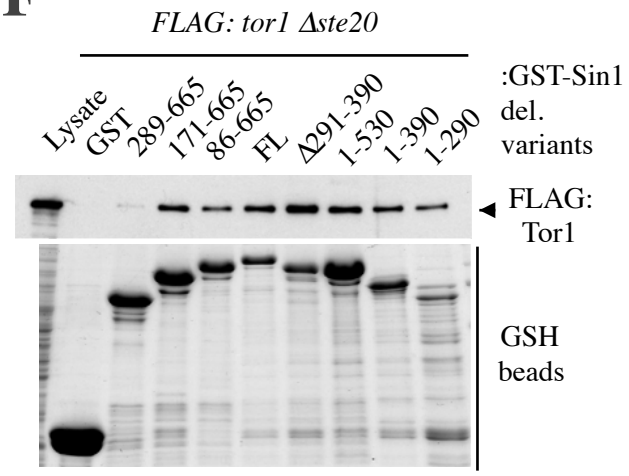


**G**

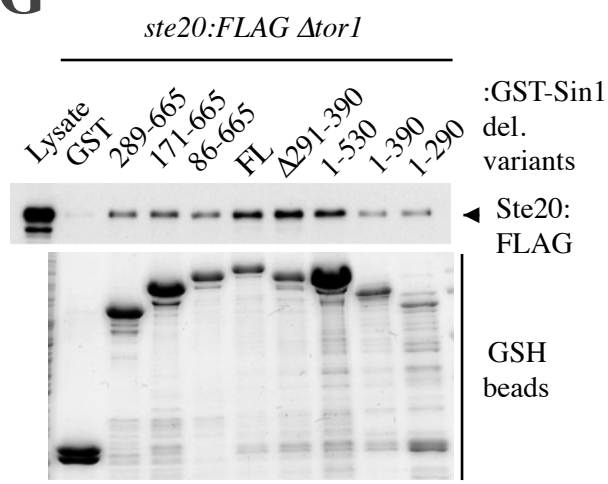


**H** **Putative Ste20 binding site at the N-terminus of Sin1**

*S.p.*Sin1 (1 - 85 a.a.)

```
1---------11--------21--------31--------41--------51--------61
--------71--------81----
```

Splicing site

```
MELTREKVLLLTFLRMQYSHILPDSIENRVISTEAPEWELDKSLQDLLIHDYDYSKTSFSS
SPPIVANDTVSNVRKPSDTKQVNGA
```

The residues coded by Exon1 = MELTREK

**first 15 residues**

Jnet - Final secondary structure prediction for query

```
-------EEEHHHHHHHHH-+--------EEEE--------+-HHHHHHHHH---------+-
---EEE---+----------+------
```

Jnet_25 - Jnet prediction of burial, less than 25% solvent accessibility

```
-B----BBBBBBBBBBB--B---B---BB-B----B-B-+--BB--BB--+--------B-+-
BBBBB---B--B--B-----B----
```

## Figure 22.

**Figure 22. Mapping Tor1 associating domain (TAD) of Sin1**

(A) Deletion analysis of Sin1 to identify the region which is required for Sin1 to be incorporated into TORC2. Three fragments of the Sin1 deletion variants were prepared to probe which parts of Sin1 are required to form TORC2 complex in an immunoprecipitation assay. Dash line shows the region deleted in Δ291-300 construct.

(B) Sin1 preferentially interacts with Tor1 through it N-terminal half. The Sin1 deletion variants as in (A) as well as the wild-type Sin1 were expressed as a Myc-tag fusion from Sin1 native promoter in *FLAF:tor1 Δsin1* cells and wild-type Sin1 in *Δsin1* cells. The cell lysates were subject to immunoprecipitation with anti-FLAG beads. The precipitated beads were probed for the presence of co-precipitated Sin1 variants with an antibody against Myc-tag.

(C) Deletion analysis of Sin1 to identify Tor1 associating domain (TAD). A diagram shows the Sin1 deletion set used to identify Tor1 associating domain in GST-pulldown assay. Dash line shows the region deleted in Δ291-300 construct.

(D) Sin1 interacts with Tor1 through the region of 171-290 amino acid residues. GST-fused Sin1 deletion constructs listed in (C) along with full-length Sin1 (FL) and GST alone were expressed from pGEX-KG plasmids in an *E. coli* strain, BL21. The bacterial cells were cultured at 16˚C after IPTG addition for about 24hrs to induce the expression of the GST-fusion proteins. The proteins were affinity purified onto GSH bead by incubating the beads with bacterial cell lysates. The GSH beads were incubated with a yeast cell lysate prepared from *FLAG:tor1 Δsin1* strain. Co-purification of FLAG:Tor1 as well as the amount of FLAG:Tor1 in the crude cell lysates (input) was checked by immunobloting with anti-FLAG antibody. GST-fusion proteins in the pulldown samples were visualized by Coomassie Brilliant Blue staining.

(E) Sin1 fragments that are able to interact with Tor1 can rescue the stress sensitivity of *Δsin1* cells. The growth of the *Δsin1* cells expressing Sin1 deletion variants along with full-length Sin1 and an empty vector from the plasmids under the control of Sin1 native promoter were tested in mild to high osmolality (1M KCl) and $Ca^{2+}$ stress (0.1M $CaCl_2$ ) by streaking onto the agar plates which were then incubated at 28˚C.

(F) Sin1 deletion fragments can interact with Tor1 kinase in the absence of Ste20. GST-pulldown assay was carried out using the cell lysate of *FLAG:tor1 Δste20* in the same procedure as in (B).

(G) Sin1 deletion fragments can interact with Ste20 in the absence of Tor1. GST-pulldown assay was carried out using *ste20:FLAG Δtor1* cell lysate in the same procedure as in (B).

(H) The primary structure of the Sin1 N-terminal region (1 -85 a.a.) that is partly responsible for the association with Ste20 is examined for predicting Ste20 binding site. The predicted secondary structure and the solvent accessibility of each residue by Jnet are shown. The short sequence at the tip of the N-terminus (colored in red) encodes the exon1. The first 15 residues missing in the study of Wilkinson *et. al.*, were highlighted with light green (Wilkinson *et. al.*, 1998).

### 3.3.2. TAD2 is confined within a small region of the N-terminal part of the Sin1 CRIM domain

In order to define the TAD boundaries, a series of Sin1 fragments were generated through serial truncations by 10 residues from 171 to 289 (Figure 23A). The Gad8 phosphorylation level at Ser546 as well as the ability to complement the stress sensitivity of Sin1-deficient cells was examined with *Δsin1* cells expressing those Sin1 truncated variants. As shown in Figure 23B, the immunoblotting analysis against phospho-Ser546 Gad8 and Gad8 revealed that the phosphorylation of Gad8 at Ser546 could be mediated by the Sin1 251-665 variant or the longer variants, but not by the 261-665 variant or the shorter variants. Consistently, the ability to complement the cell growth defects under stress conditions was abolished in *Δsin1* cells expressing the 261-655 variant or the shorter truncated variants (Figure 23C). These results suggest that the 251-665 variant, but not the 261-655 variant, can bind Tor1 to assemble functional TORC2. To biochemically confirm this conclusion, the binding capabilities of the Sin1 truncated variants to Tor1 were tested in *in-vitro* binding assays. The Sin1 truncated variants listed in Figure 23A were prepared as GST-fused recombinant proteins from *E. coli* cells, and the fusion proteins collected on GSH-beads were incubated with the cell lysate of a *FLAG:tor1 Δsin1* strain. Significant amounts of the Tor1 kinase were co-purified with the 241-655 or 251-665 variants, whereas no Tor1 co-purification was observed with the shorter variants (Figure 23D). These data suggest that the region that spans residues 251-260 of Sin1 is a critical part of the TAD region. However, the amount of Tor1 co-purified with these two variants (241-665 and 251-665) was evidently reduced when compared to that with the 171-665 variant. This indicates that the 171-250 region might also play an important role in mediating the interaction with Tor1. The secondary structure prediction reveals a clear difference in the structure between the two regions; whilst the small region spanning residues 251-260 is particularly well structured within the TAD region, the 171-250 region seems less structured, probably taking a loop

structure, and rather exposed to the surface (Figure 23E). Hereafter, the 171-250 region and the 251-260 region are referred to as TAD1 and TAD2, respectively.

A sequence alignment of the TAD2 regions from various Sin1 orthologs shows that some of the residues of TAD2 are particularly well conserved among species, implying an evolutionarily conserved mechanism of TORC2 complex formation (Figure 23F). Interestingly, TAD2 is located within the CRIM (253-383), N-terminal to the GAD region. When *S. pombe* Sin1 and *H. sapiens* SIN1 are compared, their GAD portions occupy the core region of CRIM with 30% identity, while their putative TAD2 regions show 25% identity. The CRIM structure where the kinase binding site is located next to the substrate binding site may provide a clue as to how a kinase within a multi-subunit complex engages its substrate.

**Figure 23.**

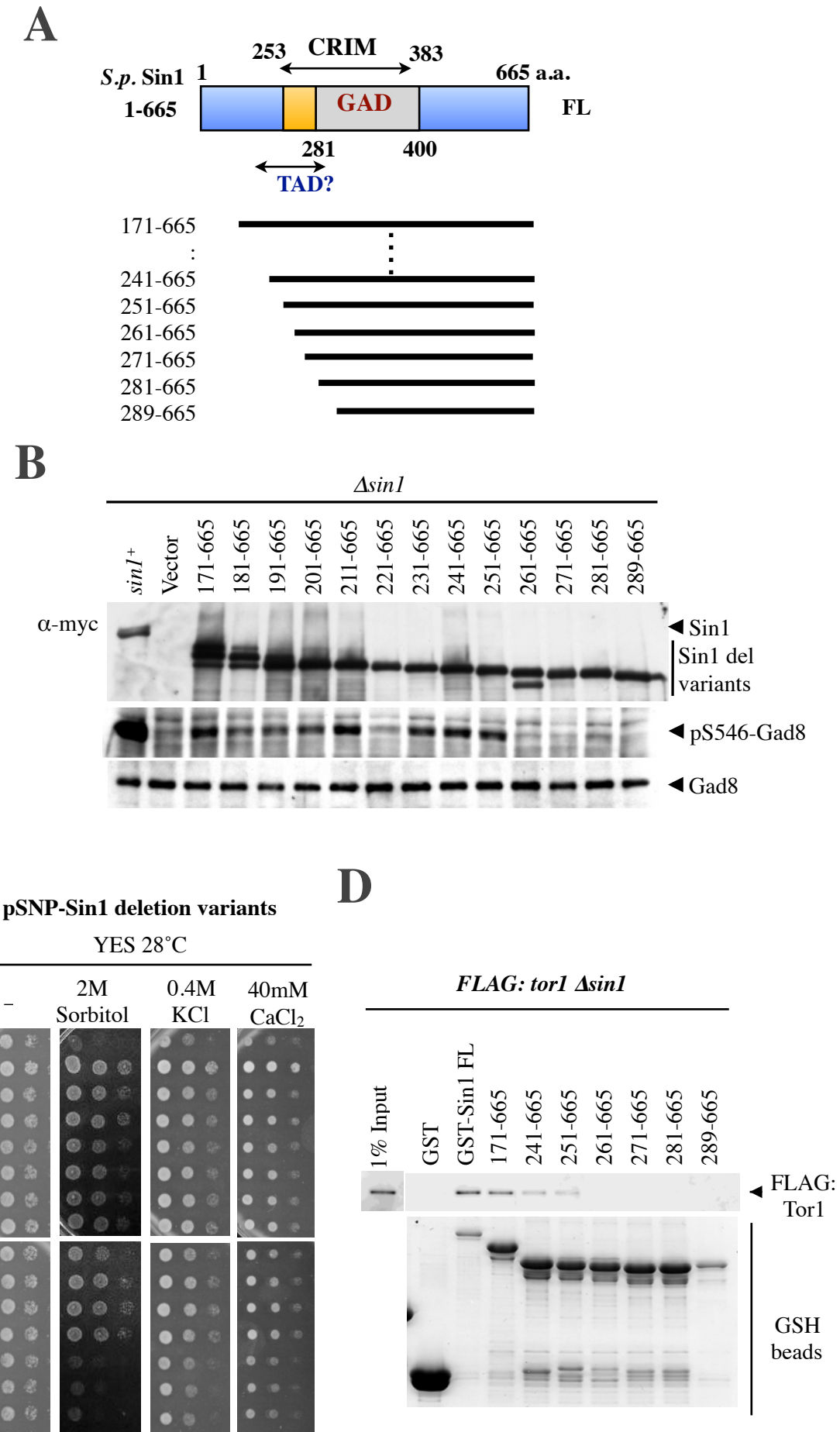
A
S.p. Sin1
1-665
1
253
CRIM
383
665 a.a.
GAD
FL
281
400
TAD?
171-665
241-665
251-665
261-665
271-665
281-665
289-665
B
Δsin1
sin1+
Vector
171-665
181-665
191-665
201-665
211-665
221-665
231-665
241-665
251-665
261-665
271-665
281-665
289-665
α-myc
Sin1
Sin1 del variants
pS546-Gad8
Gad8
C
Δsin1 / pSNP-Sin1 deletion variants
YES 28°C
–
2M Sorbitol
0.4M KCl
40mM CaCl2
Vector
sin1+
165-665
171-665
181-665
191-665
201-665
211-665
221-665
231-665
241-665
251-665
261-665
271-665
281-665
289-665
D
FLAG: tor1 Δsin1
1% Input
GST
GST-Sin1 FL
171-665
241-665
251-665
261-665
271-665
281-665
289-665
FLAG: Tor1
GSH beads

**Figure 23.**

# E

**Putative Tor1 associating domains (TADs) of Sin1**

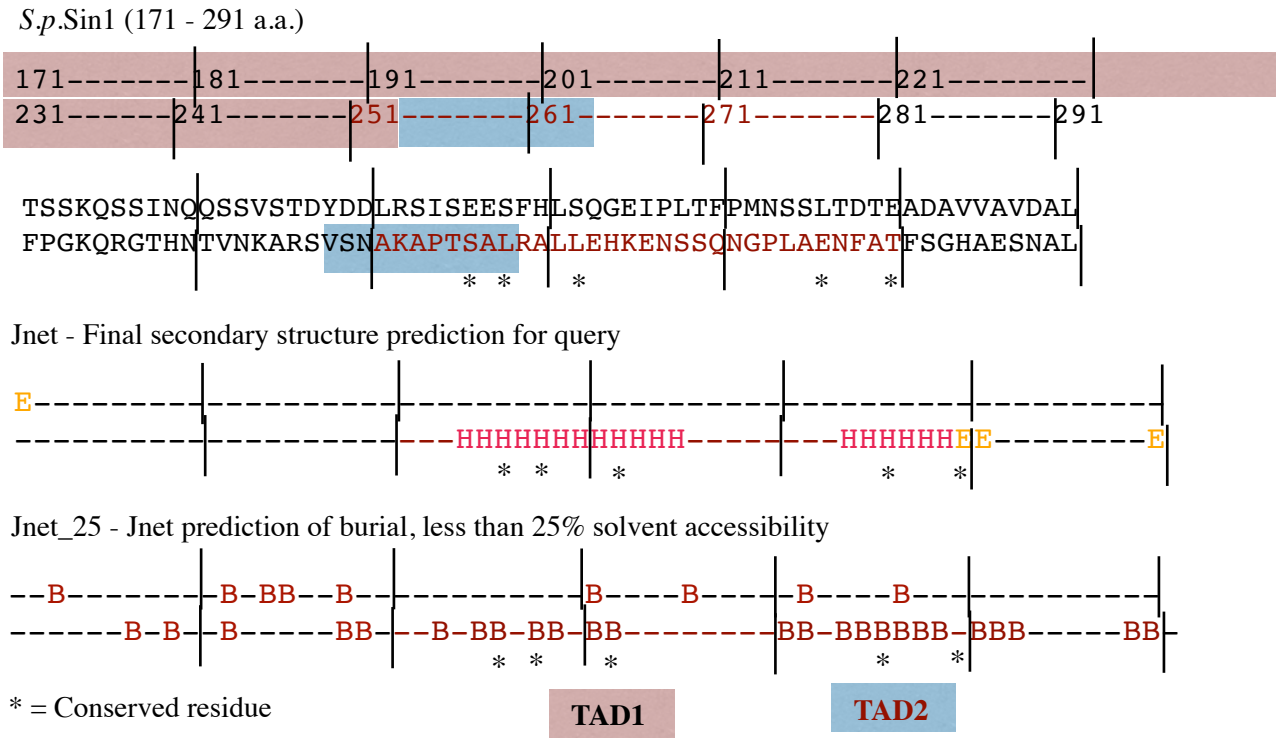


# F

**A sequence alignment of the TAD2 region**

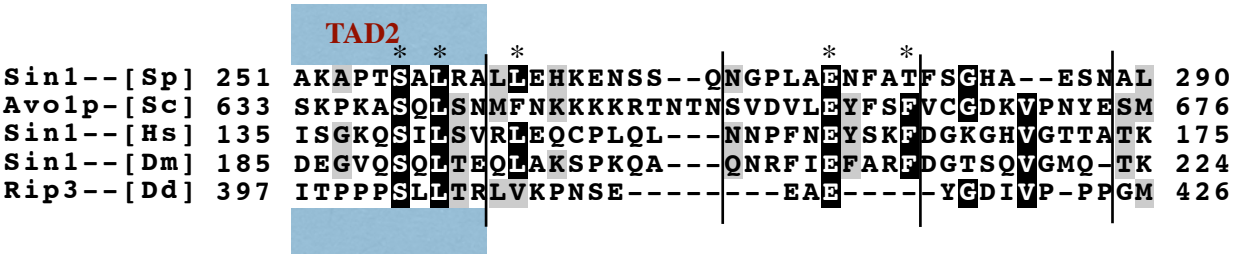

## Figure 23.

**Figure 23. Identifying the N-terminal boundary of Tor1 associating domain (TAD) of Sin1**

(A) Identifying the N-terminal boundary of Sin1TAD. A selection of Sin1 deletion variants to be tested in a GST-pulldown assay was made according to the results of the above experiments (A, B).

(B) The Sin1 fragment of 251-665 amino acid residues but not the shorter ones is able to bring about the Gad8 phosphorylation at Ser546. A series of Sin1 variants were constructed by deleting the putative Tor1 binding domain from 171 to 289 residue at every 10 amino acids and tested for their ability to bring about the Gad8 phosphorylation. The *Δsin1* cells were transformed to express the series of Sin1 deletion constructs under the control of Sin1 native promoter along with wild-type Sin1 and an empty vector. The cell lysates were TCA-extracted and the samples were subject to immunoblotting against Gad8, phospho-Ser546 Gad8 and the Sin1 deletion variants with Myc-tag at the C-terminus.

(C) The Sin1 fragment of 251-665 amino acid residues but not the shorter ones can compliment the stress sensitivity of *Δsin1 cells*. The *Δsin1* cells expressing the series of the Sin1 deletion constructs along with wide-type Sin1 and an empty vector were spotted in serial dilution onto a control YES plate ("–") as well as the stress plates containing 2M sorbitol, 0.4M KCl and 40mM $CaCl_2$ .

(D) GST-fused Sin1 deletion constructs listed in (C) along with full-length Sin1 (FL) and GST alone were expressed in *E. coli* cells. After IPTG addition (0.1mM final conc.), the bacterial cells were cultured at 16˚C for about 24hrs to induce the expression of the recombinant proteins. GSH beads were incubated with bacterial cell lysates and the recombinant proteins were affinity-purified onto the GSH beads. The GSH beads were then incubated with the yeast cell lysate prepared from a *FLAG:tor1 Δsin1* strain. Co-purification of FLAG:Tor1 as well as FLAG:Tor1 in the crude cell lysates (input) were detected by immunobloting with anti-FLAG antibody. GST-fusion proteins in the pulldown samples were visualized by Coomassie Brilliant Blue staining.

(E) The TAD2 contains some highly conserved amino acid residues through evolution. The primary structure of the region predicted to contain the TAD of Sin1 (171-281 a.a.) was subject to the secondary structure prediction by Jnet to characterize the Tor1 binding sites. The predicted secondary structure and the solvent accessibility (the degree of burial) of each residue by Jnet are shown. The letters represent extended (E), helical (H) and other (-) types of secondary structure respectively. In the solvent accessibility predictions they represent buried (B) and exposed (-) for a 25% solvent accessibility cut-off. The TAD2 is colored in red and highlighted in blue.

(F) The sequence alignment of the TAD region between species. The alignment was obtained using Clustal omega server. Identical residues are shaded black and conserved residues grey at 50% level. *Sp, Schizosaccharomyces pombe; Sc, Saccharomyces cerevisiae; Hs, Homo sapiens; Dm, Drosophila melanogaster; Dd, Dictyostelium discoideum*

# 4. DISCUSSION

It was not until 2005 that TORC2 was proved to be PDK2, a putative protein kinase that phosphorylates Akt in its hydrophobic motif (Sarbassov et al., 2005). Since then, the subunit composition and regulation of TORC2 have been intensively studied. However, how TORC2 discerns different AGC-family kinases and recognizes specific substrates has remained elusive. Unlike other organisms, TORC2 deficiency in fission yeast does not result in lethality but is manifested as stress sensitivity. Hence, fission yeast is highly instrumental in dissecting the molecular mechanisms of TORC2 regulation and function. I have found that the Sin1 subunit of *S. pombe* TORC2 is essential for the interaction with Gad8. Based on the NMR structure of Sin1 CRIM, I have extensively characterized Sin1 as the substrate-binding subunit of TORC2, through mutagenesis and protein interaction assays. Furthermore, the molecular mechanisms of Sin1 incorporation into TORC2 and the role of Sin1 in the activation of Gad8 by TORC2 have been explored.

## 4.1. Rab-family small GTPase Ryh1 as upstream regulator of TORC2-Gad8 signaling

Rhy1, a Rab-family small GTPase, has been identified as a key upstream regulator of the TORC2-Gad8 signaling pathway in fission yeast; the TORC1 signaling pathway is also known to be regulated by small GTPases such as Rheb and Rag (Durán and Hall, 2012; Tatebe and Shiozaki, 2010). As an underlying molecular mechanism by which Ryh1 activates TORC2, I showed that Ryh1 promotes Gad8 phosphorylation by augmenting the Sin1-Gad8 interaction. Indeed, co-precipitation of Sin1 with Gad8 was detected, though their interaction was very limited, which probably reflects the transient nature of the Sin1-Gad8 interaction (Figure 8A). Moreover, the GTP-bound form of Ryh1 augmented the Sin1-Gad8 association,

resulting in the hyper-activation of Gad8 in a TORC2-dependent manner (Figure 8C). While a previous study indicated that the absence of Ryh1 did not impair the stability of the TORC2 complex (Tatebe et al., 2010), it is possible that the conformational change of TORC2 induced by GTP-bound Ryh1 leads to the improved interaction between Sin1 and Gad8. Of note, the expression of the GTP-bound form of Ryh1 remarkably reduces the degradation of Sin1 in crude cell lysates (Figure 8C, E), implying the involvement of Ryh1 in the regulation of the TORC2 complex integrity. This observation may be a key to understand the molecular mechanism of TORC2 activation by Ryh1, but it needs more information before drawing any conclusion.

In fission yeast, TORC2-Gad8 signaling communicates environmental fluctuations, such as glucose availability and environmental stresses, to cellular machinery (Cohen et al., 2014; Hatano et al., 2015; Ikeda et al., 2008). Therefore, if and how Ryh1 mediates glucose signals to TORC2-Gad8 signaling would be a key question to understand how yeast cells sense extracellular stimuli. If Ryh1 activity reflects the glucose availability, then both Ryh1 and glucose signaling should employ the same molecular mechanism to regulate TORC2; for example, the intrinsic Tor1 kinase activity within TORC2 should respond to the availability of both glucose and GTP-locked Ryh1. The fusion protein technique has enabled investigation of the intrinsic activity of Tor kinases. The results showed that whilst the intrinsic kinase activity of Tor1 is not affected by the nucleotide binding state of Ryh1 (Figure 16A), it dose respond to glucose availability (Figure 16B). The possibility remains that glucose availability also affects the Sin1-Gad8 interaction in addition to the intrinsic Tor1 kinase activity and, in this case, Ryh1 would be partly responsible for mediating glucose signaling.

### 4.2. Sin1 interacts with Gad8 through conserved residues in CRIM domain

In order to understand how the Ryh1-mediated signals to TORC2 are further conveyed onto

Gad8, it would be useful to characterize the molecular architecture of the TORC2-Gad8 docking interface. This study showed that Sin1 recruits Gad8 onto TORC2 through the newly defined Gad8/Akt associating domain (GAD) within the Sin1 CRIM domain conserved among diverse eukaryotic species. The following observations established the central region of Sin1 as GAD (residues 281-400), which is essential for TORC2 to bind its substrates. First, the GAD region of Sin1 was mapped to the core region within the CRIM domain (Figure 9C). Second, the single amino acid substitutions that disrupt the interaction with Gad8 were isolated within the GAD region. Consistent with the observation that Sin1 is not required for the stable assembly of the other TORC2 subunits (Figure 10), the Sin1 variants carrying any of those single substitutions were stably incorporated into TORC2. As expected, those Sin1 variants failed to cause the TORC2-dependent phosphorylation of Gad8 at Ser546 and to complement the stress sensitivity when expressed in *Δsin1* cells (Figure 11E, F). Third, the Sin1GAD fragment fused to the Ste20 subunit restored the Ser546 phosphorylation and activity of Gad8 in the absence of endogenous Sin1, demonstrating that the recruitment of Gad8 onto TORC2 takes place on the GAD region (Figure 14). Fourth, the Ste20-Gad8 fusion experiment in the *Δsin1* background showed that Gad8 can be phosphorylated when the direct interaction with Tor1 kinase is forced to occur, indicating that Sin1 is not essential for the kinase activity of Tor1 (Figure 15A). Collectively, these observations demonstrated that the failure of Gad8 activation in strains expressing Sin1 with the GAD mutations is not due to disruption of the TORC2 integrity, but can be attributed to the loss of the interaction with Gad8 through Sin1GAD. These results illustrate the role of Sin1GAD in recruiting Gad8 onto TORC2 in order to bring the substrate to the proximity of Tor1 kinase.

However, the NMR structure of Sin1 CRIM has revealed that most of the residues that correspond to the isolated substitutions were rather buried from the molecular surface of Sin1 and those exposed on the surface have only weak inhibitory effects on the Sin1 function

(Figure 11G). By comparing the crystal structures of the active and inactive forms of Akt, a putative Sin1-binding site was spotted on the hydrophobic pockets composed of residues F150, Y152 and L153 (Figure 12A, Figure 21A), partly because the Sin1-Gad8 association appears to involve hydrophobic interaction (Figure 12B). In addition, the Akt crystal structure shows a relatively large basic region adjacent to the hydrophobic pocket. Based on the NMR structure of Sin1 CRIM, its surface residues that may interact with the putative Sin1-binding sites above were selected and intensively verified for their involvement in the interaction with Gad8 (Figure 12, 13, and Table 4). Mutations to the Acid2 region, an acidic loop protruding from the surface with the nearby hydrophobic residues (those found in-between the acidic residues; L357, F361, and those found in KFGF motif; F373, F375) were found to have considerable impacts on the interaction with Gad8. Particularly, F361 and F373 have larger contributions than the other ones to the Sin1-Gad8 interaction. It is interesting to note that, structurally, the F361 and F373 residues are facing each other across a hollow-like structure in the densely conserved region of CRIM (Figure 12E, right panel).

The above results indicate that the substrate specificity of TORC2 is conferred by a specific subunit. The fusion protein technique has enabled presentation of Gad8, a TORC2 substrate, to TORC1; the Mip1-Gad8 fusion protein was phosphorylated at Ser546 of the Gad8 part in a Tor2-dependent manner, independently of recruitment through the substrate binding site of Mip1 (Figure 17A, B). These data indicate that Tor kinases themselves are not selective at least for different AGC-family kinases and that TORC2 recognizes its substrate through the interaction between the substrate and the GAD domain within the Sin1 CRIM region.

### 4.3. Sin1 docking on Gad8 and the conformational changes of Gad8 upon activation

Next, the position of Sin1 binding site on Gad8 was investigated. Because the amino acid substitutions affected the conformation of Gad8, it was difficult to conclusively determine the Sin1-binding site within Gad8 (Figure 18, 20). Yet, it was noted that Gad8 might undergo conformational changes upon its activation, like AGC-family kinases in mammals. In the present study, I first isolated Gad8 point mutations that abolish the interaction between Gad8 and Sin1, hoping to locate the Sin1-binding site in Gad8. Within the Gad8 N-terminal region, eight amino acid substitutions that disrupt the interaction with Sin1 were isolated, out of which six turned out to activate Gad8 independently of TORC2. Those activating mutations include D153A, which is equivalent to the known activating mutation D239A in budding yeast Ypk2 (Figure 18A, Table 5) (Kamada et al., 2005). The results indicate that Gad8 would lose the interacting potency with Sin1, when the integrity of the N-terminal, non-catalytic domain is disrupted. However, those N-terminal variants of Gad8 were found phosphorylated and activated in a TORC2-dependent manner. This observation implies that Gad8 with the N-terminal substitutions can still transiently interact with Sin1 and this transient interaction would be sufficient for TORC2 to phosphorylate the Gad8 variants at Ser546. This interpretation further suggests that these N-terminal Gad8 variants might take an intermediate form in the activation process, which can be further activated by the TORC2-dependent phosphorylation.

A similar conclusion can be drawn by the analysis of the Gad8 N-terminal deletion variants (215-569 residues), which lack the N-terminal non-catalytic region. The deletion analysis of Gad8 in this study and similar analyses of budding yeast Ypk2, mammalian Akt and PKC by others (Cameron et al., 2011; Lu et al., 2011) suggested that the N-terminal regions of these protein kinases do not serve as the binding site for Sin1. However, paradoxically, the N-terminally truncated variant of Gad8 lost most of the interaction with

Sin1, though some residual interaction was still evident (Figure 19B, Figure 21G). Surprisingly, the N-terminal deletion variant could further be activated by TORC2 (Figure 19A). The reduced affinity of the N-terminal deletion variant for Sin1 might be due to the conformational change caused by the N-terminal truncation, which could affect the integrity of the Sin1 binding site within Gad8. Similar speculation may also be applied to the Gad8 variants carrying a single substitution in the N-terminal non-catalytic region.

Interestingly, the N-terminal, non-catalytic region of AGC family kinases are known to have *cis*-inhibitory effects on the kinase activation; one well-known example is the PH domain in the N-terminal region of Akt kinase (Alessi, 1998; Warfel et al., 2011). An inactive Akt takes a closed conformation where the PH domain is folded onto the kinase domain (Calleja et al., 2009; Huang et al., 2011; Wu et al., 2010). Binding of $PIP_3$ to the PH domain releases the PH domain from the kinase domain, leading to an open conformation. The Akt crystal structures predict that global conformational changes are brought about upon the Akt activation, with its αB and αC helices stabilized (Yang et al., 2002a; 2002b); in the closed conformation, the PH domain is positioned in a way that causes a steric hindrance with those two helices (Wu et al., 2010). Inhibition of the kinase domain by the N-terminal, non-catalytic domain was also reported with another AGC-family kinase, S6K (Dennis et al., 1998). In budding yeast, the D239A mutation in the N-terminal region of Ypk2, a Gad8 ortholog, brings about TORC2-independent activation of this kinase, and it was proposed that the N-terminal, non-catalytic domain of Ypk2 contains a "*cis*-inhibitory motif" (Kamada et al., 2005). It can be inferred that Gad8 might also undergo conformational changes in its activation process, including the dissociation of the N-terminal region from the kinase domain. I have shown that the Gad8 N-terminal non-catalytic domain can interact with the Gad8 protein in an immunoprecipitation assay (Supplemental Figure 2). In addition, chemical cross-linking coupled with MS (CX-MS) analysis of the inactive form of Gad8 detected

crosslinks between the N-terminal non-catalytic domain and the kinase domain (Supplemental Figure 3). Finally, a theoretical structure model of the Gad8 N-terminal region predicts that residues K128 and D153 protrude towards the same direction, implying their roles as potential interaction interface (Supplemental Figure 4). Thus, it is conceivable that, like Akt, Gad8 might take an inactive, closed conformation with its N-terminal region inhibiting its catalytic domain, and that the point mutations and deletions of the N-terminal region of Gad8 might compromise this auto-inhibitory mechanism.

### 4.4. The analysis of the Gad8 kinase domain variants

The truncation analyses of Gad8 (Figure 19B, Figure 21G) suggested that Sin1 interacts with the kinase domain of Gad8. A reverse yeast 2-hybrid screen successfully isolated within the Gad8 kinase domain eight amino acid substitutions of six different residues that strongly inhibit the interaction with Sin1 (Figure 20A, B). Four out of the six Gad8 kinase domain variants were able to complement the stress sensitivity of *Δgad8* cells even though they were not phosphorylated at Ser546, whereas the L303P variant was unable to do so despite the phosphorylation at Ser546 (Figure 20C). Interestingly, L303 of Gad8 is equivalent to Akt2 L225, which is flanked by F471 and F473 of the C-terminal hydrophobic motif in the active form of Akt2 (Yang et al., 2002a; 2002b). Notably, the nearby S474 residue is the TORC2 phosphorylation target. As shown in Supplemental Figure 1, Gad8 L303 is also predicted to be flanked by F542 and W545, and S546 is phosphorylated by TORC2. In the crystal structure of the active form of Akt2, the C-terminal loop with the hydrophobic motif is tethered into the PIF-like pocket formed by the αB and αC helices (Yang et al., 2002a; 2002b). If this mechanism is conserved in Gad8, it is likely that L303P substitution would prevent the phosphorylated hydrophobic-motif from binding to the PIF-like pocket and thereby disrupt the proper positioning of the Gad8 C-terminal loop within the kinase domain,

resulting in an erroneous conformation (Figure 20F).

### 4.5. Prediction of a putative Sin1-binding site on Gad8 using the reported Akt structures

The analyses through random mutagenesis of Gad8 did not yield a clear conclusion to identify the Sin1-binding site on Gad8; therefore, I turned my attention to the reported crystal structures of Akt, the mammalian ortholog of Gad8. On the surface of the inactive, but not active, form of Akt, residues F150, Y152 and L153 form a hydrophobic pocket, which appears to be a good candidate as a Sin1-binding site to mediate the TORC2-dependent phosphorylation of inactive Akt. The three residues are conserved in Gad8 as F230, L232, and L233, all of which are within the putative Sin1-binding region identified by the truncation analysis of Gad8 (Figure 21E, F, G). The F230A variant was not phosphorylated and activated by TORC2; expression of this mutant Gad8 was unable to rescue *Δgad8* cells under the stress condition (Figure 21D, Table 7). L232 and L233 are exposed on the molecular surface and their substitutions did not seem to affect the kinase structure; evidently the L232A and L233A variants can still be phosphorylated and activated by TORC2 (Figure 21D, Table 7). Further study is required to more accurately evaluate the contribution of these three residues to the Sin1-binding function.

In order to provide an integrated view of the above observations, a model of the Sin1-Gad8 docking was constructed using the available 3D structure data. The crystal structure of the inactive form of Akt1 with its PH domain was employed to mimic the putative Sin1 binding site of the inactive form of Gad8, by substituting the tyrosine residue (Y152) of Akt1 with leucine (L232) in Gad8. It was not possible to fulfill all of the following conditions, which are predicted to be required for the Sin1-Gad8 interaction; (1) the Sin1 F361 residue inserts into the hydrophobic pocket; (2) L232 of Gad8 (L152 in this model) is placed between

F361 and F375 of Sin1; (3) Acidic Region 2 interacts with the basic region of Gad8; and (4) Sin1 binds to Gad8 T252 (T172) as suggested by the series of analyses in this study. Therefore, the tentative docking model shown in Figure 24 fulfills only conditions (1) and (2). If all of the four conditions need to be fulfilled for the proper interaction between Sin1 and Gad8, it would be most likely that their interaction involves temporal changes in their conformations.

## Figure 24.

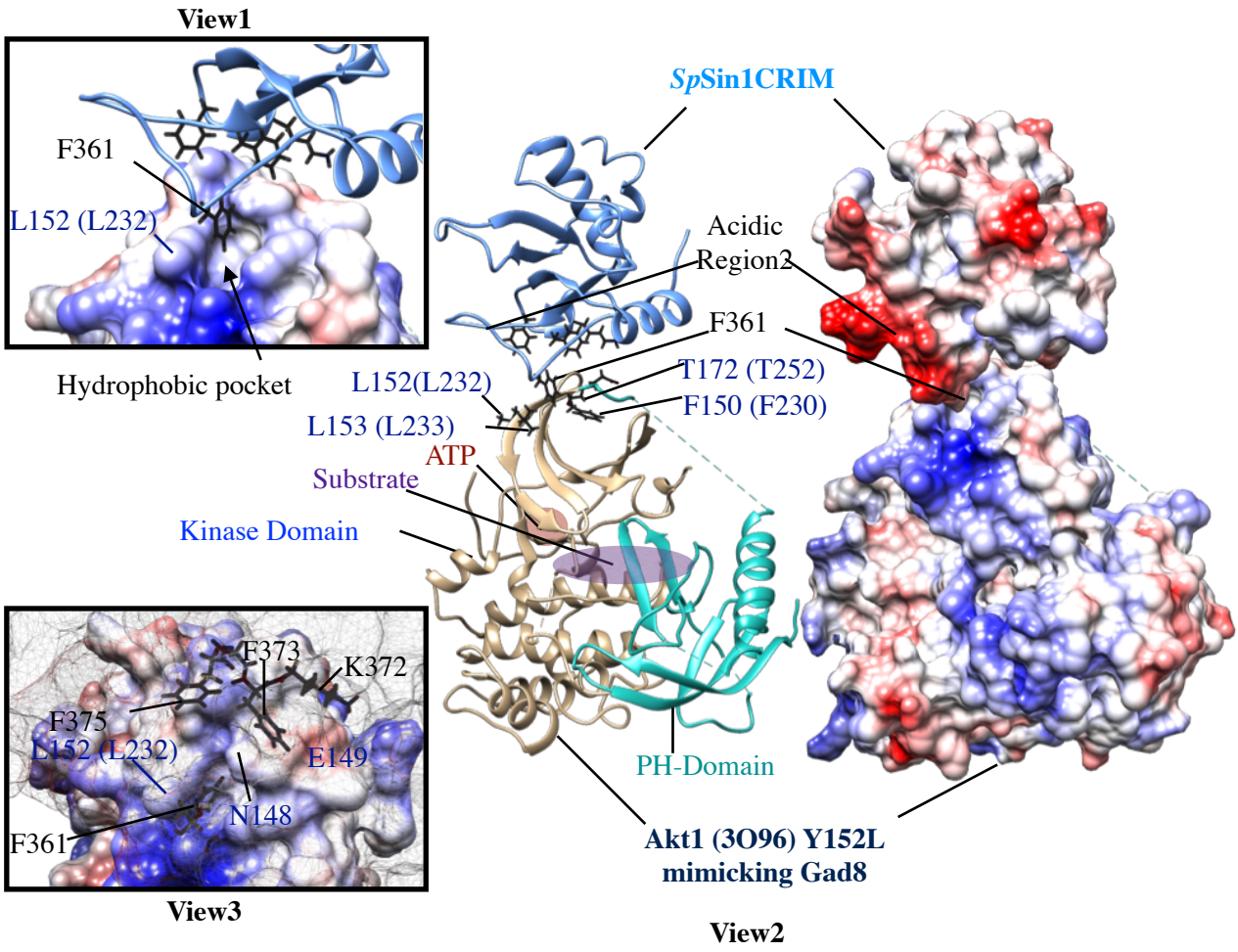


**Figure 24. Prediction of the docking interface between Sin1CRIM and Gad8.**

(I) Tentative docking model of Sin1 CRIM and Gad8 where F361 at the end of the acidic protrusion of Sin1 is inserted into the hydrophobic pocket of the inactive form of Gad8/Akt (View1). The crystal structure of inactive form of Akt1 with its PH domain (3O96) is used to predict the docking of Sin1 and Gad8; the tyrosine residue (Y152) of Akt1 is substituted with leucine to mimic Gad8 - the residues from Gad8 represented in parenthesis. View2 provides the overview of the Sin1-Gad8 docking model, giving the sense of positioning of the docking site relative to the other important sites such as ATP and substrate binding sites. View 3 shows the side chain of positively charged K372 can reach the negatively charged residue of E149 next to F150 with an arbitrary positioning of this inserted model.

### 4.6. Identification of the Sin1TAD

The Gad8 associating domain (GAD) spans the majority of the most conserved part of the Sin1 protein (CRIM region), raising the question of which parts of Sin1 are responsible for the integration of Sin1 into TORC2. The Sin1 variant lacking the entire GAD region was still able to interact with Tor1 (Figure 22B), indicating that the GAD region is not required for the interaction with Tor1 kinase. Subsequent analysis using the Sin1 deletion variants identified a Tor1 associating domain (TAD) within the N-terminal 171-280 amino acid region of Sin1 (Figure 22D). Consistent with this result, Cameron *et al*. (2011) showed that human SIN1 interacts with mTOR through its N-terminal region from 1 to 192 amino acid residues (Cameron et al., 2011). In *S. pombe*, the TAD region was further narrowed down to the minimum region of residues 251-260 (TAD2), which was shown to be necessary to sustain the interaction with Tor1 kinase (Figure 23A, B, D). For more stable interaction with Tor1 kinase, however, the TAD1 region (171-250) was also required (Figure 23D). According to the results from Figure 10B and Supplemental Figure 5, Wat1 is bound firmly with Tor1 in the absence of the other TORC2 subunits and, in the absence of Wat1, Sin1 becomes unstable and hardly retains the interaction with Tor1. These observations raise the possibility that Wat1 might play a critical role in mediating the interaction between Tor1 and the Sin1TAD regions. One possible subunit arrangement in TORC2 is that Wat1 binds to TAD2 and Tor1 is in contact with TAD1, as shown in the diagram of Figure 25. The diagram illustrates that Tor1 kinase and the substrate Gad8 interact with Sin1 through the domains within the CRIM region, thereby bringing the kinase and its substrate in close proximity.

Taken together, this study revealed that the GAD and the TAD are localized next to each other within the evolutionarily conserved CRIM domain (Figure 25). Such molecular architecture of Sin1 offers a simple solution for the kinase to come in contact with its substrate in the multi-subunit kinase complex TORC2. The TAD region of Sin1 can also be

an attractive target for protein-protein interaction inhibitors. However, although I named it Tor1 associating domain (TAD), the possibility still remains that Sin1 indirectly interacts with Tor1 kinase through the association with Wat1. Further analysis will be carried out to reveal the more detailed architecture of TORC2.

Figure 25.

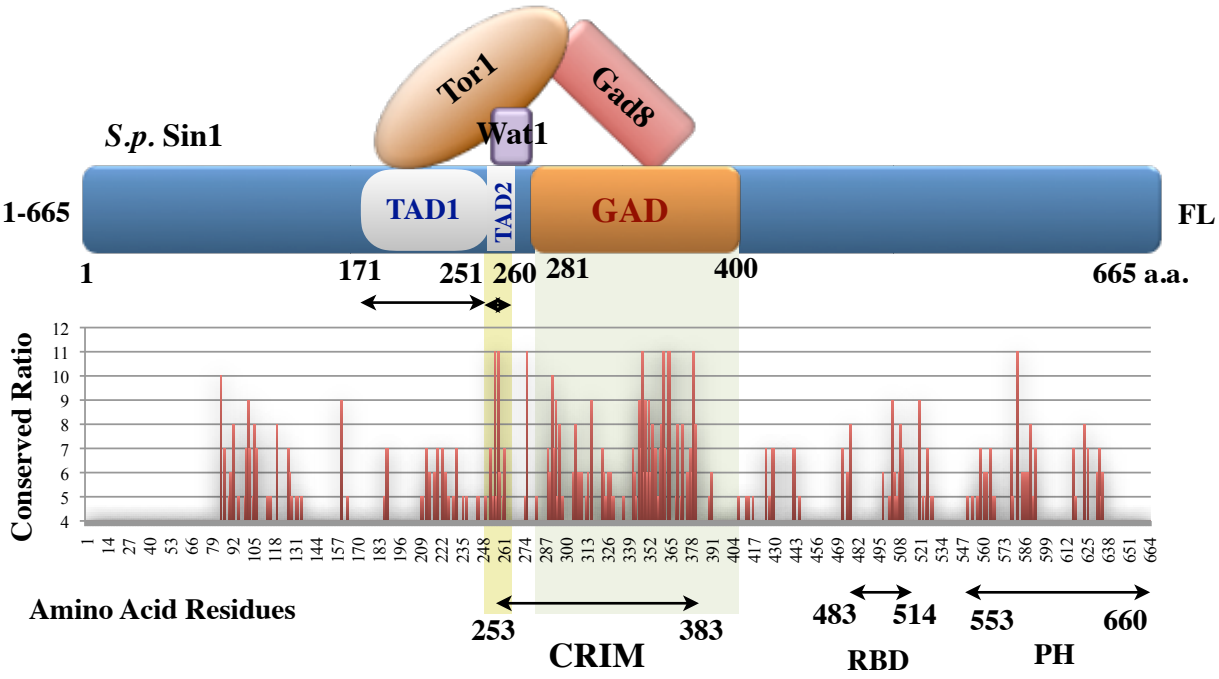


**Figure 25. A tentative model of how Gad8 protein is recruited onto Tor1 kinase through the association with Sin1 CRIM.**

Schematic diagram represents the primary design of Sin1 protein architecture exhibiting the GAD region and the putative TAD domains along with the CRIM region. Sin1 CRIM is the most densely conserved region throughout the entire Sin1 protein, on which the association of Tor1, Wat1 and Gad8 are orchestrated. The degree of sequence conservation is expressed as the bar graph on each amino acid residue: the higher the value, the more conserved.

### 4.7. TORC2 pathway as an therapeutic target

When considering therapeutic interventions against the mTOR pathways, it would be of note that TORC2-Akt signaling is responsible for the progression through the cell cycle upon the inhibition of TORC1 by rapamycin (Breuleux et al., 2009). Tumor micro-environments, especially deep inside the tumors, are known to be nutrient-limiting and hypoxic, yet a malignant tumor do not stop dividing (Yang et al., 2015). Even a subset of malignant tumors with activated PI3K/Akt signaling is known to be resistant to dietary restriction (Kalaany and Sabatini, 2009). Therefore, combined with aberrant cell growth often seen in malignant cancers, the fueling from the TORC2-Akt axis towards cell cycle progression is likely to result in further acceleration of tumor development. From these perspectives, the inhibition of the TORC1 pathway such as by rapamycin may not be a very good option to treat malignant cancer. Indeed, the limited anti-tumor activity and the development of drug resistance in patients have hampered the use of TORC1-specific inhibitors such as rapamycin as anti-cancer drug (Mi et al., 2015; O'Reilly et al., 2006; Xie et al., 2016). These phenomena can be attributed to the TORC1-S6K pathway, the inhibition of which leads to the activation of TORC2 signaling (Breuleux et al., 2009; Chica et al., 2016; Hsu et al., 2011; Manning, 2004; Martín et al., 2017; Um et al., 2004; Xie and Proud, 2013; Yu et al., 2011).

Although aberrantly elevated cellular translation is evident in some cancer types, constitutive activation of the TSC1/2-Rheb-TORC1 axis only results in hypertrophy and rarely progress into malignancy (Inoki et al., 2005a). On the other hand, many examples of aberrant activation of the PI3K-Akt pathway have been reported in a wide variety of cancers (Table 8) (Libra, 2011), indicating that acceleration of the mitotic cell cycle must be a key step for malignant transformation. In addition, the TORC1-regulated translation constitutes a branch of the Akt signaling pathway (Wang et al., 2014). These observations make the TORC2-Akt signaling pathway an attractive target of therapeutic intervention (Sparks and

Guertin, 2010). Therefore, the selective inhibition of TORC2-Akt signaling by therapeutic intervention would bring a new paradigm into cancer therapy. The emergence of the 2nd generation TOR inhibitors that target both TORC1 and TORC2 are promising. However, being ATP-binding competitor for the kinase domain of mTOR, these drugs need further evaluation, particularly for their specificities. The lack of TORC2-specific inhibitor, like rapamycin for TORC1, has also limited detailed analysis of TORC2 signaling. The present findings propose Sin1GAD as an attractive target of protein-protein interaction inhibitors (PPIIs). During this study, other groups also reported the interaction between the Sin1 central domain and PKCα (Cameron et al., 2011), between the Sin1 N-terminal part and SGK1 (Lu et al., 2011), as well as the interaction between the budding yeast Sin1 ortholog Avo1 and the Gad8 equivalent Ypk2 (Liao and Chen, 2011). Together, these studies warrant further research into the drug developments against the Sin1GAD interface.

**Table 8. Frequency of PI3K, PTEN and Akt somatic mutations by tumor type.**

| Gene | Cancer Type | Mutated/tested case (%) |
|---|---|---|
| **PI3KCA** | | |
| | Breast | 1493/5839 (26%) |
| | Endometrium | 230/938 (25%) |
| | Urinary tract | 189/942 (20%) |
| | Skin | 116/753 (15%) |
| | Large intestine | 764/6153 (12%) |
| **PTEN** | | |
| | Endometrium | 690/1837 (38%) |
| | Central Nerve System | 618/3638 (17%) |
| | Prostate | 92/658 (14%) |
| | Skin | 107/768 (14%) |
| | Large intestine | 75/1114 (7%) |
| **Akt** | | |
| | Breast | 61/1328 (5%) |
| | Thyroid | 10/292 (3%) |
| | Urinary tract | 9/301 (3%) |
| | Endometrium | 5/227 (2%) |

*Data are obtained from the COSMIC website.

# 5. CONCLUSIONS

In this thesis study, I have characterized Sin1 as the substrate binding subunit of TORC2, which is essential for the Gad8 recruitment onto TORC2 in fission yeast. This function of the Gad8 recruitment is mediated through the domain termed GAD found within the evolutionarily conserved CRIM domain of Sin1. The substrate specificity of the CRIM domain most likely constitutes the molecular basis for TORC2 to distinguish different AGC-family kinases. Furthermore, the analysis of Sin1-binding site on Gad8 through mutagenesis has provided a new insight into Gad8 activation. I have also shown that Sin1 interacts with Tor1 kinase through the TAD regions, one of which is found within the CRIM region. Thus, the molecular architecture of the CRIM domain enables Sin1 to bring Tor1 kinase and its substrate in proximity; the GAD region binds Gad8, while the TAD region associates with Tor1 kinase. Hence, Sin1 CRIM is an attractive target of pharmacological interventions by protein-protein interaction inhibitors which are expected to exhibit high specificity against the targeted pathway.

# 6. SUPPLEMENTAL INFORMATION

## 6.1. L303P substitution in the HM-site of Gad8 reveals the regulatory role of the C-terminal region

Through collaborative research, Dr. Kawabata constructed a theoretical 3D structure of the active form of Gad8 by the homology modeling based on the available 3D structure of the active form of Akt2 (PDB ID: 1O6K) (Supplemental Figure 1). The left panel, which shows the structure of the entire kinase domain, indicates the position of L303 in the N-lobe of the kinase domain. The close-up view on the right shows that the side-chain of L303 is placed between the side-chains of the F542 and F545 in the hydrophobic-motif, guiding the aromatic ring of F542 into the pocket formed in between αB and αC helices.

## Supplemental Figure 1.

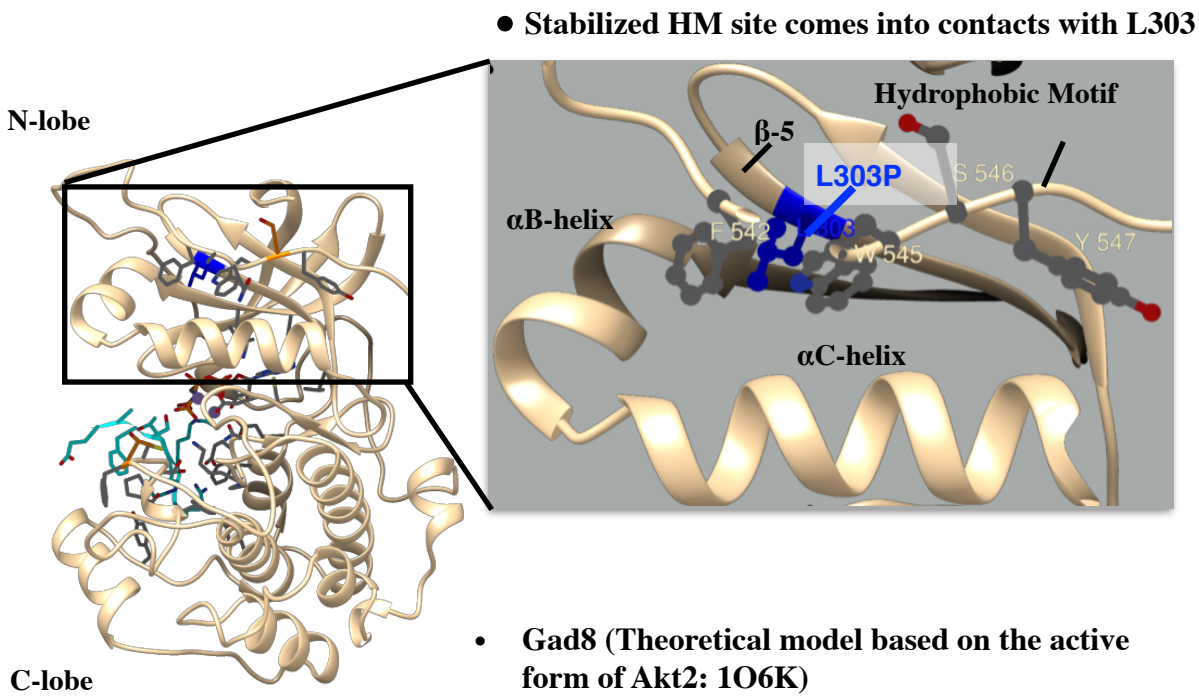


**Supplemental Figure 1. Theoretical model of an active form of Gad8 reveals an action of L303 residue.**

The theoretical model of a crystal structure of Gad8 (230-569 a.a.) was constructed based on the active form of Akt2 (AKT2_HUMAN: 1o6k) through homology modeling using an in-house alignment program and Modeller 9.11 by Dr. Kawabata. A whole kinase domain (left) and the hydrophobic motif (HM) site docks αB and αC-helices (magnified panel; right ) showing the positioning of the L303 residue in relation to the HM site, and the αB and αC-helices in an active form of Gad8. The side-chain of L303 residue on β-5 sheet is flanked by the side-chains of F525 and W545.

## 6.2. Possible role for the N-terminal non-catalytic region in the inactive conformation of Gad8

The TORC2-independent activity of the N-terminally truncated Gad8 suggests that the dissociation of the N-terminal domain from the kinase domain could be a prerequisite for the full-activation of Gad8. The activating mutations in the N-terminal region (Table 5) might disrupt such intramolecular inhibitory interaction. Indeed, it has been reported that Akt, the mammalian counterpart of Gad8, was shown to take a closed conformation where the N-terminal PH domain binds to the kinase domain (Calleja et al., 2007; 2009; Huang et al., 2011; Wu et al., 2010). In order to investigate if, in its inactive form, the Gad8 N-terminal domain is physically associated with its kinase domain to form a closed conformation, the MBP-fused wild-type as well as mutant Gad8 N-terminal fragments (1-229 a.a.) with the K128E or D153A substitution were purified onto amylose resins, and the resins were further incubated with the lysates of *Δsin1* cells expressing a chromosomal copy of Gad8:FLAG. After extensive wash, the amylose resins were recovered and the samples were probed for the co-purification of Gad8:FLAG by immunoblotting with anti-FLAG antibody. Compared to a wild-type control, the amounts of the co-purified Gad8:FLAG with the MBP-Gad8 N-terminal fragments carrying the K128E or D153A substitution were significantly reduced (Supplemental Figure 2). This indicates that the N-terminal non-catalytic domain interacts with Gad8 and residues K128 and D153 are responsible for interdomain association of Gad8 protein, although which part of Gad8 mediates this interdomain association is yet to be determined. Furthermore, a cross-linking study combined with a subsequent mass spectrometric analysis (CX-MS) on an inactive form of Gad8 co-purified with Sin1 revealed that a cross-link was formed between the Gad8 N-terminal non-catalytic domain (NCD) and the kinase domain (KD) (K7, 8 of NCD-K456 of KD and K48, 51, 56 of NCD-K249 of KD) (Supplemental Figure 3). To illustrate these observations, I requested Dr. Kawabata to

construct a theoretical 3D structure of the Gad8 N-terminal region. He kindly modeled the structure through the homology modeling based on the available 3D structure of the C2 domain of Human Synaptotagmin-2 (PDB ID:4p42), which has 14 % sequence identity to the N-terminal C2 domain of Gad8. The amino acid residues isolated through the mutagenesis study were mapped on the molecular surface of the structural model of the Gad8 N-terminal region (Supplemental Figure 4). Intriguingly, residues K128 and D153 are protruded from the molecular surface on the same side of the structural model, while most others are buried. Furthermore, the two residues are placed such that they could flank a target residue or two between them. The fact that the N-terminal substitutions as well as the N-terminal deletion of Gad8 partially eliminate the need for the association with Sin1 for their activation suggests that the dissociation of the N-terminal region from the kinase domain consists of an important step for the Gad8 activation process.

## Supplemental Figure 2.

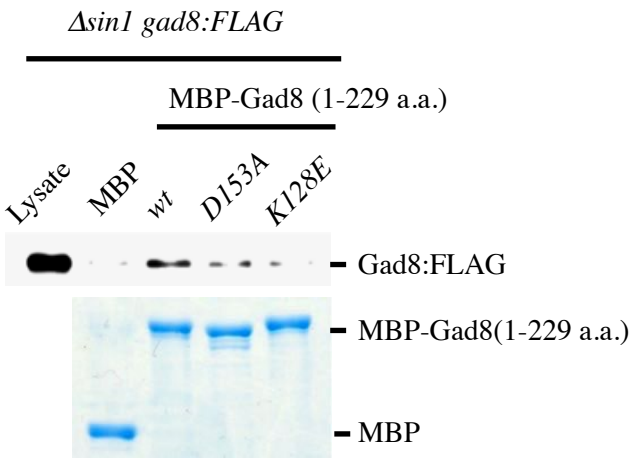


**Supplemental Figure 2. Inter-domain interaction of Gad8.**

The fragment of the wild-type Gad8 N-terminal domain but not those carrying the amino acid substitution bind to Gad8. Wild-type Gad8 N-terminal fragment as well as the fragments carrying D153A or K128E amino acid substitutions were expressed as MBP fusion in bacterial cells and recovered onto amylose resins. The amylose resins were incubated with the lysates derived from *Δsin1 gad8:FLAG* cells. After extensive wash, the precipitated amylose resins were probed for the co-purification of Gad8:FLAG by immunoblotting with anti-FLAG antibody

## Supplemental Figure 3.

**A**

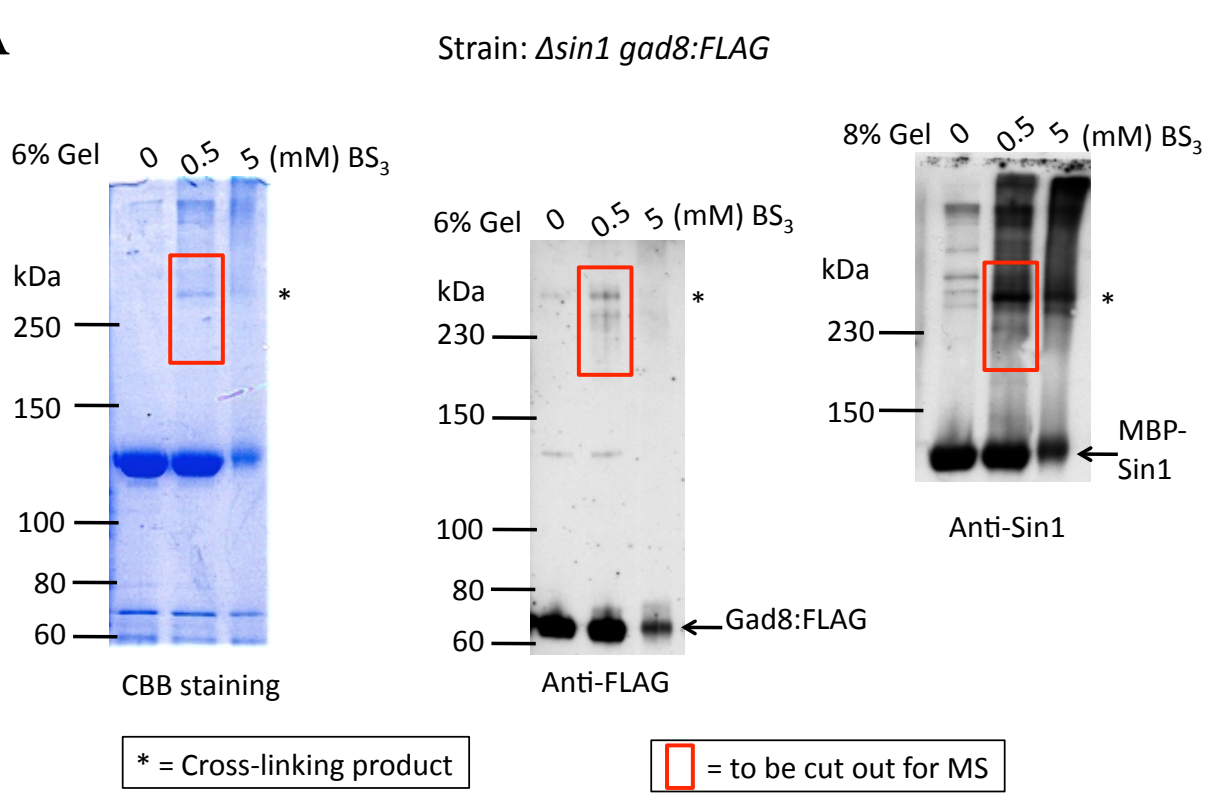


**B**

**Gad8**

| | | | | | |
|---|---|---|---|---|---|
| 1 | 1-8aa | MSWKLTKK | 4 | 447-456aa | FPDNIDEKAK |
| 2 | 44-57aa | SSDEKSRKSSEDKR | 3 | 249-254aa | KRDTSR |
| 3 | 249-254aa | KRDTSR | 5 | 466-470aa | APEKR |
| 5 | 466-470aa | APEKR | 6 | 481-492aa | NHPFFDDIDWKK |

| Gad8 | Start | End |
|---|---|---|
| C2 calcium/lipid-binding domain, CaLB | 62 | 222 |
| Protein kinase, catalytic domain | 230 | 485 |
| Protein kinase, ATP binding site | 236 | 259 |
| Serine/threonine-protein kinase, active site | 349 | 361 |
| AGC-kinase, C-terminal | 486 | 557 |

**Supplemental Figure 3. Cross-linking study followed by mass spectrometry (CX-MS) analysis on an inactive form of Gad8 complexed with Sin1.**

(A) Recombinant MBP-Sin1 bound onto amylose resins was prepared from bacterial lysates. The resultant resins were incubated with the cell lysates prepared from the *Δsin1 gad8:FLAG*. The purified resins were subjected to incubation with and without a cross-linking reagent BS3 at the final concentration of either 0.5 or 5 mM. The reaction mixture was heated in the sample buffer at 65C for 15min to elute proteins. The samples were analyzed by CBB staining and immunobloting with anti-Sin1 and anti-FLAG antibodies to detect co-purified with Gad8. the cross-linked product of Sin1-Gad8 complex was cleaved out from the gel (red square) and subjected mass spectrometry.

(B) The data from the CX-MS assay was analyzed by a computer software. The cross-linked peptides from Gad8 were classified in different colors according to the domains (table), from which these peptides are derived and listed.

## Supplemental Figure 4.

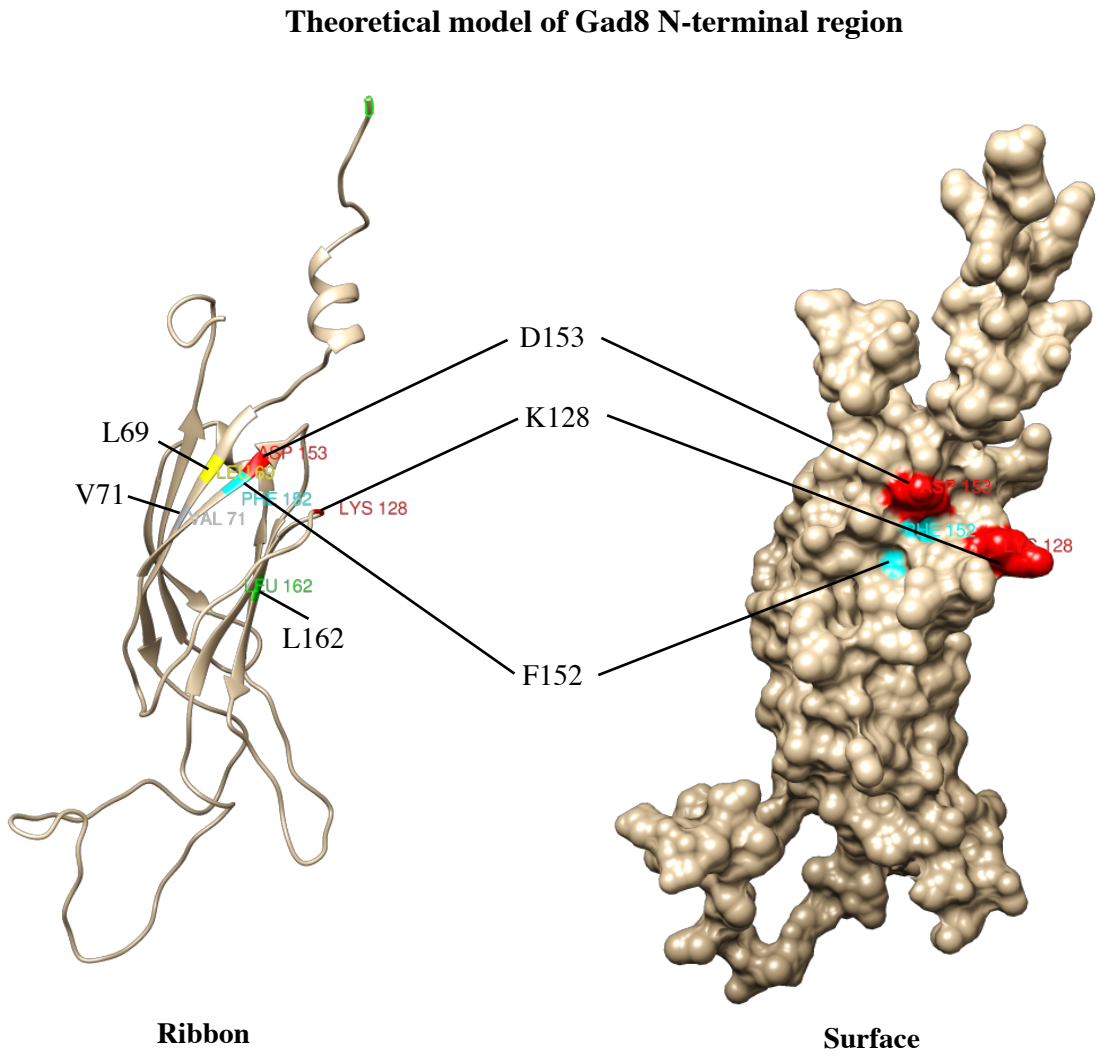


**Supplemental Figure 4. The theoretical 3D model of Gad8 C2 domain.**

The theoretical model of a crystal structure of Gad8 C2 domain (44-228 a.a.) was constructed based on the C2 domain of human Synaptotagmin-2 (ESYT2_HUMAN: 4p42) through homology modeling using PSI-BLAST and Modeller 9.11 by Dr. Kawabata. The sequence identity was 14 %. The model is shown in ribbon (left) and surface (right) representations. The amino acids residues isolated from the mutagenesis study are mapped on the model structure. Residues K128 and D153 were placed on the same side of the molecular surface.

### 6.3. Sin1 integration into TORC2 is dependent upon one of the other three essential subunits; Tor1, Ste20 and Wat1

It would be of an interest to know if Sin1 can be integrated into TORC2 even in the absence of the other subunit. However, upon cell lysis under a native condition, Sin1 seemed to get unstable and degraded in both the Ste20 and Wat1 deletion backgrounds (Supplemental Figure 5). The observation that the absence of Sin1 did not affect the associations between the Tor1 kinase and the other TORC2 subunit is particularly important, because this predicts incorporation of the Sin1 variant with a single amino acid substitution will not disturb the integrity of TORC2. This is consistent with the observation in the previous section that the Sin1 variants were stably associated with the Tor1 kinase (Figure 11D, Figure 13E).

The above experiments did not give clear results as to if Sin1 interacts with Tor1 in the absence of another essential TORC2 subunit, because the Sin1 protein is degraded in crude cell lysates. I therefore decided to use the GST-fused Sin1 recombinant protein produced in bacterial cells for GST-pulldown assays. This approach is less susceptible to the degradation in crude cell lysates, because a relatively large amount of GST-Sin1 can be inputted into the assay system. From the bacterial lysate, GST-Sin1 as well as GST alone was affinity-purified onto GSH beads. The GSH beads bound with GST-Sin1 or GST were then incubated with yeast cell lysates prepared from wild-type, *Δste20* or *Δwat1* strains expressing a chromosomal copy of FLAG:Tor1 as well as wild-type, *Δtor1* or *Δwat1* strains expressing a chromosomal copy of Ste20:FLAG. In the wild-type strains, Tor1 or Ste20 was successfully co-purified with GST-Sin1, compared to the GST alone control (Supplemental Figure 5B, C; left panel). In each deletion background, the amounts of Tor1 and Ste20 co-purification with Sin1 were significantly reduced, indicating the significant contributions of Tor1, Ste20, and Wat1 in forming TORC2 (Supplemental Figure 5B, C; middle and right panels). The greater reduction in the level of the Sin1-Tor1 association in the absence of Wat1 implies that Wat1 plays a

major role in connecting Sin1 and Tor1. However, the reduced but the significant amounts of the Tor1 or Ste20 co-purification were still observed, indicating that Sin1 is still able to form a complex with Tor1 independently of Ste20 or Wat1, and Sin1 with Ste20 independently of Tor1 or Wat1 (Supplemental Figure 5B, C; middle and right panels). Whether or not Sin1 forms a heterodimer with Tor1 or Ste20 in the complete absence of the other subunits and, if any, how stable the heterodimer might be, will be subject to future studies.

**Supplemental Figure 5.**

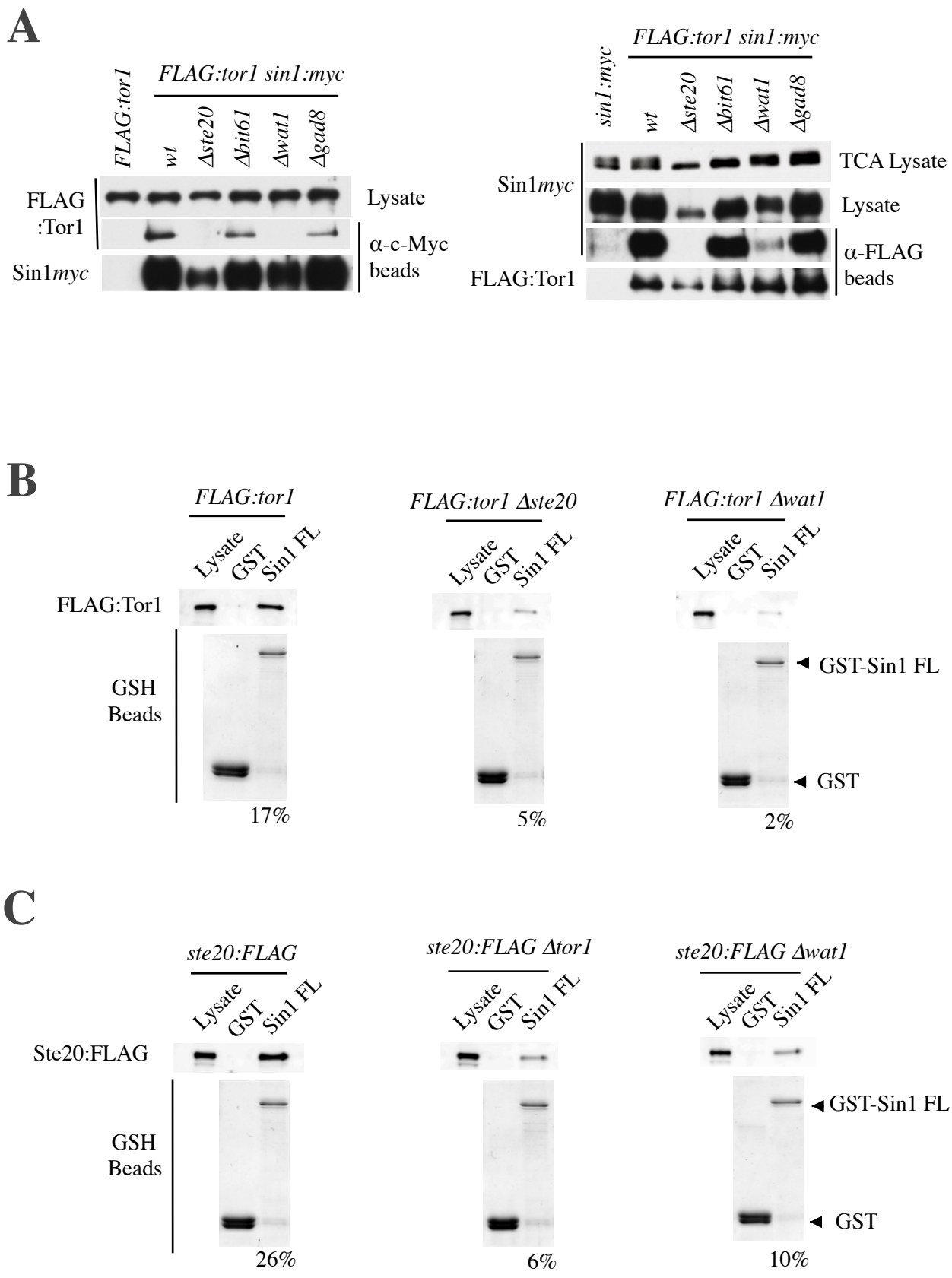

## Supplemental Figure 5.

**Supplemental Figure 5. Tor1 or Ste20 is co-purified with the recombinant Sin1 in the absence of the other.**

(A) Tor1-Sin1 interaction. *FLAG:tor1 sin1:myc* strains with the different genetic background of *wt*, *Δste20*, *Δsin1*, *Δbit61*, and *Δgad8* were subject to immunoprecipitation assay as in (A). The Sin1 proteins in the TCA samples are shown in the right panel.

(B) Sin1 interacts with Tor1 independently of Ste20 or Wat1. Cell extracts of the *FLAG:tor1*, *FLAG:tor1 Δste20*, or *FLAG:tor1 Δwat1* strains were subject to the GST-pulldown assay with the GSH beads bound with either GST alone or GST-Sin1 Full-length (FL) recombinant proteins prepared by the affinity purification from bacterial lysates. Immunobloting assay was performed to detect FLAG:Tor1 in the lysates and the purified fraction with anti-FLAG antibodies. The recombinant proteins on the GSH beads were visualized with CBB staining. The numbers shown at the bottom of each panel represent the percentage of the co-purified FLAG:Tor1 relative to the total amount of FLAG:Tor1 present in the crude cell extract used for the incubation. The same signal intensity from the co-purified fraction with that of the input (1%) means a 20% of the FLAG:Tor1 inputted into the pulldown assay was recovered with Sin1. Images were taken by LAS so linearity of signal intensity can be expected, and quantification was done through densitometric analysis using ImageJ.

(C) Sin1 interacts with Ste20 independently of Tor1 and Wat1. The crude cell extracts of the *Ste20:FLAG*, ste20:*FLAG Δtor1*, or ste20:*FLAG Δwat1* strains were subject to the GST-pulldown assay procedures as in (A). Ste20:FLAG in the purified fraction and in the input was detected by immunobloting analysis of the precipitated GSH beads with anti-FLAG antibody.

# 7. ACKNOWLEDGMENTS

I would like to first extend my gratitude to my supervisor Professor Kazuhiro Shiozaki for having me in his laboratory and educating me with his sincere mentorship. I also appreciate Dr. Hisashi Tatebe for training me with his great patience. My deep appreciation goes to Professors Hisaji Maki who gave me an opportunity to study in UC Davis and Hiroshi Takagi took care of me as a supervisor at NAIST. I thank all the members of Shiozaki's lab in UC Davis and NAIST for helpful discussion and encouragement. I especially note the following. I appreciate the talent and expertise of David Richter in yeast two-hybrid assay that he exerted fully throughout this study. The great technical assistances that I received during the period in UC Davis from Boram You and Tahara Nozomi were vital for the success of this study. I also thank Toshiya Yonekura for his work in mammalian system. Special thanks go to Dr. Takuya Ogawa, Dr. Norihiro Kitagawa, Tomoyuki Hatano and Mariko Maenish for their kind help during the preparation of this manuscript. Last but not the least I would like to express my sincere appreciation to my wife Yuki Murayama for her devotion.

# 8. REFERENCES


Alessi, D.R., Andjelkovic, M., Caudwell, B., Cron, P., Morrice, N., Cohen, P., and Hemmings, B.A. (1996). Mechanism of activation of protein kinase B by insulin and IGF-1. *15*, 6541–6551.

Alessi, D.R., Deak, M., Casamayor, A., Caudwell, F.B., Morrice, N., Norman, D.G., Gaffney, P., Reese, C.B., MacDougall, C.N., Harbison, D., et al. (1997). 3-Phosphoinositide-dependent protein kinase-1 (PDK1): structural and functional homology with the Drosophila DSTPK61 kinase. *7*, 776–789.

Alessi, D. (1998). ScienceDirect - Current Opinion in Genetics & Development : Mechanism of activation and function of protein kinase B. Curr Opin Genet Dev.

Ali, S.M., and Sabatini, D.M. (2005). Structure of S6 kinase 1 determines whether raptor-mTOR or rictor-mTOR phosphorylates its hydrophobic motif site. *280*, 19445–19448.

Altomare, D.A., and Testa, J.R. (2005). Perturbations of the AKT signaling pathway in human cancer. Oncogene- … *24*, 7455–7464.

Alvarez, B., and Moreno, S. (2006). Fission yeast Tor2 promotes cell growth and represses cell differentiation. J Cell Sci *119*, 4475–4485.

Arkin, M. (2004). Small-molecule inhibitors of protein–protein interactions: progressing towards the dream. Nature Reviews Drug Discovery.

Aylett, C.H.S., Sauer, E., Imseng, S., Boehringer, D., Hall, M.N., Ban, N., and Maier, T. (2016). Architecture of human mTOR complex 1. Science *351*, 48–52.

Balendran, A., Casamayor, A., Deak, M., Paterson, A., Gaffney, P., Currie, R., Downes, C.P., and Alessi, D.R. (1999). PDK1 acquires PDK2 activity in the presence of a synthetic peptide derived from the carboxyl terminus of PRK2. *9*, 393–404.

Barbet, N.C., Schneider, U., Helliwell, S.B., Stansfield, I., Tuite, M.F., and Hall, M.N. (1996). TOR controls translation initiation and early G1 progression in yeast. *7*, 25–42.

Benjamin, D., Colombi, M., Moroni, C., and Hall, M.N. (2011). Rapamycin passes the torch: a new generation of mTOR inhibitors. Nature Reviews Drug Discovery *10*, 868–880.

Berchtold, D., and Walther, T.C. (2009). TORC2 plasma membrane localization is essential for cell viability and restricted to a distinct domain. *20*, 1565–1575.

Betz, C., Stracka, D., Prescianotto-Baschong, C., Frieden, M., Demaurex, N., and Hall, M.N. (2013). mTOR complex 2-Akt signaling at mitochondria-associated endoplasmic reticulum membranes (MAM) regulates mitochondrial physiology. Proc Natl Acad Sci USA *110*, 12526–12534.

Betz, C., and Hall, M.N. (2013). Where is mTOR and what is it doing there? J Cell Biol *203*, 563–574.

Betzi, S., Guerlesquin, F., and Morelli, X. (2009). Protein-protein interaction inhibition

(2P2I): fewer and fewer undruggable targets. Comb Chem High Throughput Screen *12*, 968–983.

Biondi, R.M., Kieloch, A., Currie, R.A., and Deak, M. (2001). The PIF-binding pocket in PDK1 is essential for activation of S6K and SGK, but not PKB : Abstract : The EMBO Journal. *20*, 4380–4390.

Breuleux, M., Klopfenstein, M., Stephan, C., Doughty, C.A., Barys, L., Maira, S.-M., Kwiatkowski, D., and Lane, H.A. (2009). Increased AKT S473 phosphorylation after mTORC1 inhibition is rictor dependent and does not predict tumor cell response to PI3K/mTOR inhibition. Mol Cancer Ther *8*, 742–753.

Brown, E.J., Albers, M.W., Shin, T.B., Ichikawa, K., Keith, C.T., Lane, W.S., and Schreiber, S.L. (1994). A mammalian protein targeted by G1-arresting rapamycin-receptor complex. Nature *369*, 756–758.

Brown, E.J., Beai, P.A., Keith, C.T., Chen, J., and Shin, T.B. (1995). Control of p70 S6 kinase by. Nature.

Brunn, G.J., Hudson, C.C., Sekulić, A., Williams, J.M., Hosoi, H., Houghton, P.J., Lawrence, J.C., and Abraham, R.T. (1997). Phosphorylation of the Translational Repressor PHAS-I by the Mammalian Target of Rapamycin. *277*, 99–101.

Calleja, V., Alcor, D., Laguerre, M., Park, J., Vojnovic, B., Hemmings, B.A., Downward, J., Parker, P.J., and Larijani, B. (2007). Intramolecular and Intermolecular Interactions of Protein Kinase B Define Its Activation In Vivo. PLoS Biol *5*, e95.

Calleja, V., Laguerre, M., Parker, P.J., and Larijani, B. (2009). Role of a Novel PH-Kinase Domain Interface in PKB/Akt Regulation: Structural Mechanism for Allosteric Inhibition. PLoS Biol *7*, e1000017.

Cameron, A.J.M., Linch, M.D., Saurin, A.T., Escribano, C., and Parker, P.J. (2011). Dissecting the role of Sin1 in AGC kinase regulation by TORC2. Biochem J *439*, 287–297.

Chang, F., Lee, J.T., Navolanic, P.M., Steelman, L.S., Shelton, J.G., Blalock, W.L., Franklin, R.A., and McCubrey, J.A. (2003). Involvement of PI3K/Akt pathway in cell cycle progression, apoptosis, and neoplastic transformation: a target for cancer chemotherapy. Leukemia *17*, 590–603.

Chen, C.-H., and Sarbassov, D.D. (2011). Integrity of mTORC2 is dependent on phosphorylation of SIN1 by mTOR. J Biol Chem.

Chica, N., Rozalén, A.E., Pérez-Hidalgo, L., Rubio, A., Novak, B., and Moreno, S. (2016). Nutritional Control of Cell Size by the Greatwall-Endosulfine-PP2A·B55 Pathway. *26*, 319–330.

Chou, M., and Blenis, J. (1995). The 70 kDa S6 kinase: regulation of a kinase with multiple roles in mitogenic signalling. Curr Opin Cell Biol.

Cloonan, N. (2006). SIN1 AND SIN1 ISOFORMS: An investigation into the biological significance of a novel human protein family.

Cohen, A., Kupiec, M., and Weisman, R. (2014). Glucose activates TORC2-Gad8 protein via positive regulation of the cAMP/cAMP-dependent protein kinase A (PKA) pathway and negative regulation of the Pmk1 protein-mitogen-activated protein kinase pathway. J Biol Chem *289*, 21727–21737.

Colicelli, J., Nicolette, C., Birchmeier, C., Rodgers, L., Riggs, M., and Wigler, M. (1991). Expression of three mammalian cDNAs that interfere with RAS function in Saccharomyces cerevisiae. Proc Natl Acad Sci USA *88*, 2913–2917.

Dennis, P.B., Pullen, N., Pearson, R.B., Kozma, S.C., and Thomas, G. (1998). Phosphorylation sites in the autoinhibitory domain participate in p70(s6k) activation loop phosphorylation. *273*, 14845–14852.

Durán, R.V., and Hall, M.N. (2012). Regulation of TOR by small GTPases. EMBO Rep.

Facchinetti, V., Ouyang, W., Wei, H., Soto, N., Lazorchak, A., Gould, C., Lowry, C., Newton, A.C., Mao, Y., Miao, R.Q., et al. (2008). The mammalian target of rapamycin complex 2 controls folding and stability of Akt and protein kinase C. *27*, 1932–1943.

Fatrai, S., Elghazi, L., Balcazar, N., Cras-Méneur, C., Krits, I., Kiyokawa, H., and Bernal-Mizrachi, E. (2006). Akt Induces β-Cell Proliferation by Regulating Cyclin D1, Cyclin D2, and p21 Levels and Cyclin-Dependent Kinase-4 Activity. Diabetes *55*, 318–325.

Fernández-Sáiz, V., Targosz, B.-S., Lemeer, S., Eichner, R., Langer, C., Bullinger, L., Reiter, C., Slotta-Huspenina, J., Schroeder, S., Knorn, A.-M., et al. (2013). SCFFbxo9 and CK2 direct the cellular response to growth factor withdrawal via Tel2/Tti1 degradation and promote survival in multiple myeloma. *15*, 72–81.

Fields, S., and Song, O.-K. (1989). A novel genetic system to detect protein–protein interactions. Nature *340*, 245–246.

Fingar, D.C., and Blenis, J. (2004). Target of rapamycin (TOR): an integrator of nutrient and growth factor signals and coordinator of cell growth and cell cycle progression. Oncogene- … *23*, 3151–3171.

Foster, D.A., Yellen, P., Xu, L., and Saqcena, M. (2010). Regulation of G1 Cell Cycle Progression Distinguishing the Restriction Point from a Nutrient-Sensing Cell Growth Checkpoint(s). Genes & Cancer *1*, 1124–1131.

Frias, M.A., Thoreen, C.C., Jaffe, J.D., Schroder, W., Sculley, T., Carr, S.A., and Sabatini, D.M. (2006). mSin1 is necessary for Akt/PKB phosphorylation, and its isoforms define three distinct mTORC2s. *16*, 1865–1870.

Garami, A., Zwartkruis, F.J.T., Nobukuni, T., Joaquin, M., Roccio, M., Stocker, H., Kozma, S.C., Hafen, E., Bos, J.L., and Thomas, G. (2003). Insulin activation of Rheb, a mediator of mTOR/S6K/4E-BP signaling, is inhibited by TSC1 and 2. *11*, 1457–1466.

García-Martínez, J.M., and Alessi, D.R. (2008). mTOR complex 2 (mTORC2) controls hydrophobic motif phosphorylation and activation of serum- and glucocorticoid-induced protein kinase 1 (SGK1). Biochem J *416*, 375–385.

Gaubitz, C., Oliveira, T.M., Prouteau, M., Leitner, A., Karuppasamy, M., Konstantinidou, G.,

Rispal, D., Eltschinger, S., Robinson, G.C., Thore, S., et al. (2015). Molecular Basis of the Rapamycin Insensitivity of Target Of Rapamycin Complex 2. *58*, 977–988.

Gaubitz, C., Prouteau, M., Kusmider, B., and Loewith, R. (2016). TORC2 Structure and Function. Trends Biochem Sci *41*, 532–545.

Glaser, F., Pupko, T., Paz, I., Bell, R.E., Bechor-Shental, D., Martz, E., and Ben-Tal, N. (2003). ConSurf: Identification of Functional Regions in Proteins by Surface-Mapping of Phylogenetic Information. Bioinformatics *19*, 163–164.

Guertin, D.A., Stevens, D.M., Thoreen, C.C., Burds, A.A., Kalaany, N.Y., Moffat, J., Brown, M., Fitzgerald, K.J., and Sabatini, D.M. (2006). Ablation in mice of the mTORC components raptor, rictor, or mLST8 reveals that mTORC2 is required for signaling to Akt-FOXO and PKCalpha, but not S6K1. Dev. Cell *11*, 859–871.

Hara, K., Yonezawa, K., Kozlowski, M.T., Sugimoto, T., Andrabi, K., Weng, Q.P., Kasuga, M., Nishimoto, I., and Avruch, J. (1997). Regulation of eIF-4E BP1 phosphorylation by mTOR. *272*, 26457–26463.

Hara, K., Yonezawa, K., Weng, Q.P., Kozlowski, M.T., Belham, C., and Avruch, J. (1998). Amino acid sufficiency and mTOR regulate p70 S6 kinase and eIF-4E BP1 through a common effector mechanism. *273*, 14484–14494.

Hara, K., Maruki, Y., Long, X., Yoshino, K.-I., Oshiro, N., Hidayat, S., Tokunaga, C., Avruch, J., and Yonezawa, K. (2002). Raptor, a binding partner of target of rapamycin (TOR), mediates TOR action. *110*, 177–189.

Hardt, M., Chantaravisoot, N., and Tamanoi, F. (2011). Activating mutations of TOR (target of rapamycin).

Hatano, T., Morigasaki, S., Tatebe, H., Ikeda, K., and Shiozaki, K. (2015). Fission yeast Ryh1 GTPase activates TOR Complex 2 in response to glucose. Cell Cycle *14*, 848–856.

Hauge, C., Antal, T.L., Hirschberg, D., Doehn, U., Thorup, K., Idrissova, L., Hansen, K., Jensen, O.N., Jørgensen, T.J., Biondi, R.M., et al. (2007). Mechanism for activation of the growth factor-activated AGC kinases by turn motif phosphorylation. *26*, 2251–2261.

Hayashi, T., and Yanagida, M. (2011). The reverse, but coordinated, roles of Tor2 (TORC1) and Tor1 (TORC2) kinases for growth, cell cycle and separase-mediated mitosis in Schizosaccharomyces pombe. Rsob.Royalsocietypublishing.org.

Hayashi, T., Hatanaka, M., Nagao, K., Nakaseko, Y., Kanoh, J., Kokubu, A., Ebe, M., and Yanagida, M. (2007). Rapamycin sensitivity of the Schizosaccharomyces pombe tor2 mutant and organization of two highly phosphorylated TOR complexes by specific and common subunits. *12*, 1357–1370.

He, Y., Sugiura, R., Ma, Y., Kita, A., Deng, L., Takegawa, K., Matsuoka, K., Shuntoh, H., and Kuno, T. (2006). Genetic and functional interaction between Ryh1 and Ypt3: two Rab GTPases that function in S. pombe secretory pathway. *11*, 207–221.

Heitman, J., Movva, N., and Hall, M. (1991). Targets for cell cycle arrest by the immunosuppressant rapamycin in yeast.

Helliwell, S.B., Howald, I., Barbet, N., and Hall, M.N. (1998). TOR2 is part of two related signaling pathways coordinating cell growth in Saccharomyces cerevisiae. Genetics *148*, 99–112.

Helliwell, S., Wagner, P., and Kunz, J. (1994). TOR1 and TOR2 are structurally and functionally similar but not identical phosphatidylinositol kinase homologues in yeast. Molecular Biology of ….

Ho, H.-L., Shiau, Y.-S., and Chen, M.-Y. (2005). Saccharomyces cerevisiaeTSC11/AVO3 participates in regulating cell integrity and functionally interacts with components of the Tor2 complex. *47*, 273–288.

Hosokawa, N., Hara, T., Kaizuka, T., Kishi, C., Takamura, A., Miura, Y., Iemura, S.-I., Natsume, T., Takehana, K., Yamada, N., et al. (2009). Nutrient-dependent mTORC1 association with the ULK1-Atg13-FIP200 complex required for autophagy. Mol. Biol. Cell *20*, 1981–1991.

Hsu, P.P., Kang, S.A., Rameseder, J., Zhang, Y., Ottina, K.A., Lim, D., Peterson, T.R., Choi, Y., Gray, N.S., Yaffe, M.B., et al. (2011). The mTOR-regulated phosphoproteome reveals a mechanism of mTORC1-mediated inhibition of growth factor signaling. *332*, 1317–1322.

Huang, B.X., Akbar, M., Kevala, K., and Kim, H.-Y. (2011). Phosphatidylserine is a critical modulator for Akt activation. J Cell Biol *192*, 979–992.

Huang, X., Begley, M., Morgenstern, K.A., Gu, Y., Rose, P., Zhao, H., and Zhu, X. (2003). Crystal structure of an inactive Akt2 kinase domain. Structure *11*, 21–30.

Huggins, D.J. (2016). Studying the role of cooperative hydration in stabilizing folded protein states. Journal of Structural Biology *196*, 394–406.

Ikeda, K., Morigasaki, S., Tatebe, H., Tamanoi, F., and Shiozaki, K. (2008). Fission yeast TOR complex 2 activates the AGC-family Gad8 kinase essential for stress resistance and cell cycle control. Cell Cycle *7*, 358–364.

Ikenoue, T., Inoki, K., Yang, Q., Zhou, X., and Guan, K.-L. (2008). Essential function of TORC2 in PKC and Akt turn motif phosphorylation, maturation and signalling. *27*, 1919–1931.

Inoki, K., Corradetti, M.N., and Guan, K.-L. (2005a). Dysregulation of the TSC-mTOR pathway in human disease. Nat Genet *37*, 19–24.

Inoki, K., Ouyang, H., Li, Y., and Guan, K.-L. (2005b). Signaling by Target of Rapamycin Proteins in Cell Growth Control. Microbiology and Molecular Biology Reviews *69*, 79–100.

Inoki, K., Zhu, T., and Guan, K.-L. (2003). TSC2 Mediates Cellular Energy Response to Control Cell Growth and Survival. *115*, 577–590.

Jacinto, E., and Lorberg, A. (2008). TOR regulation of AGC kinases in yeast and mammals. Biochem J *410*, 19–37.

Jacinto, E., Facchinetti, V., Liu, D., Soto, N., Wei, S., Jung, S.Y., Huang, Q., Qin, J., and Su, B. (2006). SIN1/MIP1 maintains rictor-mTOR complex integrity and regulates Akt

phosphorylation and substrate specificity. *127*, 125–137.

Jacinto, E., Loewith, R., Schmidt, A., Lin, S., Rüegg, M.A., Hall, A., and Hall, M.N. (2004). Mammalian TOR complex 2 controls the actin cytoskeleton and is rapamycin insensitive. *6*, 1122–1128.

Janes, M.R., Limon, J.J., So, L., Chen, J., Lim, R.J., Chavez, M.A., Vu, C., Lilly, M.B., Mallya, S., Ong, S.T., et al. (2010). Effective and selective targeting of leukemia cells using a TORC1/2 kinase inhibitor. Nat Med *16*, 205–213.

Jorgensen, P. (2004). How Cells Coordinate Growth and Division 10.1016/j.cub.2004.11.027 : Current Biology | ScienceDirect.com. Current Biology.

Kalaany, N.Y., and Sabatini, D.M. (2009). Tumours with PI3K activation are resistant to dietary restriction. Nature *458*, 725–731.

Kamada, Y., Fujioka, Y., Suzuki, N.N., Inagaki, F., Wullschleger, S., Loewith, R., Hall, M.N., and Ohsumi, Y. (2005). Tor2 Directly Phosphorylates the AGC Kinase Ypk2 To Regulate Actin Polarization. *25*, 7239–7248.

Kamada, Y., Yoshino, K.-I., Kondo, C., Kawamata, T., Oshiro, N., Yonezawa, K., and Ohsumi, Y. (2010). Tor directly controls the Atg1 kinase complex to regulate autophagy. Molecular and Cellular Biology *30*, 1049–1058.

Kannan, N., Haste, N., Taylor, S.S., and Neuwald, A.F. (2007). The hallmark of AGC kinase functional divergence is its C-terminal tail, a cis-acting regulatory module. Proc Natl Acad Sci USA *104*, 1272–1277.

Kawai, M., Nakashima, A., Ueno, M., Ushimaru, T., Aiba, K., Doi, H., and Uritani, M. (2001). Fission yeast tor1 functions in response to various stresses including nitrogen starvation, high osmolarity, and high temperature. *39*, 166–174.

Kim, D.-H., Sarbassov, D.D., Ali, S.M., King, J.E., Latek, R.R., Erdjument-Bromage, H., Tempst, P., and Sabatini, D.M. (2002). mTOR interacts with raptor to form a nutrient-sensitive complex that signals to the cell growth machinery. *110*, 163–175.

Kim, S.G., Hoffman, G.R., Poulogiannis, G., Buel, G.R., Jang, Y.J., Lee, K.W., Kim, B.-Y., Erikson, R.L., Cantley, L.C., Choo, A.Y., et al. (2013). Metabolic stress controls mTORC1 lysosomal localization and dimerization by regulating the TTT-RUVBL1/2 complex. *49*, 172–185.

Kominami, K., Seth-Smith, H., and Toda, T. (1998). Apc10 and Ste9/Srw1, two regulators of the APC-cyclosome, as well as the CDK inhibitor Rum1 are required for G1 cell-cycle arrest in fission yeast. *17*, 5388–5399.

Kunz, J., Henriquez, R., Schneider, U., Deuter-Reinhard, M., Movva, N.R., and Hall, M.N. (1993). Target of rapamycin in yeast, TOR2, is an essential phosphatidylinositol kinase homolog required for G1 progression. *73*, 585–596.

Kuo, C.J., Chung, J., Fiorentino, D.F., Flanagan, W.M., Blenis, J., and Crabtree, G.R. (1992). Rapamycin selectively inhibits interleukin-2 activation of p70 S6 kinase. Nature *358*, 70–73.

Lakkaraju, A.K., Abrami, L., Lemmin, T., Blaskovic, S., Kunz, B., Kihara, A., Dal Peraro, M., and van der Goot, F.G. (2012). Palmitoylated calnexin is a key component of the ribosome-translocon complex. *31*, 1823–1835.

Liang, J., and Slingerland, J.M. (2003). Multiple roles of the PI3K/PKB (Akt) pathway in cell cycle progression. Cell Cycle *2*, 339–345.

Liao, H.-C., and Chen, M.-Y. (2011). TARGET OF RAPAMYCIN COMPLEX 2 SIGNALS TO THE DOWNSTREAM EFFECTOR YEAST PROTEIN KINASE 2 (YPK2) THROUGH ADHERES-VORACIOUSLY-TO-TARGET OF-RAPAMYCIN-2 PROTEIN 1 (AVO1) IN SACCHAROMYCES CEREVISIAE. J Biol Chem.

Libra, M. (2011). Gene alterations in the PI3K/PTEN/AKT pathway as a mechanism of drug-resistance (Review). Int J Oncol.

Liu, P., Gan, W., Chin, Y.R., Ogura, K., Guo, J., Zhang, J., Wang, B., Blenis, J., Cantley, L.C., Toker, A., et al. (2015). PtdIns(3,4,5)P3-Dependent Activation of the mTORC2 Kinase Complex. Cancer Discovery *5*, 1194–1209.

Loewith, R., Jacinto, E., Wullschleger, S., Lorberg, A., Crespo, J.L., Bonenfant, D., Oppliger, W., Jenoe, P., and Hall, M.N. (2002). Two TOR complexes, only one of which is rapamycin sensitive, have distinct roles in cell growth control. *10*, 457–468.

Lu, M., Wang, J., Jones, K.T., Ives, H.E., Feldman, M.E., Yao, L.J., Shokat, K.M., Ashrafi, K., and Pearce, D. (2010). mTOR Complex-2 Activates ENaC by Phosphorylating SGK1. Journal of the American Society of Nephrology *21*, 811–818.

Lu, M., Wang, J., Ives, H.E., and Pearce, D. (2011). mSIN1 mediates SGK1 interaction with mTORC2 and is required for selective activation of the epithelial sodium channel. J Biol Chem.

Luo, J., Manning, B.D., and Cantley, L.C. (2003). Targeting the PI3K-Akt pathway in human cancer: rationale and promise. Cancer Cell *4*, 257–262.

Manning, B.D. (2004). Balancing Akt with S6K. J Cell Biol *167*, 399–403.

Manning, B.D., and Cantley, L.C. (2003). Rheb fills a GAP between TSC and TOR. Trends Biochem Sci *28*, 573–576.

Martín, R., Portantier, M., Chica, N., Nyquist-Andersen, M., Mata, J., and Lopez-Aviles, S. (2017). A PP2A-B55-Mediated Crosstalk between TORC1 and TORC2 Regulates the Differentiation Response in Fission Yeast. Current Biology *27*, 175–188.

Matsuo, T., Kubo, Y., Watanabe, Y., and Yamamoto, M. (2003). Schizosaccharomyces pombe AGC family kinase Gad8p forms a conserved signaling module with TOR and PDK1-like kinases. Embo J. *22*, 3073–3083.

Matsuo, T., Otsubo, Y., Urano, J., Tamanoi, F., and Yamamoto, M. (2007). Loss of the TOR kinase Tor2 mimics nitrogen starvation and activates the sexual development pathway in fission yeast. *27*, 3154–3164.

Maundrell, K. (1990). nmt1 of fission yeast. A highly transcribed gene completely repressed

by thiamine. *265*, 10857–10864.

Mei Sun, G.W.J.E.P.R.I.F.Z.-Q.Y.X.-L.M.S.A.S.R.J.P.N.T.S.V.N.J.Q.C. (2001). AKT1/PKBα Kinase Is Frequently Elevated in Human Cancers and Its Constitutive Activation Is Required for Oncogenic Transformation in NIH3T3 Cells. The American Journal of Pathology *159*, 431.

Mi, W., Ye, Q., Liu, S., and She, Q.-B. (2015). AKT inhibition overcomes rapamycin resistance by enhancing the repressive function of PRAS40 on mTORC1/4E-BP1 axis. Oncotarget *6*, 13962–13977.

Mitsuhiro Yanagida, N.I.M.S.K.S. (2011). Nutrient limitations alter cell division control and chromosome segregation through growth-related kinases and phosphatases. Philosophical Transactions of the Royal Society B: Biological Sciences *366*, 3508.

Nakashima, A., Otsubo, Y., Yamashita, A., Sato, T., Yamamoto, M., and Tamanoi, F. (2012). Psk1, an AGC kinase family member in fission yeast, is directly phosphorylated and controlled by TORC1 as S6 kinase. J Cell Sci.

Nishiuma, T., Hara, K., Tsujishita, Y., Kaneko, K., Shii, K., and Yonezawa, K. (1998). Characterization of the phosphoproteins and protein kinase activity in mTOR immunoprecipitates. Biochem Biophys Res Commun *252*, 440–444.

Nojima, H., Tokunaga, C., Eguchi, S., Oshiro, N., Hidayat, S., Yoshino, K.-I., Hara, K., Tanaka, N., Avruch, J., and Yonezawa, K. (2003). The Mammalian Target of Rapamycin (mTOR) Partner, Raptor, Binds the mTOR Substrates p70 S6 Kinase and 4E-BP1 through Their TOR Signaling (TOS) Motif. *278*, 15461–15464.

O'Reilly, K.E., Rojo, F., She, Q.-B., Solit, D., Mills, G.B., Smith, D., Lane, H., Hofmann, F., Hicklin, D.J., Ludwig, D.L., et al. (2006). mTOR Inhibition Induces Upstream Receptor Tyrosine Kinase Signaling and Activates Akt. Cancer Res *66*, 1500–1508.

Oh, W.J., Wu, C.-C., Kim, S.J., Facchinetti, V., Julien, L.-A., Finlan, M., Roux, P.P., Su, B., and Jacinto, E. (2010). mTORC2 can associate with ribosomes to promote cotranslational phosphorylation and stability of nascent Akt polypeptide. *29*, 3939–3951.

Otsubo, Y., and Yamamato, M. (2008). TOR signaling in fission yeast. Crit Rev Biochem Mol Biol *43*, 277–283.

Pan, D., and Matsuura, Y. (2012). Structures of the pleckstrin homology domain of Saccharomyces cerevisiaeAvo1 and its human orthologue Sin1, an essential subunit of TOR complex 2. Acta Crystallogr F Struct Biol Cryst Commun *68*, 386–392.

Pearce, L.R., Huang, X., Boudeau, J., Pawłowski, R., Wullschleger, S., Deak, M., Ibrahim, A.F.M., Gourlay, R., Magnuson, M.A., and Alessi, D.R. (2007). Identification of Protor as a novel Rictor-binding component of mTOR complex-2. Biochem J *405*, 513–522.

Petersen, J., and Hagan, I.M. (2005). Polo kinase links the stress pathway to cell cycle control and tip growth in fission yeast. *435*, 507–512.

Poston, C.N., Krishnan, S.C., and Bazemore-Walker, C.R. (2013). In-depth proteomic analysis of mammalian mitochondria-associated membranes (MAM). J Proteomics *79*, 219–

230.

Price, D.J., Grove, J.R., Calvo, V., Avruch, J., and Bierer, B.E. (1992). Rapamycin-induced inhibition of the 70-kilodalton S6 protein kinase. Science *257*, 973–977.

Pupko, T., Bell, R.E., Mayrose, I., Glaser, F., and Ben-Tal, N. (2002). Rate4Site: an algorithmic tool for the identification of functional regions in proteins by surface mapping of evolutionary determinants within their homologues. Bioinformatics *18*, S71–S77.

Roelants, F.M., Torrance, P.D., and Thorner, J. (2004). Differential roles of PDK1- and PDK2-phosphorylation sites in the yeast AGC kinases Ypk1, Pkc1 and Sch9. Microbiology (Reading, Engl) *150*, 3289–3304.

Saltiel, A.R. (1996). Regulation of Both Glycogen Synthase and PHAS-I by Insulin in Rat Skeletal Muscle Involves Mitogen-activated Protein Kinase-independent and Rapamycin-sensitive Pathways. *271*, 5033–5039.

Sarbassov, D.D., Ali, S.M., Kim, D.-H., Guertin, D.A., Latek, R.R., Erdjument-Bromage, H., Tempst, P., and Sabatini, D.M. (2004). Rictor, a novel binding partner of mTOR, defines a rapamycin-insensitive and raptor-independent pathway that regulates the cytoskeleton. *14*, 1296–1302.

Sarbassov, D.D., Guertin, D.A., Ali, S.M., and Sabatini, D.M. (2005). Phosphorylation and regulation of Akt/PKB by the rictor-mTOR complex. *307*, 1098–1101.

Sato, T., Nakashima, A., Guo, L., and Tamanoi, F. (2009). Specific activation of mTORC1 by Rheb G-protein in vitro involves enhanced recruitment of its substrate protein. *284*, 12783–12791.

Schalm, S.S., Fingar, D.C., Sabatini, D.M., and Blenis, J. (2003). TOS Motif-Mediated Raptor Binding Regulates 4E-BP1 Multisite Phosphorylation and Function. Current Biology *13*, 797–806.

Schmidt, A., Kunz, J., and Hall, M.N. (1996). TOR2 is required for organization of the actin cytoskeleton in yeast. Proc Natl Acad Sci USA *93*, 13780–13785.

Schroder, W.A., Buck, M., Cloonan, N., Hancock, J.F., Suhrbier, A., Sculley, T., and Bushell, G. (2007). Human Sin1 contains Ras-binding and pleckstrin homology domains and suppresses Ras signalling. Cell Signal *19*, 1279–1289.

Schroder, W., Bushell, G., and Sculley, T. (2005). The human stress-activated protein kinase-interacting 1 gene encodes JNK-binding proteins. Cell Signal *17*, 761–767.

Schroder, W., Cloonan, N., Bushell, G., and Sculley, T. (2004). Alternative polyadenylation and splicing of mRNAs transcribed from the human Sin1 gene. Gene *339*, 17–23.

Shinozaki-Yabana, S., and Watanabe, Y. (2000). Novel WD-Repeat Protein Mip1p Facilitates Function of the Meiotic Regulator Mei2p in Fission Yeast. Molecular and Cellular ….

Sparks, C.A., and Guertin, D.A. (2010). Targeting mTOR: prospects for mTOR complex 2 inhibitors in cancer therapy. Oncogene- … *29*, 3733–3744.

STEINBERG, S.F. (2008). Structural Basis of Protein Kinase C Isoform Function. Physiological Reviews *88*, 1341–1378.

Tanford, C. (1997). How protein chemists learned about the hydrophobic factor. Protein Science *6*, 1358–1366.

Tatebe, H., Murayama, S., Yonekura, T., and Hatano, T. (2017). Substrate specificity of TOR complex 2 is determined by a ubiquitin-fold domain of the Sin1 subunit. Elife.

Tatebe, H., and Shiozaki, K. (2010). Rab small GTPase emerges as a regulator of TOR complex 2. Small Gtpases *1*, 180–182.

Tatebe, H., Morigasaki, S., Murayama, S., Zeng, C.T., and Shiozaki, K. (2010). Rab-family GTPase regulates TOR complex 2 signaling in fission yeast. *20*, 1975–1982.

Testa, J.R., and Bellacosa, A. (2001). AKT plays a central role in tumorigenesis. Proc Natl Acad Sci USA *98*, 10983–10985.

Tiwary, P., Mondal, J., Morrone, J.A., and Berne, B.J. (2015). Role of water and steric constraints in the kinetics of cavity–ligand unbinding. Proc Natl Acad Sci USA *112*, 12015–12019.

Ubersax, J.A., and Ferrell, J.E., Jr (2007). Mechanisms of specificity in protein phosphorylation. Nat Rev Mol Cell Biol *8*, 530–541.

Um, S.H., Frigerio, F., Watanabe, M., Picard, F., Joaquin, M., Sticker, M., Fumagalli, S., Allegrini, P.R., Kozma, S.C., Auwerx, J., et al. (2004). Absence of S6K1 protects against age- and diet-induced obesity while enhancing insulin sensitivity. Nature *431*, 200–205.

Urano, J., Comiso, M.J., Guo, L., Aspuria, P.-J., Deniskin, R., Tabancay, A.P., Kato-Stankiewicz, J., and Tamanoi, F. (2005). Identification of novel single amino acid changes that result in hyperactivation of the unique GTPase, Rheb, in fission yeast. *58*, 1074–1086.

Uritani, M., Hidaka, H., Hotta, Y., Ueno, M., Ushimaru, T., and Toda, T. (2006). Fission yeast Tor2 links nitrogen signals to cell proliferation and acts downstream of the Rheb GTPase. *11*, 1367–1379.

Vivanco, I., and Sawyers, C. (2002). The phosphatidylinositol 3-kinase–AKT pathway in human cancer. Nat. Rev. Cancer.

Wang, J., Ye, Q., and She, Q.-B. (2014). New insights into 4E-BP1-regulated translation in cancer progression and metastasis. Cancer Cell Microenviron *1*.

Wang, S.-Z., and Roberts, R.M. (2005). The evolution of the Sin1 gene product, a little known protein implicated in stress responses and type I interferon signaling in vertebrates. BMC Evol Biol *5*, 13.

Wang, T., Blumhagen, R., Lao, U., Kuo, Y., and Edgar, B.A. (2012). LST8 Regulates Cell Growth via Target-of-Rapamycin Complex 2 (TORC2). *32*, 2203–2213.

Warfel, N.A., Niederst, M., and Newton, A.C. (2011). Disruption of the interface between the PH and kinase domains of Akt is sufficient for hydrophobic motif site phosphorylation in the

absence of mTORC2. J Biol Chem.

Wedaman, K.P., Reinke, A., Anderson, S., Yates, J., McCaffery, J.M., and Powers, T. (2003). Tor kinases are in distinct membrane-associated protein complexes in Saccharomyces cerevisiae. *14*, 1204–1220.

Weisman, R., and Choder, M. (2001). The fission yeast TOR homolog, tor1+, is required for the response to starvation and other stresses via a conserved serine. *276*, 7027–7032.

Weisman, R., Roitburg, I., Schonbrun, M., Harari, R., and Kupiec, M. (2007). Opposite effects of tor1 and tor2 on nitrogen starvation responses in fission yeast. Genetics *175*, 1153–1162.

Wilkinson, M.G., Pino, T.S., Tournier, S., Buck, V., Martin, H., Christiansen, J., Wilkinson, D.G., and Millar, J.B. (1999). Sin1: an evolutionarily conserved component of the eukaryotic SAPK pathway. *18*, 4210–4221.

Wu, W.-I., Voegtli, W.C., Sturgis, H.L., Dizon, F.P., Vigers, G.P.A., and Brandhuber, B.J. (2010). Crystal Structure of Human AKT1 with an Allosteric Inhibitor Reveals a New Mode of Kinase Inhibition. PLoS ONE *5*, e12913.

Wullschleger, S., Loewith, R., and Hall, M.N. (2006). TOR signaling in growth and metabolism. *124*, 471–484.

Wullschleger, S., Loewith, R., Oppliger, W., and Hall, M.N. (2005). Molecular Organization of Target of Rapamycin Complex 2. *280*, 30697.

Xie, J., and Proud, C.G. (2013). Crosstalk between mTOR complexes. *15*, 1263–1265.

Xie, J., Wang, X., and Proud, C.G. (2016). mTOR inhibitors in cancer therapy. F1000Res *5*, 2078.

Yang, H., Rudge, D.G., Koos, J.D., Vaidialingam, B., Yang, H.J., and Pavletich, N.P. (2013). mTOR kinase structure, mechanism and regulation. Nature.

Yang, J., Cron, P., Good, V.M., Thompson, V., Hemmings, B.A., and Barford, D. (2002a). Crystal structure of an activated Akt/protein kinase B ternary complex with GSK3-peptide and AMP-PNP. Nat Struct Biol *9*, 940–944.

Yang, J., Cron, P., Thompson, V., Good, V.M., Hess, D., Hemmings, B.A., and Barford, D. (2002b). Molecular mechanism for the regulation of protein kinase B/Akt by hydrophobic motif phosphorylation. *9*, 1227–1240.

Yang, Q., Inoki, K., Ikenoue, T., and Guan, K.-L. (2006). Identification of Sin1 as an essential TORC2 component required for complex formation and kinase activity. *20*, 2820–2832.

Yang, X., Yu, D.-D., Yan, F., Jing, Y.-Y., Han, Z.-P., Sun, K., Liang, L., Hou, J., and Wei, L.-X. (2015). The role of autophagy induced by tumor microenvironment in different cells and stages of cancer. Cell & Bioscience *5*, 8.

Yip, C.K., Murata, K., Walz, T., Sabatini, D.M., and Kang, S.A. (2010). Structure of the human mTOR complex I and its implications for rapamycin inhibition. *38*, 768–774.

Yu, Y., Yoon, S.-O., Poulogiannis, G., Yang, Q., Ma, X.M., Villén, J., Kubica, N., Hoffman, G.R., Cantley, L.C., Gygi, S.P., et al. (2011). Phosphoproteomic analysis identifies Grb10 as an mTORC1 substrate that negatively regulates insulin signaling. *332*, 1322–1326.

Yuan, H.-X., and Guan, K.-L. (2016). Structural insights of mTOR complex 1. Cell Res *26*, 267–268.

Zhang, Y., Gao, X., Saucedo, L.J., Ru, B., Edgar, B.A., and Pan, D. (2003). Rheb is a direct target of the tuberous sclerosis tumour suppressor proteins. *5*, 578–581.

Zinzalla, V., Stracka, D., Oppliger, W., and Hall, M.N. (2011). Activation of mTORC2 by Association with the Ribosome. *144*, 757–768.